ABSTRACT

Title of Dissertation: Morphology, Mineralogy, and Hydrology of Soils in the Triassic Culpeper Basin of Maryland

Mark Peter Elless, Doctor of Philosophy, 1992

Dissertation directed by: Dr. Martin C. Rabenhorst
Associate Professor
Department of Agronomy

Soils derived from red parent materials are problematic in terms of morphologically assessing their hydrology because these parent materials are known to retard the development of redoximorphic features within their sola. This retardation phenomena may lead to misinterpretations of these soils for both agricultural and engineering purposes. Such soils occur within the Triassic Culpeper Basin of Maryland. Eleven pedons along two topohydrosequences within this basin were therefore investigated to determine the interrelationships between the soil morphology, mineralogy, and hydrology, particularly as these pertain to the development of redoximorphic features in these soils. These soils are derived from dusky red (5YR 4/4) parent materials which retard the development of redoximorphic features. Morphological descriptions of each pedon were made and the water table was monitored in both open boreholes and slotted PVC pipes at staggered depths. Bulk samples of each horizon were collected for mineralogical and chemical analyses. Results indicate that hematite is the only iron oxide in the underlying red shales and sandstones of this basin. The

hematite in the soils is then inherited during pedogenesis and is responsible for the red hues exhibited throughout the profiles of the better-drained pedons and in the lower sola of the more poorly-drained pedons. Results of parent material uniformity indicate the presence of either loess, colluvium, alluvium, or mixtures of these materials with residuum within the upper sola of these same pedons. Residual, or principally residually-derived, soils remain predominantly red throughout their profile, independent of hydrology. Soils formed from non-uniform parent materials exhibit yellower hues, particularly within their upper sola. Thus, the pedogenic yellowing of these pedons may be due to either the incorporation of more easily altered foreign material than that derived from weathering of the red residual parent materials or to the presence of a seasonally-high water table in the upper sola of these pedons. Even though redoximorphic features are created through redox processes, the nature of the parent materials appears to mediate their degree of development. This study suggests that the degree of parent material uniformity be assessed prior to any judgment on the drainage classes of similar soils.

THE MORPHOLOGY, MINERALOGY, AND HYDROLOGY OF SOILS IN THE TRIASSIC CULPEPER BASIN OF MARYLAND

by

Mark Peter Elless

Dissertation submitted to the Faculty of the Graduate School
of The University of Maryland in partial fulfillment
of the requirements for the degree of
Doctor of Philosophy
1992

Advisory Committee:

Associate Professor Martin Rabenhorst, Chairman/Advisor
Professor Luke Chang
Professor Delvin Fanning
Professor Richard Weismiller
Associate Professor Bruce James

DEDICATION

To my father, Richard Elless,

for being the best teacher I ever had

To my mother, Clare Elless,

for encouraging me to reach for the stars

and

To my fiancee, Fatima Kasim

The Star of Sierra Leone never shone so bright

Thank you --- for everything

ACKNOWLEDGEMENTS

To my advisor and friend, Dr. Martin Rabenhorst, for his guidance and counsel throughout this study,

To the rest of my graduate committee for their assistance and support in completing this dissertation,

A special thank you to Dr. Delvin Fanning for "finding" me in North Dakota and persuading me to do my graduate work at Maryland,

To the landowners at each of my research sites, Mr. and Mrs. Walter Reilly and Mr. Phil Valentine, for their permission and willingness to allow me free access unto their respective lands,

To all my friends who have either assisted me at some time during my research or have shared our graduate lives together, particularly Margaret Condron, Randy Stahl, Mike Blaylock, David Verdone, Joey Shaw, and Ahmed Hussein,

To Carl Robinnette for his assistance during the site selection process,

To David Verdone and George Lulandela for assisting me in my laboratory work,

To my brothers and sisters (Debra, Rick, Tari, Michael, and Judy) for encouraging me to continue my education, and

To the entire Kasim family for "adopting" me into their wonderful family, particularly to Mary for being much like a second mother to me, to Aysha whose enthusiasm as a nine-year old was a welcome escape from strictly my studies, and

to Dr. Prince Kassim for sharing both his sound counsel and humorous stories at times when they were most needed.

TABLE OF CONTENTS

LIST OF TABLES

LIST OF FIGURES

INTRODUCTION

The morphological properties of soils have been commonly used to evaluate the relative "wetness" or drainage class of various soils. It has become known that soils derived from red parent materials are problematic in terms of assessing their drainage class, because these soils are less apt to show the morphological features associated with a given degree of wetness (redoximorphic features such as gleying, low chroma mottling, Fe/Mn nodules, etc.). The absence of commonly identifiable redoximorphic features in wet soils may cause erroneous interpretations regarding the suitability of these soils for agricultural, engineering or environmental uses. This could have serious ramifications for homeowners such as failure of septic systems, wet basements and foundations, or may result in erroneous delineation of wetlands.

In Maryland, such problematic red soils are found in the Triassic Culpeper Basin of Maryland. This basin occupies western Montgomery County, portions of central Frederick County, and western Carroll County and constitutes one member of a series of Triassic basins which extend fairly continuously throughout the Mid-Atlantic USA from North Carolina to New Hampshire. The dominant geological parent materials in this basin are dusky red sedimentary rocks dominated by shales with lesser amounts of fine-grained sandstone and siltstone.

The overall objective of this research is to determine

the interrelationships between the morphology, mineralogy, and hydrology of the soils derived from these red parent materials, particularly as these interrelationships pertain to the occurrence and distribution of redoximorphic features in these soils.

To fulfill this overall objective, each of the four chapters in this dissertation (Chapters 2-5) examines a particular portion of this larger objective. The objective of Chapter 2 is to determine the mineralogical makeup and degree of homogeneity of the red shales in this basin. The objective of Chapter 3 is to examine the degree of parent material uniformity in the soils derived from these red parent materials. The objective of Chapter 4 is to determine the factor(s) controlling the development of redoximorphic features in these soils. The objective of the Chapter 5 is to examine the iron oxide chemistry and mineralogy in soils and selected redoximorphic features, and to evaluate the origin of these features.

The results from this investigation should provide insight regarding the genesis of these soils and the conditions required for the development of redoximorphic features in parent materials known to retard such development.

CHAPTER 1

REVIEW OF LITERATURE

Geology and Geography of the Maryland Piedmont

The Piedmont physiographic province in Maryland occupies approximately 2500 square miles or roughly 1/4 of the state (Vokes and Edwards, 1974). The Piedmont occupies portions or encompasses fully the following counties: Frederick, Montgomery, Carroll, Howard, Baltimore, Harford, and Cecil. The Piedmont is bounded by the other two recognized physiographic regions in Maryland---to the east, the Coastal Plain Province and to the west, the Appalachian Province. The physiography of the Piedmont is characterized by broad undulating topography with low knobs and ridges together with numerous stream valleys which incise the rolling topography.

Two divisions, eastern and western, of the Piedmont Province have been differentiated based on their underlying geology (Vokes and Edwards, 1974). In the eastern division, the underlying geology is a complex series of metamorphic rocks (i.e., gneisses, slates, phyllites, serpentines) and granitic (gabbroic) rocks. In the western division, the underlying geology is dominated by a series of metamorphic rocks in its easterly portion, but less strongly metamorphosed than in the eastern division. The larger western portion of the western division is underlain by Cambro-Ordivician (geologic ages representing 600 $\pm$ 20 to 440 $\pm$ 10 mya) limestone which are folded but have not recrystallized to form marble and upon which lie, with

pronounced angular unconformity, red Triassic (a geologic age representing 225 ± 5 to 180 ± 5 mya) sandstones, siltstones, and shales. This collection of Triassic sandstones, siltstones, and shales is called the Newark Group.

Two formations comprise the Newark Group: 1) the upper Gettysburg formation which is composed mainly of sandstone and associated siltstone and shale, and 2) the lower New Oxford formation which is composed mainly of shale and associated sandstone and siltstone (Fisher, 1964; Vokes and Edwards, 1974). Following deposition of these sediments, dikes of diabase composition intruded upon these Triassic sediments and pre-Triassic metamorphic rocks and occur sporadically throughout the province. These dikes, however, are more abundant in the western division than in the eastern division or the Appalachian province.

Geographical Extent of Triassic Basins in the USA

Triassic-aged basins occur in the Mid-Atlantic region of the USA extending somewhat linearly from North Carolina through central Virginia and Maryland and then arcing through southeastern Pennsylvania and central New Jersey before extending northward into the Connecticut Valley and the Acadian area (Figure 1-1). These basins are the result of tensional forces created during the breakup of the supercontinent Pangaea II at the start of the Triassic

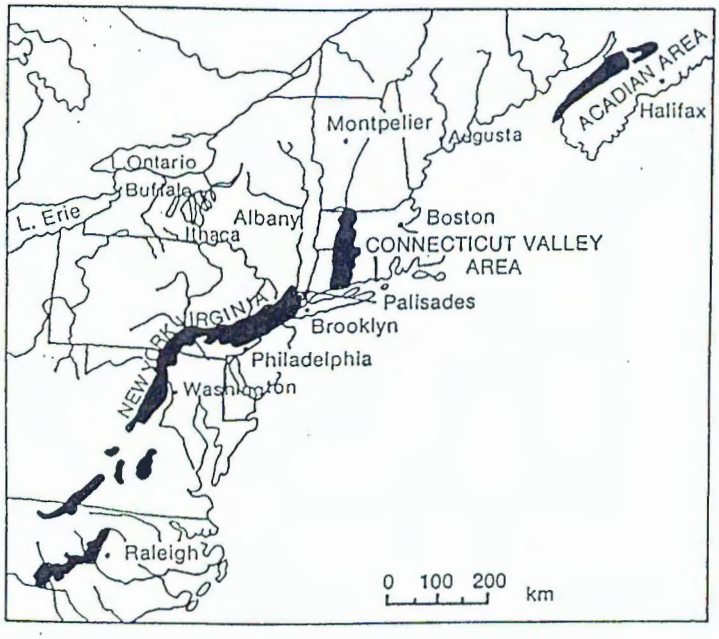

Figure 1-1. Location of Triassic Basins occurring along the Mid-Atlantic USA. After Levin (1978).

Period (Levin, 1978). Infilling of alluvial sediments into each basin subsequently occurred, resulting in the deposition of the Newark Group of sediments.

The Culpeper Basin in Maryland is but one member in this series of basins. A portion of this particular basin occurs in the Piedmont physiographic province of central Maryland and occupies portions of western Montgomery county, extends as a narrow discontinuous belt trending SSW to NNE in central Frederick county, and finally extends into northwestern Carroll county. Through reconnaissance survey by the current author, the dominant geologic parent material of this basin is dusky red shales with lesser amounts of fine-grained sandstone comprising the Newark Group of red Triassic sediments.

Description of MD Soil Series Developed from the Newark Group

The Penn series is defined as a well-drained to somewhat excessively drained, droughty to very droughty, moderately shallow to very shallow soil which occurs on the upland topographic positions. Penn soils are considered to be immature soils because they show only minor profile development (Matthews, 1960). The Penn series is classified as a fine-loamy, mixed, mesic Ultic Hapludalf.

The Readington series is closely associated with the Penn series but is less well-drained, more deeply weathered, and has a higher moisture-supplying capacity than the Penn

series (Matthews, 1960). This series occurs in upland flats and has its drainage restricted internally by the presence of a fragipan within the solum. The Readington series is classified as a fine-loamy, mixed, mesic Typic Fragiudalf.

The Croton series is defined as a poorly-drained, shallow to moderately deep, well-developed soil which occurs in upland flats, depressions, and near heads of drains. Its drainage is also restricted internally by the presence of a fragipan. In Montgomery County, this series is believed to be partly colluvial in nature with downwashing of surface material from the adjacent and slightly higher Penn, Lewisberry, Readington, and Bucks soils (Matthews et al., 1961). The Croton series is classified as a fine-silty, mixed, mesic Typic Fragiaqualf.

The Abbottstown series is very similar to the Croton series, but it is slightly better-drained and is in the fine-loamy particle-size family. It also occurs in depressions and on broad upland flats like the Croton series as well as having its drainage restricted internally by the presence of a fragipan. The Abbottstown series is classified as fine-loamy, mixed, mesic Aeric Fragiaqualf.

The Bucks series is similar to the Penn series, but has a deeper solum. This series also is well-drained and occurs in similar landscape positions as the Penn series. The Bucks series, however, has a lower base status than the Penn

series. The Bucks series is classified as a fine-loamy, mixed, mesic Typic Hapludult.

The Lewisberry series is defined as somewhat excessively-drained, shallow, sandy soil that has weak subsoil development. This series commonly occurs on uplands, near the Penn and Klinesville series. Because of their drainage, they have a low moisture-supplying capacity. The Lewisberry series is classified as a coarse-loamy, mixed, mesic Ultic Hapludalf.

The Klinesville series is defined as gently sloping to very steep, reddish brown soil that is shallow (the most shallow soils in Carroll county) and droughty. This series is often associated with the Penn and Lewisberry series but contains less silt than the Penn series and less sand than the Lewisberry series. Also, the Klinesville series has no argillic horizon. The Klinesville series is therefore classified as a loamy-skeletal, mixed, mesic, Lithic Dystrochrept.

Previous Investigations on Soils Developed from Triassic Rocks

Only two soil investigations on soils developed from these Triassic red beds occurring in the Piedmont Province of the Mid-Atlantic region of the United States have been found to date. The first, McCracken et al. (1964), compared mineralogically similar soils occurring on very different parent materials in the North Carolina Piedmont.

The soil series which they studied were the Iredell and the White Store. The Iredell and White Store series both have very high smectite contents in B horizons underlying thin A horizons, thereby promoting restricted internal drainage. The Iredell series is formed from mafic igneous rocks such as diorite, whereas the White Store series is derived from Triassic Basin sediments. These researchers found that both of these soils shared similar physical properties but not chemical properties. The White Store soils were found to have high exchangeable acidity whereas the Iredell series was found to have high exchangeable bases via the weathering of the mafic parent material. They also found that exchangeable magnesium levels exceeded exchangeable calcium levels in the B horizons and attributed this possibly to the release of magnesium from the octahedral sheets in montmorillonite. Additionally, the relatively low concentrations of free iron in the solum of the White Store series was apparently due to the low iron content in the parent material and/or loss of iron through leaching following episodes of reduction. The Iredell series is classified as a Typic Hapludalf whereas the White Store series is classified as a Vertic Hapludalf.

The second investigation examined soil and saprolite characteristics of Vertic and Aquic Hapludults in the Triassic Basin of North Carolina (Griffin and Buol, 1988). Specifically, these researchers examined a White Store

(fine, mixed, thermic Vertic Hapludalfs) and a Creedmoor (clayey, mixed, thermic Aquic Hapludults) soil. The White Store soil was derived from weathered, red, fine sandstone whereas the Creedmoor soil was derived from a coarse-grained gray sandstone. Mineralogically, the two parent materials have similar mineral constituents, including quartz, feldspars, muscovite mica, chlorite, and smectite. The White Store soil, however, contained more chlorite and much less feldspar than the Creedmoor soil. This was attributed to increased weathering in the White Store soil. Both soils had smectite as their dominant clay mineral. Due to the differing amounts of mineral precursors for smectite formation in both soils, two differing modes of smectite formation were suggested in these soils: neogenetic smectite via the weathering of ferro-magnesian minerals in the Creedmoor soils and transformation smectite via chlorite intermediates in the White Store soil. Kaolinite is most abundant in the argillic horizons of both soils and possibly formed from acid attack of randomly interstratified smectite in overlying horizons or from feldspar weathering. Iron oxide mineralogy was not discussed in this investigation.

The parent materials in these two studies are different from those within the Triassic Culpeper Basin of Maryland and thus are responsible for the morphological differences in the soils derived from these two parent materials. The

dominant parent material for soils of the Culpeper Basin is red shale whereas red fine sandstone is the parent material for the White Store series. The fine sandstone appears to have a higher feldspar content than that of the shale. The difference in the weatherable mineral content of these parent materials as well as climatic differences favor increased authigenic clay formation within the soils of the southern basins and thus allow for greater expression of the argillic horizon as compared to the soils of the Culpeper Basin in Maryland.

Soil Color

The color of soils is perhaps the first soil property one observes when examining soils. Because of this innate bias common to all of us, the writers of Soil Taxonomy (Soil Survey Staff, 1975) have relied heavily upon easily identifiable physical properties, such as soil color, in the formation of this morpho-genetic classification scheme. For example, the definitions for the epipedons and some diagnostic subsurface horizons have color requirements. Reliance on the absence or near absence of color (Munsell chroma $\leq$ 2) is found within the classification scheme at both the subgroup and suborder levels. Therefore, a grasp of the factors which influence the soil color is important in terms of understanding the classification and genesis of soils.

Soil color is the result of the interaction of both the inorganic and organic soil coloring agents. Organic material often accumulates within the uppermost layers or horizons within the soil and tends to "paint" the soil brown to black due to the thin coating of the dark organic material upon the inorganic soil particles. The dominant inorganic coloring agents in soils are iron oxides, manganese oxides, calcium carbonate, and the color of mineral grains themselves (i.e. glauconite is green; jarosite is straw yellow, etc). Iron and manganese oxides persists in well-aerated soils whereas calcium carbonate persists in soils within sub-humid and drier regions of the world. Due to the relative importance of the various iron oxides towards the coloration of the B and C horizons in the soils within the Mid-Atlantic region, only these coloring agents will be further discussed concerning their mineralogy and stability.

The term "iron oxides" is actually a misnomer because not only true iron oxides but also iron oxyhydroxides are often included within this group of minerals. I will use the term "iron oxides" throughout this review and dissertation to mean all oxyhydroxides and oxides of iron, regardless of their degree of crystallinity.

There are four prevalent crystalline forms of iron oxides observed in soils. They are hematite (α-Fe_2O_3), goethite (α-FeOOH), ferrihydrite ($5Fe_2O_3*9H_2O$), and

lepidocrocite (γ-FeOOH). Goethite and lepidocrocite are polymorphs (i.e. same chemical composition but different structure) with goethite considered the more stable of these two polymorphs (Schwertmann and Taylor, 1989). Ferrihydrite is considered a precursor to its more stable cousin, hematite (Schwertmann and Taylor, 1989).

Pure end members of each of these iron oxides yield a color commonly associated with that particular mineral. Pure hematite often exhibits reddish hues (5YR and redder), perhaps even purplish with increasing particle size, and is considered the strongest pigmenting agent among the iron oxides (Schwertmann and Taylor, 1989). Torrent et al. (1983) and Schwertmann et al. (1982) both observed the impact of the pigmenting power of hematite by noting the change from yellow to red hues when only a small proportion of hematite was incorporated in a goethite-rich soil. Goethite commonly exhibits yellower hues (7.5YR and yellower). Lepidocrocite is commonly associated with an orange color such as 7.5YR 6-7/4-8 (Fitzpatrick et al., 1985) whereas ferrihydrite exhibits colors similar to hematite. Ferrihydrite and hematite can be distinguished by both mineralogical and chemical analyses.

Because of the widespread occurrence and dominance of both hematite and goethite among soil iron oxides, several researchers have come to correlate red colors with a higher proportion of hematite to goethite whereas yellower colors

are correlated with a high proportion of goethite to hematite (Bigham et al., 1978; Schwertmann et al., 1982). Quantification of hematite has even been successful based upon the Munsell hue, value, and chroma of the material through the application of artificial redness ratings as suggested by Hurst (1977) and Torrent et al. (1980, 1983)

As the name implies, iron oxides persist in a well-aerated soil. Upon reduction, iron oxides become unstable and are susceptible to total dissolution if the episode of reduction is prolonged. Once in soluble form, Fe^{2+} either is leached away or reprecipitates in oxygenated areas. If these soil coloring agents are dissolved and removed, the neutral colors associated with uncoated mineral grains (mainly quartz) left behind are exhibited. Because in soils, Fe and Mn reduction is associated with the hydrological conditions, soil scientists and mappers rely on the depth at which these low-chroma neutral colors occur to assess the depth of the seasonally-high water table. In most soils which contain iron oxides, this wetness-induced reduction of iron oxides is indeed correlated to the depth of the seasonally high water table (Latshaw and Thompson, 1968; Veneman et. al, 1976; Franzmeier et. al, 1983). However, soils derived from parent materials whose iron oxide mineralogy exists solely as hematite appear less apt to form redoximorphic features associated with wetness-induced reduction (Niroomand and Tedrow, 1991). Possible

mechanisms responsible for this reluctance to form redoximorphic features from such sediments are discussed below.

Inhibition of Redoximorphic Features in Red Sediments

The morphological properties of soils have been commonly used to evaluate the relative "wetness" or drainage class of various soils. It has become known from field soil scientists (Carl Robinnette, SCS, personal communication) that soils derived from red parent materials (such as those in the Triassic Culpeper Basin of Maryland) are problematic in terms of assessing their drainage class, because these soils seem less apt to show the morphological features associated with a given degree of wetness (redoximorphic features such as gleying, low chroma mottling, Fe/Mn nodules, etc.). The absence of commonly identifiable redoximorphic features in wet soils may cause erroneous interpretations regarding the suitability of these soils for agricultural, engineering, or environmental uses. This could have serious ramifications for homeowners such as failure of septic systems, wet basements and foundations, or may result in erroneous delineation of wetlands.

This inhibition of gleying phenomena of red sediments was recently demonstrated in a three-month incubation study involving red C-horizon material and glucose even though incipient gley formation was observed in a gray shale after

only eight days of incubation (Niroomand and Tedrow, 1991). The researchers believed that the presence of hematite was responsible for the color stability of the red sediments during the incubation period. These soils, even under extended periods of water saturation, display few, if any, gleyic features.

Fey (1983) as stated by Schwertmann and Taylor (1989), using thermodynamic data to calculate the relative stabilities of the iron oxides, observed the effect of Al-substitution upon the thermodynamic stabilities of both hematite and goethite. He concluded that increasing Al-substitution in these iron oxides caused an increase in their stability relative to the end-member state for each iron oxide. In other words, the difficulty in forming gleyic features from red, hematite-rich, parent materials may also be due to the degree of isomorphous substitution of Al for Fe within the structure of hematite. The structure of hematite can withstand approximately 16 mole % Al as Al_2O_3 in Fe_2O_3 whereas the structure of goethite can withstand approximately 33 mole % Al as AlOOH in FeOOH (Schwertmann and Taylor, 1989).

Langmuir and Whittemore (1971), also relying upon thermodynamic data, found that for equal particle sizes less than 76 micrometers, hematite is more stable than goethite. Their data essentially confirms the reluctance of soils or parent materials which contain hematite as a fine-grained

soil coloring agent to exhibit gleyic features (Niroomand and Tedrow, 1991).

Additionally, differences in the crystal structures of hematite and goethite suggests that goethite is more susceptible to reduction due to exposed OH^- groups rather than only O^{2-} groups at crystal edges (Schwertmann and Taylor, 1989).

Because the current morphological criterion for wet soils is based upon the reduction and segregation of iron oxides, information on the stability of each iron oxide, the factors which control their stability, and possible transformations between the various iron oxides are essential for understanding soil color phenomena and gleyic feature development.

Stability of Iron Oxides in the Soil Environment

Based upon derived thermodynamic data and assuming aerobic conditions, goethite is considered the most stable iron oxide in the soil environment (Schwertmann and Taylor, 1989). Its solubility product (expressed as pFe + 3pOH) is slightly greater (pk = 43.3-44.0) than that of hematite (pK = 42.2-43.3) but is orders of magnitude greater than the solubility products for both lepidocrocite (pk = 40.6-42.5) and ferrihydrite (pk = 37.0-39.4). These stability constants are dependent upon particle size and are responsible for the range of stabilities associated with

each iron oxide (Langmuir and Whittemore, 1971).

Another factor which influences the relative stabilities of the iron oxides is the degree of aluminum substitution within each iron oxide (Fey, 1983). The observed increase in stability by Al-substitution may be caused simply by the fact that aluminum is not an element affected by redox activity and thus as more of the structure becomes infused with aluminum, the structure becomes increasingly desensitized to episodes of reduction. Because soil goethites often have a higher proportion of aluminum substitution than soil hematites, they should, at a given pH, then be more stable than hematite. Thus, if both hematite and goethite coexist, hematite should preferentially dissolve via episodes of reduction prior to the presumably greater Al-substituted goethite. A morphological color change from red hues associated with hematite to the yellow hues associated with the coexisting goethite should therefore result. This argument has been used successfully to explain pedogenic yellowing in soils derived from red sediments in Brazil where both hematite and goethite coexist in the parent material (Macedo and Bryant, 1987, 1989; Bryant and Macedo, 1990).

Another factor which modifies the stability of the less-crystalline and less stable iron oxides is the adsorption of both inorganic ions or organic molecules onto their surfaces. Schwertmann and Cornell (1972) and Cornell

et al. (1987) demonstrated that the transformation of ferrihydrite to goethite and\or hematite was strongly inhibited by the adsorption of silicate species. These researchers believe that the adsorption of silicate species onto the surface of the ferrihydrite stabilizes the ferrihydrite by linking the particles into an immobile network and retards the nucleation stage of the transformation. A similar inhibitory effect on this transformation was observed for manganese (Cornell and Giovanoli, 1987). The effect of aluminum on the formation of the various iron oxides has also been extensively studied by Schwertmann and others (Schwertmann et al., 1979; Taylor and Schwertmann, 1978, 1980; and many others).

Cornell (1985) observed the inhibitory effect on the transformation of ferrihydrite to goethite or hematite by organic molecules. He showed that all simple sugars ($\geq 10^{-4}$ M) retard the transformation to some degree but that the molecular geometry of the organic species also affects the extent of the transformation. He found that this inhibitory steric effect is most prevalent in acyclic molecules rather than cyclic molecules.

These above-mentioned factors which influence the relative stabilities of each iron oxide are either predicted by thermodynamics or determined by field-simulated laboratory studies. This next section will address the soil factors governing the conditions needed for iron oxide

instability and transformations. Particular attention will be focused upon topohydrosequences where hydrologic differences associated with topographic differences may cause iron oxide transformations to be manifest as redoximorphic features in these soils.

Soil Color Differentiation along Topohydrosequences

Several investigations concerning soil color differentiation along topohydrosequences have been reported in the literature. In these papers, the authors commonly address the conditions required for color differentiation, such as the soil moisture regime and conditions necessary for iron reduction. Specifically, five main ideas are commonly addressed, namely 1) soil moisture regime, 2) topo-hydrological effects on the soil redox status, 3) conditions necessary for iron reduction, 4) influence of iron reduction and drainage on soil color, and 5) morphological indicators of wetness. The current ideas on these five areas are summarized below.

Soil Moisture Regime

The moisture regime of any soil must be known prior to the classification of that soil. There are currently five moisture regimes defined by Soil Taxonomy (Soil Survey Staff, 1975), namely the aquic, udic, ustic, xeric, and aridic moisture regimes. Each covers a broad range of soil

moisture levels, but demonstrate increasing soil dryness in the order listed above. In Maryland, both the aquic and udic moisture regimes are observed. Because of their importance to Maryland soils, a brief description of each of these two moisture regimes is warranted.

The aquic moisture regime is often the moisture regime of "wet" soils where saturated conditions persist in the profiles of these soils. However, the definition of the aquic moisture regime is very vague:

"...implies a reducing regime that is virtually free of dissolved oxygen because the soil is saturated by groundwater or by water of the capillary fringe. An aquic moisture regime must be a reducing one. ..." (Soil Survey Staff, 1990).

In this definition, the duration of the saturation episode is not stated. Also, organic matter, microorganisms, and temperatures greater than biologic zero are needed for reduction. A problem arises in that the definition is based upon the reduction and removal of dissolved oxygen, while the morphological criterion of low chroma colors indicative of the aquic moisture regime requires that iron, not oxygen, be reduced.

Two approaches are often employed in the determination of the aquic moisture regime. The first method relies upon

in-situ monitoring of water table levels. This method is laborious and time-consuming, but direct measurements of the water table height and chemistry can be made. The second method infers the occurrence of saturation and reduction from the presence of low-chroma gleying or mottling within the solum. This method is commonly used by field personnel to discern soil wetness.

Because of the vague definition of the aquic moisture regime, the International Committee on the Aquic Moisture Regime (ICOMAQ) suggests abandoning the concept of the aquic moisture regime in favor of "aquic conditions". In fact, aquic conditions have been approved and will replace the concept of the aquic moisture regime in the next updated version of Keys to Soil Taxonomy. Aquic conditions are now defined by considering episodes of saturation (characterized by zero or positive pressure within the soil-water matrix) and reduction (by direct measurement of redox potentials or by field tests employing either 1% potassium ferric cyanide or 0.2% α'-α'-dipyridyl solution in 10% acetic acid to detect the presence of ferrous iron) in addition to the occurrence and location of redoximorphic features (gleying and associated high chroma mottling, low-chroma mottling, and Fe/Mn nodules). Aquic conditions are permitted at any depth within the soil profile (ICOMAQ, 1989).

Two subcases of aquic conditions are epiaquic and endoaquic conditions. For the epiaquic case, aquic

conditions occur due to the accumulation of meteoric water above an impermeable layer thereby forming a perched water table. If this perched water table persists, then episodes of reduction will follow those of saturation and result in the formation of redoximorphic features. For the endoaquic case, aquic conditions occur due to the occurrence of a true shallow groundwater table within the solum. If this water table persists, then episodes of reduction will follow those of saturation and result in the formation of redoximorphic features.

A less vague definition is stated for the udic moisture regime than for the aquic moisture regime:

"...implies that in most years the soil moisture control section is not dry in any part for as long as 90 days (cumulative). ...In addition, the udic moisture regime requires, except for short periods, a three-phase system, solid-liquid-gas, in part, but not necessarily in all, of the soil when the soil temperature is above 5°C. ...Water moves down through the soil at some time in most years. ..." (Soil Survey Staff, 1990).

Topo-hydrological Effects on the Soil Redox Status

Franzmeier et al. (1983) observed the heights of the water tables in well-drained soils with brownish B-horizons were not greatly different from those in somewhat poorly-drained soils with grayish B-horizons. Their results imply

that saturation without concomitant reduction will not influence the color or the associated redox status of the soil.

Evans and Franzmeier (1986) found that the topographic position of the soils influences water table heights and chemistries. They arrived at two conclusions: 1) Soils on shoulders and backslopes also had higher levels of dissolved oxygen in the soil water than soils on the swales, and 2) the grayest soils had less than 1 mg/L dissolved oxygen for significant periods, and that from the grayer to the browner soils the duration of saturation decreased. They attributed these differences in dissolved oxygen along the toposequence to either slope steepness (because as slope steepness increases, the velocity of lateral movement within the soil is expected to increase, which may cause the higher dissolved oxygen content of the soil water at the shoulder and backslope positions) or oxygen consumption due to reduction processes in the lower landscape positions.

Because dissolved oxygen should be reduced before iron, investigators often find that anaerobic conditions occur for longer periods than those favorable for iron reduction. Vepraskas and Wilding (1983) observed this relationship for soils on the upper landscape positions. Soils on the lower landscape positions, however, usually have longer periods of reduction than saturation. They attributed this difference to differences in water table recharge along the various

hillslope elements of the toposequence (i.e. water table recharge in the upper landscape positions mainly from oxygenated meteoric water whereas water table recharge in the lower landscape positions has a component of deoxygenated water via subsurface lateral flow from the upper landscape positions).

Pickering and Veneman (1984) observed that microtopography (concave versus convex slopes) also affects the incidence and duration of soil saturation, and therefore, microtopography may be important in the development of gleyic features.

Iron Reduction

When a soil is saturated, atmospheric oxygen is excluded and initially aerobic microbes consume the remaining dissolved oxygen. Once the soil becomes depleted of oxygen, anaerobic microbes dehydrogenate or oxidize organic matter and donate electrons to reduce nitrate, manganese, iron, sulfate, or other oxidized systems (Jenny, 1980). Thus, the factors necessary for iron reduction are a) organic matter, b) population of microbes, c) periodic exclusion or limited diffusion of oxygen, and d) soil temperature above biologic zero (5°C). Soil temperature, though, can be affected by drainage. Pickering and Veneman (1984) observed that in well-drained soils of central Massachusetts, a wider soil temperature range occurs

throughout the year with soil temperatures at 50 cm depth reaching freezing during the year. In the more poorly-drained soils, the soil temperature at 50 cm depth is buffered from climatic extremes by the high specific heat of water and keeps the soil temperature above biologic zero throughout the year. This enables iron reduction to be possible even in the winter. Obviously, the geographical location of the soils would influence this temperature range in both well-drained and poorly-drained soils, as poorly-drained soils in tundra areas would be frozen for a significant portion of the year.

The soil pH also affects the reduction of iron oxides. For example, the reduction of goethite is described by the following equation:

$$FeOOH + e^- + 3H^+ \longrightarrow Fe^{2+} + 2H_2O$$

In this example, both protons and electrons are required for the reduction of goethite. This equation, as well as others involving various redox phases, are shown plotted in Figure 1-2 and is constructed using thermodynamic data. As shown in the figure, lower Eh values (i.e. redox potentials) are required for iron reduction with increasing pH. Thus, neutral or basic soils will tend to retard the reduction of iron oxides more so than acidic soils at a given pe level.

Influence of Iron Reduction and Soil Drainage on Soil Color

Soil color and mottling features are considered visual

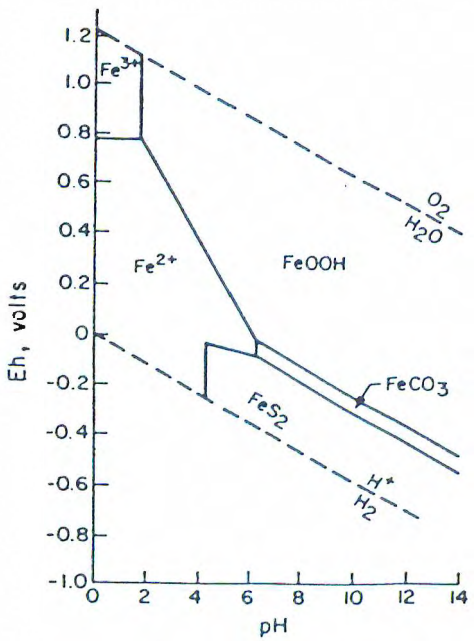

Figure 1-2. Graph of Eh vs pH for various iron phases. From Bohn et al. (1985).

evidence of the effects of soil wetness which have been caused by the oxidation, reduction, and translocation of free oxides, primarily iron (Simonson and Boersma, 1972). The dominant factor affecting hue is the hydration state of the iron oxides with red hues implying better drainage and yellow hues implying poorer drainage (Simonson and Boersma, 1972). This may be related to the type of iron "oxide" present as unhydrated hematite is red in color while the hydrated goethite is yellow in color (Schwertmann and Taylor, 1989).

Franzmeier et al. (1983) found for some Indiana soils from various particle-size families that depth to "often saturated conditions" could be better predicted from the depth to $\leq$ 3 chroma mottles and that depth to high chroma mottles could be used to predict the depth to "seldom, if ever, saturated" conditions. These researchers also found that saturated conditions occur for longer periods in somewhat poorly-drained soils than in the better drained soils during the spring and early summer. This longer saturation period when soils are warm could help explain why somewhat poorly-drained soils are grayer than their better drained counterparts which may have equally high water tables during other times (i.e. colder times) of the year.

Morphological Indicators of Wetness

The two most common morphological indicators of wetness

are the occurrence of mottling and concretions within a soil profile. Simonson and Boersma (1972) found that depth to faint and distinct mottling is strongly correlated to a high degree of waterlogging. Soil Taxonomy (Soil Survey Staff, 1975) utilizes low chroma (≤ 2) mottling as an indicator of prolonged soil wetness. According to some, high chroma mottling may be related to the depth of "seldom, if ever, saturated" conditions (Franzmeier et al., 1983).

Simonson and Boersma (1972) also believe that both the size and occurrence of concretions decreases from the poorly drained to better drained soils and that the concretions occur mainly in the A, E, and B horizons of the poorly-drained soils. According to Schwertmann and Fanning (1976) and Richardson and Hole (1979), the best area for concretion formation is in the somewhat poorly drained areas where alternating wetting/drying and oxidation/reduction occur at a greater frequency.

Besides matrix and mottle colors, other morphological features reported by some to be indicators of wetness include low chroma ped coatings or a sequum of an albic horizon over an argillic horizon. Zobeck and Ritchie (1984) caution against relying upon low chroma ped coatings to determine the moisture regime because coatings do not have to be saturated for as long a time in order to form as do low chroma mottles, so they should be evaluated differently when assessing drainage conditions. Simonson and Boersma

(1972) believe that a sequum of an albic horizon overlying an argillic horizon is correlated to and results from perched water tables, whereby the water sits upon the upper boundary of the argillic horizon and removes the soil color coatings of the albic horizon, resulting in a color given by the uncoated mineral grains themselves. Albic horizons were not observed during the reconnaissance survey of this study; however, some similar features have been described as E' horizons over fragipans in New England (Dr. Martin Rabenhorst, personal communication).

Indicators of wetness may also be on the microscopic level. The presence of channel neoalbans and neoferrans as well as coatings may provide insight into the redox behavior at the scale of individual peds.

Assessment of the Literature Review and Statement of Research Questions

This review has provided information regarding the stability of the various iron oxides in the soil environment and the effect that these oxides have upon the soil color. As this review has demonstrated, some researchers and field soils scientists have observed a retardation effect on the development of redoximorphic features in soils derived from red Triassic sediments (Niroomand and Tedrow, 1991; Carl Robinnette, personal communication). This apparent reluctance in these sediments to form such features which are comparable to their hydrological status has even been

accounted for in the waiving of several color requirements for the classification of both wet Ultisols and Alfisols in Soil Taxonomy (Soil Survey Staff, 1990). On the other hand, the Croton series (Typic Fragiaqualf), which is reported to be derived from red Triassic sediments, has been traditionally delineated at the footslope topographic positions in Maryland (Matthews, 1960; Matthews et al., 1961). This delineation is based upon the observation of well expressed redoximorphic features within the upper solum of these soils. Based upon these two conflicting observations, the following three questions may be asked: 1) What soil properties, other than hydrology may be responsible for the coloration patterns of the soils on these landscapes?, 2) Is there in fact an inhibitory effect on the development of redox-related features in soils formed from Triassic parent materials?, and 3) What is the relationship between the hydrology and the development of redoximorphic features in the soils derived from these rocks?

The overall objective of this research is then to understand the development of redox-related morphologies within soils derived from red Triassic sediments. The following five chapters of this dissertation will examine these three questions and identify the factors responsible for the coloration patterns of these soils.

CHAPTER 2

THE OCCURRENCE OF HEMATITE IN THE SHALES OF THE TRIASSIC CULPEPER BASIN OF MARYLAND

Triassic-aged basins (ca 180-225 mya) occur along the mid-Atlantic USA extending somewhat linearly from North Carolina through central Virginia and Maryland and then arcing through southeastern Pennsylvania and central New Jersey before extending northward into the Connecticut Valley (Figure 1-1). These basins are the result of the tensional forces created during the breakup of the supercontinent Pangaea II during the late Triassic Period (Levin, 1978). Infilling of alluvial sediments into each basin subsequently occurred, resulting in the deposition of sandstones, siltstones, and shales.

The Culpeper Basin of Maryland is but one member in this series of basins. A portion of this particular basin occurs in the Piedmont physiographic province of central Maryland and occupies portions of Montgomery, Frederick, and Carroll counties (Figure 1-1). Through reconnaissance survey, the dominant geologic parent material of this basin is known to be dusky red shale with lesser amounts of fine-grained sandstone.

By x-ray analysis, Fisher (1964) has shown hematite as the only iron oxide in one shale sample of the Culpeper Basin in Maryland. This finding is certainly rare because reportedly iron oxides often coexist with each other in most parent materials (Schwertmann and Taylor, 1989). The objective of this paper is to determine the mineralogical makeup of rocks in the Triassic Culpeper Basin of Maryland,

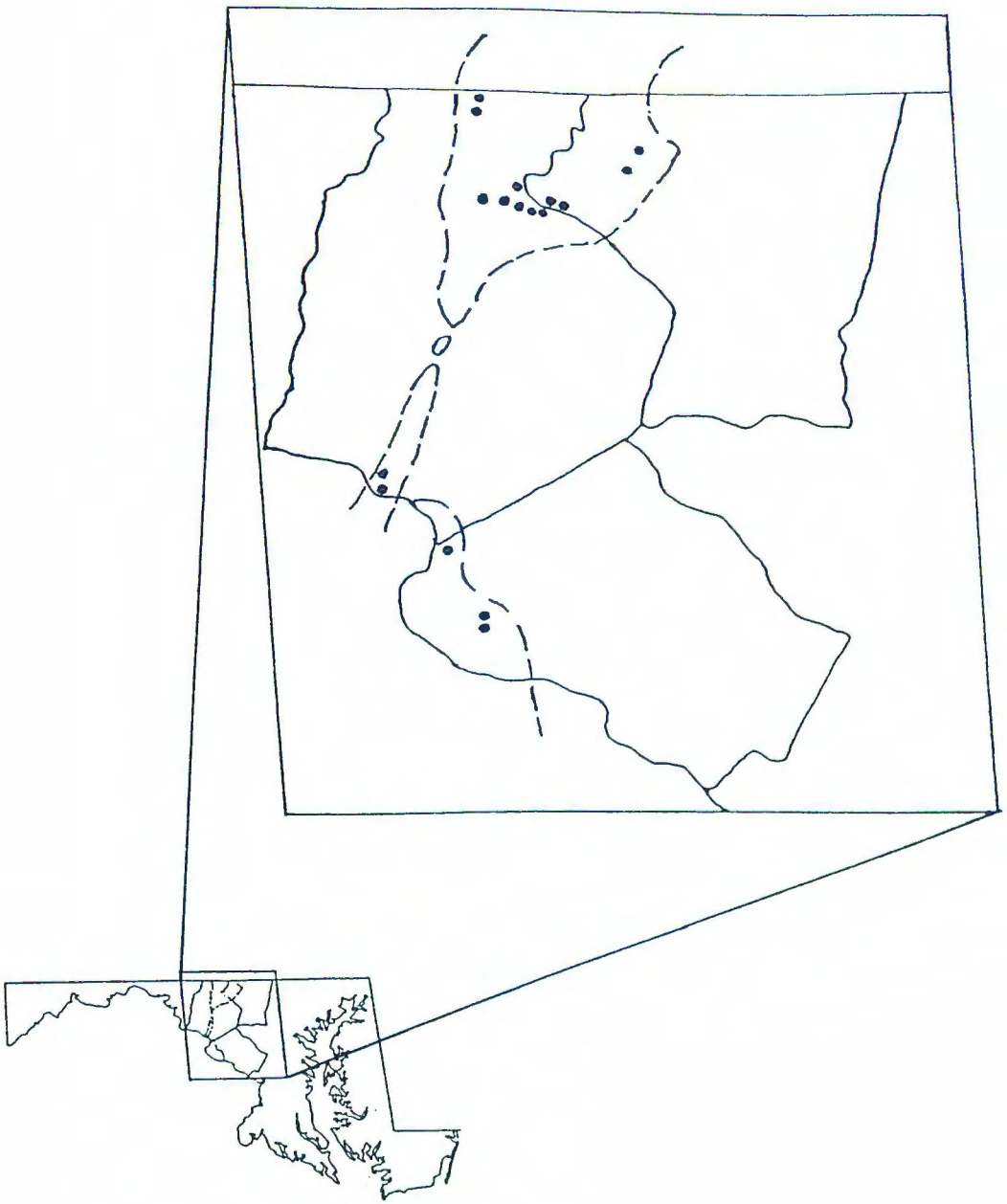

Figure 2-1. Map showing location of sampling sites within the Culpeper Basin of Maryland.

with particular emphasis on the nature of the iron oxide(s) within these shales.

Materials and Methods

Seventeen shales were sampled from roadcuts and outcrops throughout the Culpeper Basin in Maryland (Figure 2-1). All of these shales had a "dusky-red" color which had colors of 5YR 4/4 (reddish brown), 5YR 3/4 (dark reddish brown), or 2.5YR 4/4 (reddish brown). Representative fragments of each shale sample were ground in a percussion mortar and pestle prior to final grinding in a ball mill mixer for five minutes. A subfraction of the ground shale was also fractionated (using 5% Na_2CO_3 as the dispersing agent) into clay and nonclay fractions without prior removal of Fe or Si cements. This was done to determine the size partitioning of the iron oxide(s).

Chemical analyses on the ground shales were performed to both quantify the iron oxide(s) present and to determine the crystallinity of these iron oxide(s). These analyses included a) sodium dithionite citrate buffer extraction (Kittrick and Hope, 1963) on the ground whole shales and its clay/nonclay fractions, and b) acid ammonium oxalate extraction in the dark (Schwertmann, 1964) on the ground whole soils. Dithionite-extractable iron (Fe_d) is a measure of the total free iron oxide content of a sample, independent of its crystallinity, whereas oxalate-

extractable iron (Fe_o) is generally considered to measure only the poorly-crystalline or amorphous forms of iron oxides (Mehra and Jackson, 1960; Schwertmann, 1964). Additionally, total digestion following dithionite removal of the iron oxides (Fe_t) was performed to determine the quantity of non-DCB extractable iron sources such as ilmenite and iron-silicates. This was accomplished following a modification of Lim and Jackson's (1982) procedure, using HNO_3, H_2SO_4, and 30% H_2O_2 replacing concentrated $HClO_4$. Dithionite-extractable iron was determined by x-ray spectroscopy (Fanning et. al., 1970). Dithionite-extractable Al as well as oxalate and residual Fe were determined by atomic absorption spectroscopy.

X-ray diffraction (XRD) was utilized to determine the mineralogy of the shales. Slides were prepared using a slurry of ground shale and 95% ethanol. X-ray diffraction following the 5M NaOH treatment was also performed on the clay fraction to determine the iron oxide mineralogy of the shales (Norrish and Taylor, 1961). Additional silica was not added to block any iron oxide transformations during this treatment due to the abundance of silicate minerals in these soils (Kampf and Schwertmann, 1982). These slides were prepared using the filter membrane peel technique of Drever (1973). All XRD was performed using CuK alpha radiation from a Norelco diffractometer equipped with a graphite monochromator and a theta-compensating slit. Scans

were run over a range of 2-45° two-theta using a scan rate of 2° two-theta per minute.

Results and Discussion

In general, the shales possess a resistant mineralogy. The silicate fraction consists dominantly of quartz and muscovite, lesser amounts of kaolinite and chlorite, and with minor levels of both sodium plagioclase and potassium feldspar. The only iron oxide observed by XRD in all the shales is hematite, Fe_2O_3 (Figure 2-2). The fact that only one iron oxide exists in this parent material basin-wide is certainly rare, as coexistence of iron oxides is the usual case in iron oxide-containing parent materials (Schwertmann and Taylor, 1989).

Results of the chemical analyses are consistent with the sole occurrence of hematite in these shales. Dithionite-extractable iron (Fe_d) ranges between 13 and 30 g/kg for all shale samples and far exceeds the Fe_o levels, thereby suggesting that the iron oxides within the shales are of a well-crystalline nature (Table 2-1). Levels of residual iron are approximately equal to that of Fe_d and may be due to iron from the chlorite. Levels of Al substitution within the hematite range from 1.8 to 17.7 mole % and averages 7.8 mole %. Such levels of Al-substitution may induce the hematite occurring within these parent materials to be far more resistant to redox processes than its pure

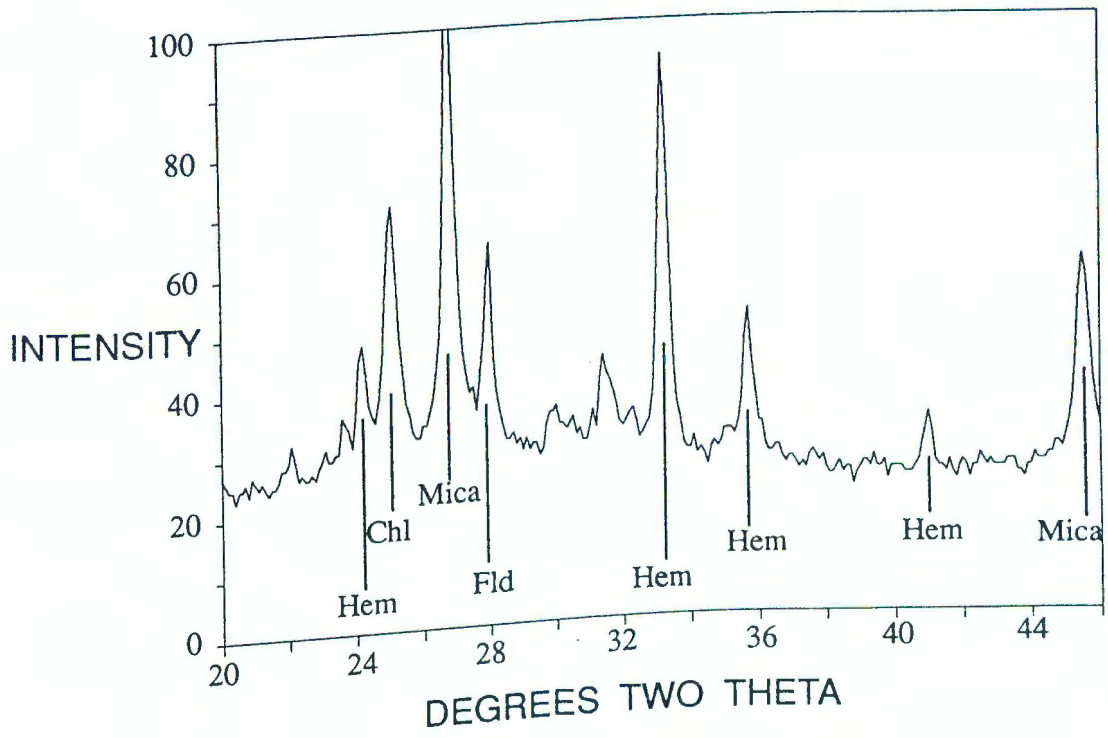

Figure 2-2. X-ray diffractogram following 5M NaOH treatment (Norrish and Taylor, 1961) of a typical red Triassic shale. Hem=hematite, Chl=chlorite, and Fld=feldspar.

Table 2-1. Iron and Aluminum Chemistry of the Triassic Shales.

County	Number of Samples	Fe_d	Fe_o	Fe_t	Clay	Fe_d in Clay	Al_2O_3 in Fe_2O_3
		<----g/kg soil--->				<-----%---->	mole%
Carroll	4	18-26	0-1	20-38	7-11	20-25	2-6
Frederick	10	13-30	0-2	9-29	4-19	14-57	4-18
Montgomery	3	16-28	0-1	17-31	2-8	14-16	2-8
Average =		21	1	20	8	23	8
Standard Dev. =		5	<1	5	4	13	4

end-member (Fey, 1983).

Results of the iron oxide size partitioning show that the iron oxides associated with the clay fraction accounts for 14 to 57% of the total free iron oxides in the shales, with 15% to 35% typically observed (Table 2-1). Thus, hematite may dominate in the clay fraction of some shales but it is often associated with the silt and/or sand fractions of the shales. These low clay-sized percentages may be due to the ineffectiveness of 5% Na_2CO_3 to disperse iron-cemented aggregates and in fact could be higher if more complete dispersion was achieved. Because thermodynamics favor the formation of goethite over hematite, and because in Maryland soils hematite forms only rarely relative to goethite (Schwertmann and Taylor, 1989), this monomineralic iron oxide parent material provides an opportunity to examine iron "oxide" transformations in the soils derived from these parent materials. The results of such an examination are presented in Chapter 5.

CHAPTER 3

PARENT MATERIAL UNIFORMITY OF THE SOILS

Residual soils may be defined as those soils formed from "unconsolidated, weathered, or partly weathered mineral material that only accumulates by disintegration of bedrock in place" (Hawley and Parsons, 1980). In Maryland, soils of the Penn and Readington series have been considered residual soils and are the respective well-drained and moderately well-drained members of a three member catena which have been traditionally delineated by landscape position. The third member, the Croton series, is considered poorly-drained and located either in upland flats or near the heads of drains. The Croton series is believed to have colluvial debris from erosion of the adjacent and slightly higher Penn and Readington series mixed within its profile and thus is not considered a truly residual soil (Matthews et al., 1958). The bedrock underlying these three soil series is dusky red shale and sandstone of the Triassic Newark Group.

During morphological examination of these soils, several rounded quartz gravels and cobbles were observed throughout the solum of the pedons in the footslope and toeslope positions. Additionally, yellower surface matrix hues (7.5YR or yellower) and greater pedogenic development (i.e. greater expression of the argillic horizon and more intricate upper solum coloring patterns) were observed within the pedons occupying the footslope or toeslope positions. In contrast, the soils occupying the backslope, shoulder, or summit landscape positions lacked any evidence

of such quartz gravels and cobbles throughout their solum, possessed redder hues (5YR or redder) associated with the surface matrix colors, and lesser pedogenic development.

The rounded quartz cobbles could not have been produced via the weathering of the underlying bedrock and thus possibly represent a colluvial/alluvial component to these soils. The more yellow/less red surface matrix colors overlying red parent materials associated with the Croton series may represent the inclusion of loess or some other material (alluvium, colluvium, or mixed) within the upper soil horizons. Loess additions to soils throughout the Coastal Plain (Wright, 1972; Foss et al., 1978) and Piedmont of Maryland (Rabenhorst, 1978; Darmody, 1980) have previously been reported.

The objectives of this paper therefore are to determine whether significant loessal or colluvial/alluvial additions have occurred along two topohydrosequences principally derived from and overlying the red sedimentary rocks of the Triassic Culpeper Basin of Maryland, and if so, to what extent these additions have impacted the morphology and genesis of these soils.

Materials and Methods

Eleven pedons located along two topohydrosequences (THS) were examined in this study. One THS was located in northern Frederick county (FC site) near the town of

Emmittsburg and the other THS was located in western Montgomery county (MC site) near the town of Boyds. Site locations are shown elsewhere (Figure 4-1).

Along these two THS pedons were described and sampled using standard techniques from either back-hoe or hand-dug soil pits at selected elevational breaks. Five pedons were examined along the transect at the MC site and six pedons were examined along the transect at the FC site. Each pedon was classified according to Soil Taxonomy (Soil Survey Staff, 1990). Composite samples from each horizon were collected and used for basic soil characterization analyses.

To evaluate the lithologic uniformity of the soil, particle size distributions were examined. The sand fractions were isolated through wet sieving and the silt fractions were fractionated by repeated centrifugation. Particle size analysis was done using the pipette method (Gee and Bauder, 1986). Following oven drying at 105°C, the sand and silt fractions were then crushed for 5 minutes within a ball mill mixer. Duplicate pellets for each fraction for every horizon were prepared from the ground samples. A 1:1 ratio by weight of the sample to the boric acid was used for all pellets. Pellets were made by pressing each sample at 20000 psi for 30 seconds. Each pellet was then stored in a desiccator prior to analysis for Ca, K, Ti, and Zr using x-ray spectroscopy. Pellets were also prepared from NIST samples 76, 77, 78, 102, 198, 199

for standards.

Results and Discussion

Occurrence of Lithologic Discontinuities

Each pedon along both THS show silty-textured A and upper B horizons overlying more sandy-textured sediments of the lower B, C, and R horizons (Table 3-1). Typically, the upper silty horizons within each pedon have textures of silt loam, silty clay loam, or loams which overlie textures of loam or sandy loam. A higher percentage of the total silt fraction as fine silt (20 to 2 um) generally occurs within the silty-textured horizons. The coarse silt fraction (50 to 20 um), however, becomes a more dominant fraction of the total silt fraction in the more sandy-textured BC, C, and R horizons. The intimate association between the shale and sandstone members which comprise these red sediments may explain the occurrence of sandy horizons found within the sola of most pedons (Vokes and Edwards, 1974; Fisher, 1964). Evaluations of lithologic discontinuities based solely upon textural variations in these shale-derived soils, however, is inconclusive because the silty-textured horizons may simply represent a product of the weathering of the shale and thereby account for the occurrence of the silty-textured horizons in the upper solum of each pedon.

Table 3-1a. Results of particle size analysis for the MC site.

Sample	Sand	C. Silt	F. Silt	Total Silt	C. Clay	F. Clay	Total Clay	CF >2mm
	<--------------------			%			-------------------->	
MC1 A	34.4	14.4	33.5	47.8	10.3	7.5	17.7	1.7
MC1 Ap	29.5	18.2	33.8	52.0	11.5	7.0	18.5	3.6
MC1 Btg1	15.9	18.6	32.0	50.6	17.8	15.7	33.5	0.0
MC1 Btg2	35.3	9.9	26.2	36.1	14.6	14.0	28.6	0.7
MC1 Btg3	25.9	12.2	31.6	43.8	16.1	14.2	30.3	0.0
MC1 2BC	59.2	18.2	14.1	32.3	3.8	4.7	8.5	13.0
MC2 A	35.1	16.0	29.6	45.6	10.9	8.4	19.3	0.7
MC2 Ap	35.6	17.4	29.4	46.7	10.6	7.0	17.7	2.9
MC2 Btg	23.1	8.5	33.2	41.7	19.2	16.0	35.2	0.1
MC2 Bx1	31.1	14.9	35.6	50.4	10.3	8.1	18.4	0.0
MC2 Bx2	22.7	29.1	30.2	59.3	11.5	6.6	18.1	0.0
MC2 2BC	70.4	12.9	9.8	22.7	5.5	1.4	6.9	1.5
MC2 3BCg	17.2	31.7	35.0	66.6	10.4	5.7	16.1	4.1
MC3 Ap	42.0	21.4	21.8	43.2	11.1	3.6	14.7	1.6
MC3 Bt	35.7	18.2	20.0	38.2	15.6	10.4	26.0	0.3
MC3 Bx1	44.9	11.2	22.5	33.8	12.9	8.5	21.4	0.2
MC3 Bx2	33.6	13.0	29.8	42.8	12.0	11.7	23.7	0.1
MC3 Bx3	36.9	32.3	18.1	50.4	5.8	6.9	12.7	0.6
MC3 2BCg	51.4	18.0	23.7	41.6	4.4	2.6	7.0	0.4
MC3 3Cr	62.6	17.3	12.3	29.6	3.9	3.9	7.8	7.5
MC4 Ap	18.7	30.5	33.6	64.2	12.5	4.7	17.1	4.8
MC4 Bt1	20.0	18.8	37.9	56.7	15.8	7.5	23.3	0.7
MC4 Bt2	23.6	28.5	29.5	57.9	8.0	10.5	18.5	4.1
MC4 Btx1	37.4	23.1	24.9	48.0	10.4	4.2	14.6	32.8
MC4 Btx2	42.7	14.8	25.5	40.3	12.5	4.4	17.0	55.8
MC4 Cr	51.3	10.7	26.2	36.9	9.4	2.4	11.9	45.1
MC5 Ap	50.1	13.9	24.4	38.3	8.5	3.1	11.6	1.2
MC5 Bt1	43.6	11.4	26.1	37.5	13.2	5.7	18.9	0.6
MC5 Bt2	54.1	10.2	19.3	29.4	11.9	4.6	16.5	1.1
MC5 BC	67.4	8.6	11.7	20.2	9.8	2.6	12.3	0.0
MC5 C1	73.4	6.1	7.5	13.6	7.3	5.6	12.9	0.0
MC5 2C2 up	31.9	38.3	18.3	56.6	6.5	4.9	11.4	0.1
MC5 2C2 lo	23.1	44.6	23.0	67.7	5.6	3.6	9.2	30.9
MC5 3R	69.1	14.8	10.4	25.2	3.2	2.5	5.7	72.1

Table 3-1b. Results of particle size analysis for the FC site.

Sample	Sand	C. Silt	F. Silt	Total Silt	C. Clay	F. Clay	Total Clay	CF >2mm
	<--------------------			%				-------------------->
FC1 Ap	29.3	8.4	36.1	44.5	17.2	8.9	26.1	4.2
FC1 Btg1	11.2	6.4	36.0	42.4	29.1	17.2	46.3	0.3
FC1 Btg2	8.9	4.3	28.0	32.3	30.4	28.5	58.8	0.2
FC1 2BC	18.3	11.5	37.3	48.7	20.1	12.9	33.0	0.7
FC1 3BC	72.7	8.3	10.1	18.4	5.6	3.2	8.9	1.0
FC1 4BCg1	78.7	5.7	8.7	14.4	4.3	2.6	6.9	0.0
FC1 4BCg2	69.1	6.6	9.8	16.3	7.9	6.7	14.6	0.0
FC1 4BCg3	47.8	9.2	22.0	31.2	12.7	8.3	21.0	3.8
FC1 5Cr	69.2	5.2	14.4	19.5	8.3	3.0	11.3	36.0
FC1A Ap	22.4	11.9	40.4	52.3	16.7	8.6	25.3	1.9
FC1A Bt1	10.4	11.6	33.4	45.0	26.3	18.3	44.6	0.2
FC1A Bt2	14.9	11.5	35.2	46.7	20.7	17.7	38.4	0.6
FC1A 2Bxup	27.2	14.6	32.9	47.5	15.5	9.8	25.2	4.3
FC1A 2Bxlo	39.4	15.8	27.4	43.2	12.4	5.0	17.5	19.3
FC1A 2Cr	58.3	7.8	20.6	28.4	8.4	4.9	13.3	56.3
FC2 Ap	19.4	17.0	36.8	53.8	17.7	9.2	26.8	2.8
FC2 BE	12.6	15.6	35.3	50.8	22.5	14.1	36.6	0.7
FC2 Bt	12.1	15.5	35.0	50.4	19.9	17.5	37.5	0.4
FC2 2Bx	39.4	8.0	31.2	39.2	12.9	8.4	21.3	5.7
FC2 2BC	38.8	7.8	28.9	36.7	15.7	8.8	24.5	0.4
FC2 3Crt	55.5	10.3	17.7	28.0	10.8	5.6	16.5	36.6
FC3 Ap	17.3	18.9	47.5	66.4	14.4	1.9	16.2	4.7
FC3 BA	26.9	16.2	40.6	56.8	14.1	2.2	16.3	8.5
FC3 Bt1	26.2	24.7	32.1	56.9	13.9	3.1	16.9	4.0
FC3 Bt2	22.4	27.8	26.6	54.4	17.4	5.9	23.2	2.3
FC3 Bt3	36.4	24.5	20.0	44.5	14.2	4.9	19.1	28.0
FC3 2Crt	40.2	35.1	14.1	49.2	8.7	2.0	10.7	55.4
FC4 Ap	32.4	20.8	29.5	50.2	13.5	3.9	17.4	10.1
FC4 Bw1	43.3	9.7	27.7	37.4	15.2	4.1	19.3	20.5
FC4 Bw2	40.1	19.0	20.7	39.7	14.6	5.7	20.3	6.8
FC4 BC	53.9	11.3	19.2	30.5	11.1	4.5	15.6	21.8
FC4 Cr	47.5	21.5	18.4	39.9	9.7	2.9	12.6	48.0

Table 3-1b (cont). Results of particle size analysis for the FC site.

Sample	Sand	C. Silt	F. Silt	Total Silt	C. Clay	F. Clay	Total Clay	CF >2mm
	<--------			-------%--------				------->
FC5 Ap	29.1	31.1	27.4	58.4	9.9	2.6	12.5	26.4
FC5 Bt1	37.7	22.3	22.5	44.8	13.2	4.3	17.5	41.5
FC5 Bt2	26.2	26.2	21.4	47.6	16.2	10.0	26.2	31.4
FC5 Bt3	22.6	36.9	17.3	54.2	15.6	7.6	23.2	42.5
FC5 2BCt1	31.7	26.6	24.6	51.2	11.9	5.2	17.2	45.9
FC5 3BCt2	48.4	32.0	10.8	42.8	5.6	3.2	8.8	40.6
FC5 4Crt	54.6	16.6	16.6	33.2	9.7	2.5	12.2	76.8

Depth functions involving various particle size and total elemental analysis were examined to either confirm the field identification of the lithologic discontinuities or identify other possible discontinuities not identified in the field. These data are presented in figures 3-1 to 3-11. Similar approaches have been recommended by Brewer (1964) and adopted for use in loess studies of Maryland soils (Wright, 1972; Rabenhorst, 1978; Darmody, 1980).

Possible types of discontinuities which may be observed in these soils include a) different lithologic strata caused by the facies change between the red shale and sandstone members of the parent materials, b) loess or alluvium/colluvium overlying residuum, and c) mixture caused by colluviation of red materials. The first and third types would still exhibit red hues because the entire solum is dominantly residually-derived throughout whereas the second type would show stronger contrasts in color because the loess-affected upper sola would not be principally derived from the underlying residuum.

FC Site

Pedon FC1 Appropriate data for this pedon are shown in Figures 3-1a to 3-1h. Abrupt changes in the clay-free particle size distribution (Figure 3-1b) were observed at the upper boundaries of the 2BC, 3BC, 4BCg, and 5Cr horizons. These discontinuities were further supported by

abrupt deviations in the depth functions of the sand/silt ratio and Zr concentration. The field identifiable lithologic discontinuity observed at the upper boundary of the 5Cr was based primarily upon variations in the coarse fragment and K concentration depth functions. The substantially higher clay content of the argillic horizon as compared to the pedons upslope (Table 3-1b) and the sharp contrast of yellowish horizons overlying red parent materials (Table 4-1, Appendix A) suggests that the upper solum discontinuity at 75 cm is the result of loessal or alluvial/colluvial debris added to this pedon. The lower discontinuities were field identifiable and interpreted as a facies change between the sandstone and shale members of the parent materials. These lithologic discontinuities were confirmed in the depth functions of the particle size distributions (Figures 3-1b and 3-1c).

Pedon FC1A Appropriate data for this pedon are shown in Figures 3-2a to 3-2h. A lithologic discontinuity at the upper boundary of the 2Bx horizon was observed for pedon FC1A. Abrupt changes in the depth functions of both K and Ti concentrations (Figures 3-2f and 3-2g) coupled with a sharp increase in the coarse fragment content (Figure 3-2d) at the upper boundary of the 2Bx horizon indicates a discontinuity at this depth. As in pedon FC1, the substantially higher clay content of the argillic horizon as compared with the pedons upslope (Table 3-1b) and the sharp

contrast of yellowish horizons overlying red parent materials (Table 4-1, Appendix A) suggests that this upper solum discontinuity is the result of loessal or alluvial/colluvial debris added to this pedon. Variations in the coarse fragment, K, and Ti depth functions occur at the upper boundary of the 3Cr horizon; however, due to a lack of supporting field evidence (Appendix A) recognition of a discontinuity at this depth is not warranted.

Pedon FC2 Appropriate data for this pedon are shown in Figures 3-3a to 3-3h. Abrupt changes in several textural depth functions (i.e. sand/silt ratio, clay-free PSD, coarse fragment content) coupled with deviations in the K and Ti concentrations indicates the presence of lithologic discontinuities at the upper boundaries of the 2Bx and 3Crt horizons. In contrast to pedon FC1 and FC1A, the stratification of yellowish horizons overlying red parent materials does not occur in pedon FC2 (Table 4-1, Appendix A). Red hues prevail throughout the profile of this pedon. The lower clay content of the argillic horizon (Table 3-1b) and the prevalence of red hues throughout the profile of pedon FC2 (Table 4-1, Appendix A) suggests that pedon FC2 is principally derived from residual materials. Therefore, the discontinuity observed at the upper boundary of the 2Bx horizon represents a mixture of colluvial debris with residual materials.

Pedons FC3, FC4, FC5 Appropriate data for each of these

pedons are shown in Figures 3-4a to 3-6h. Analysis of the four particle size and four elemental depth function curves for both pedon FC3 (Figures 3-4a to 3-4h) and FC4 (Figures 3-5a to 3-5h) indicate no upper solum discontinuities in either of these pedons. Variations in the fine silt/coarse silt ratio and Zr depth functions were observed at the BA/Bt boundary in pedon FC3; however, due to a lack of supporting evidence recognition of a discontinuity at this depth is not warranted. A sharp increase in the coarse fragment content within the 2Crt horizon in pedon FC3 corroborated the change in structure observed in the field (Appendix A) for this discontinuity. Because of the absence of any upper solum discontinuities, the lower clay contents typical of the higher pedon (Table 3-1b), and the prevalence of red colors throughout the profiles (Table 4-1, Appendix A), these two pedons are considered residual soils.

Lithologic discontinuities at the upper boundaries of the 2BCt1, 3BCt2 and 4Crt horizons for pedon FC5 were observed mainly from the particle size depth functions and from the depth functions of K and Ti (Figures 3-6a to 3-6h). The abrupt changes in these parameters suggests these variations represents a facies change characterized by differences in the texture and mica content of the shale and sandstone. Because of the absence of any upper solum discontinuities, the lower clay contents as compared to the loess-affected lower pedons (Table 3-1b), and the prevalence

of red colors throughout the profile (Table 4-1, Appendix A), pedon FC5 is considered a residual soil.

MC Site

Pedon MC1 Appropriate data for this pedon are shown in Figures 3-7a to 3-7h. Abrupt changes in several particle size depth functions (i.e. fine sand/coarse sand ratio, clay-free PSD, and coarse fragment content) indicates the presence of a lithologic discontinuity at the upper boundary of the 2BC horizon. Variations in the depth functions involving the sand and coarse fragment content at the upper boundary of the argillic horizon is probably due to the presence of both sand and gravel-sized Fe/Mn nodules at this boundary. The substantially higher clay contents of the argillic horizon as compared to the higher pedons (Table 3-1a) and the sharp contrast of yellowish horizons overlying red parent materials (Table 4-1, Appendix A) suggests that this discontinuity is the result of loessal or alluvial/colluvial debris added to this pedon.

Pedon MC2 Appropriate data for this pedon are shown in Figures 3-8a to 3-8h. Abrupt changes were observed at the upper boundaries of the 2BC and 3BCg horizons in several particle size depth functions (i.e. fine sand/coarse sand, clay-free PSD, and coarse fragment content) as well as in the depth functions involving the Ca and Zr concentration. These discontinuities probably represents a facies change

between the shale and sandstone members of the underlying parent materials. Variations in both the fine silt/coarse silt ratio and the fine sand/coarse sand ratio (Figure 3-8a) as well as the sand-sized Ti concentration at the upper boundary of the Bx1 horizon suggests a discontinuity at this depth, but their degree of contrast is considered too slight to warrant recognizing a discontinuity by horizon symbols. The loss of sharply contrasting materials at this depth may have resulted from mixing of any added components with residuum. The substantially higher clay contents of the argillic horizon as compared to the pedons upslope (Table 3-1a) and the sharp contrast of yellowish horizons overlying the red Bx1 horizon (Table 4-1, Appendix A) suggests that an upper solum discontinuity is present at the upper boundary of the Bx1 and is the result of loessal or alluvial/colluvial debris added to this pedon.

Pedon MC3 Appropriate data for this pedon are shown in Figures 3-9a to 3-9h. Abrupt changes in the fine sand/coarse sand ratio and the clay-free PSD depth functions indicates the occurrence of lithologic discontinuities at the upper boundaries of the 2BCg and 3Cr horizons. The reliance on textural changes to indicate these lower solum discontinuities suggests these discontinuities result from a facies change between the shale and sandstone members. No upper solum discontinuities were observed in this pedon and therefore this pedon is interpreted as a residual soil.

Pedon MC4 Appropriate data for this pedon are shown in Figures 3-10a to 10h. Analysis of the four particle size and four elemental depth distribution curves for pedon MC4 indicate no confirmed lithologic discontinuities within this pedon (Figures 3-10a to 3-10h). A variation in the depth function of the coarse fragment content was observed at the upper boundary of the Cr horizon; however, this discontinuity was not observed by any other parameter. These results confirm the absence of field identifiable lithologic discontinuities within this pedon. Because of the absence of any discontinuities, the lower clay contents as compared to the pedons downslope (Table 3-1a), and the prevalence of red colors throughout the profiles (Table 4-1, Appendix A), this pedon is considered a residual soil.

Pedon MC5 Appropriate data are shown for this pedon are shown in Figures 3-11a to 3-11h. Abrupt changes in the sand/silt ratio and the clay-free PSD depth functions as well as the depth functions involving the Ti and Zr concentrations were observed at the upper boundaries of the 2C2 and 3R horizons. These lower solum discontinuities represent the facies change between the shale and sandstone members of the parent materials. The absence of any upper solum discontinuities, the lower clay content of the argillic horizon as compared to the pedons downslope (Table 3-1a), and the prevalence of red hues throughout the profile (Table 4-1, Appendix A) suggests that this pedon is a

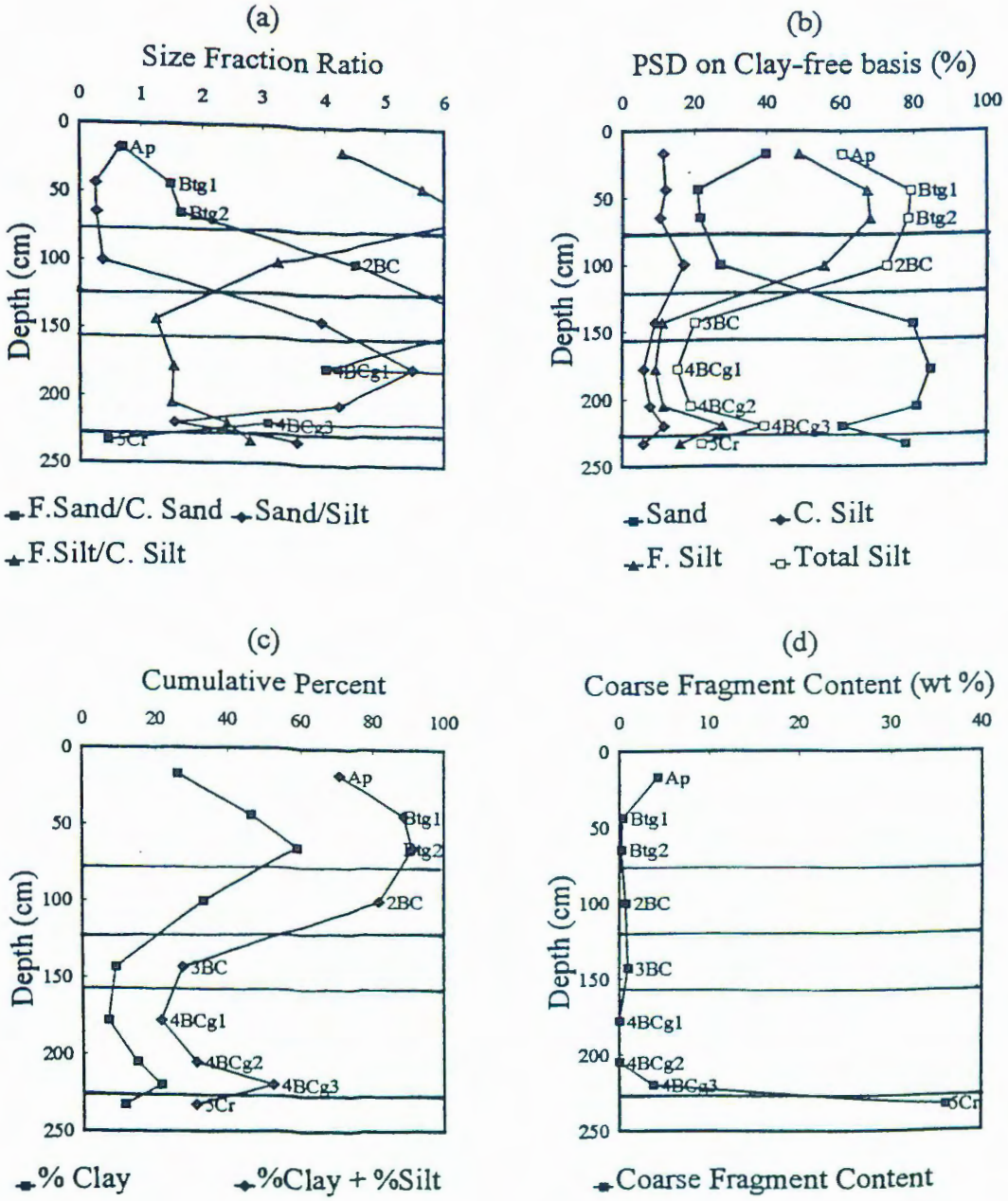

Figure 3-1. Depth functions for pedon FC1 of a) selected particle size ratios, b) PSD on clay-free basis, c) PSD with clay and d) coarse-fragment content. Discontinuities shown as solid horizontal lines. Variations shown as dashed horizontal lines.

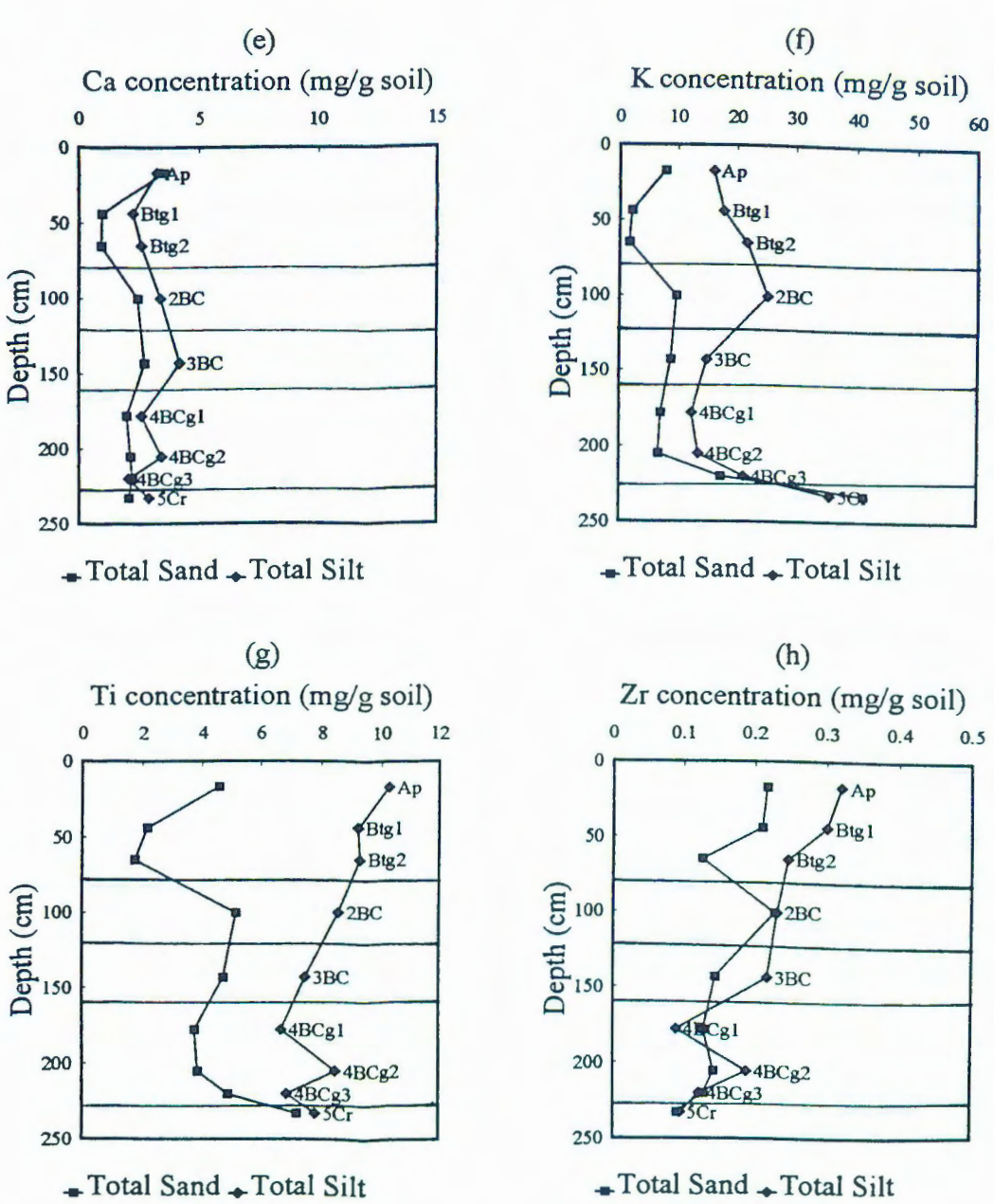

Figure 3-1. Depth distributions for pedon FC1 of e) % Ca, f) % K, g) % Ti, and h) % Zr. Discontinuities shown as solid horizontal lines. Variations shown as dashed horizontal lines.

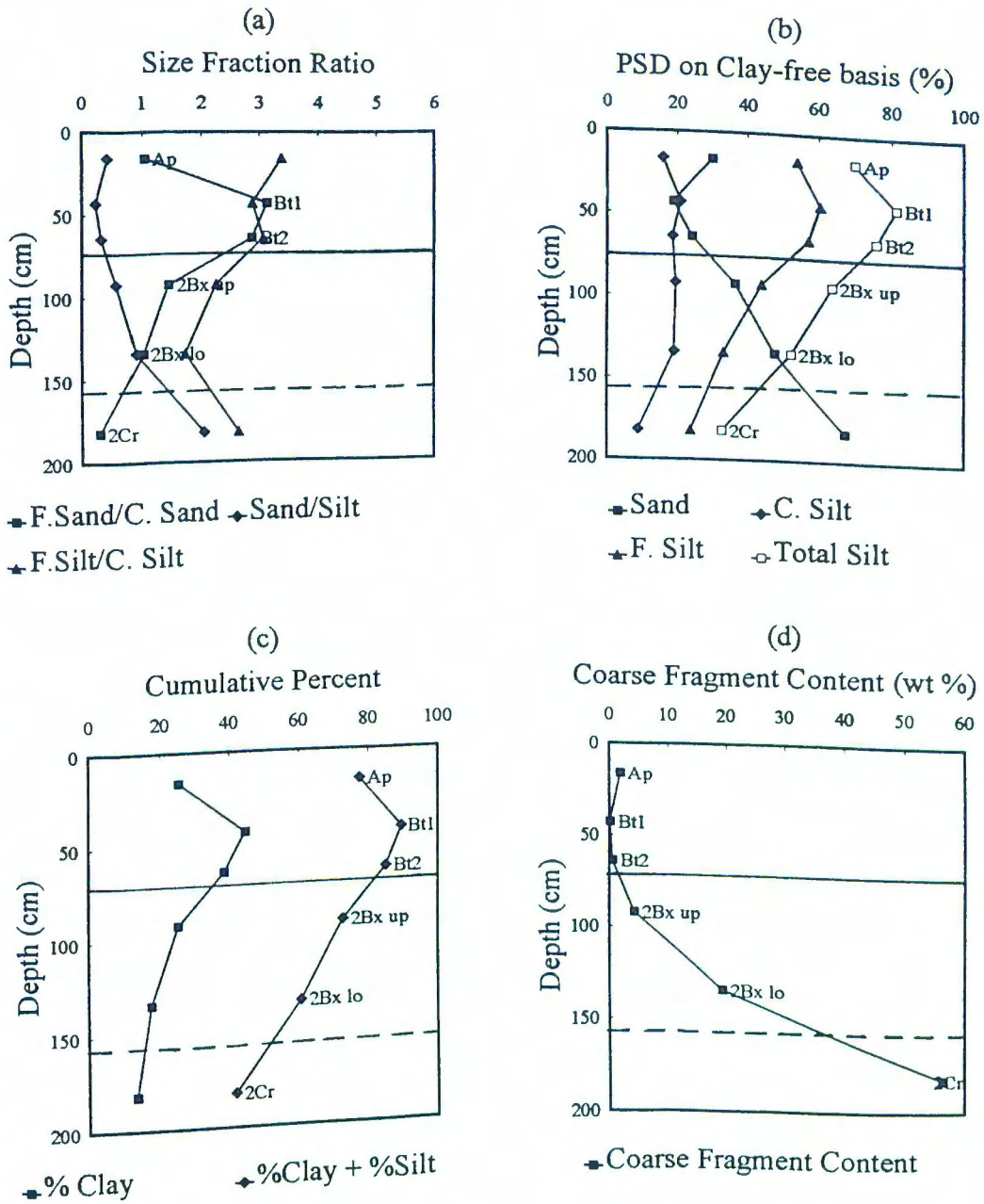

Figure 3-2. Depth functions for pedon FC1A of a) selected particle size ratios, b) PSD on clay-free basis, c) PSD with clay and d) coarse-fragment content. Discontinuities shown as solid horizontal lines. Variations shown as dashed horizontal lines.

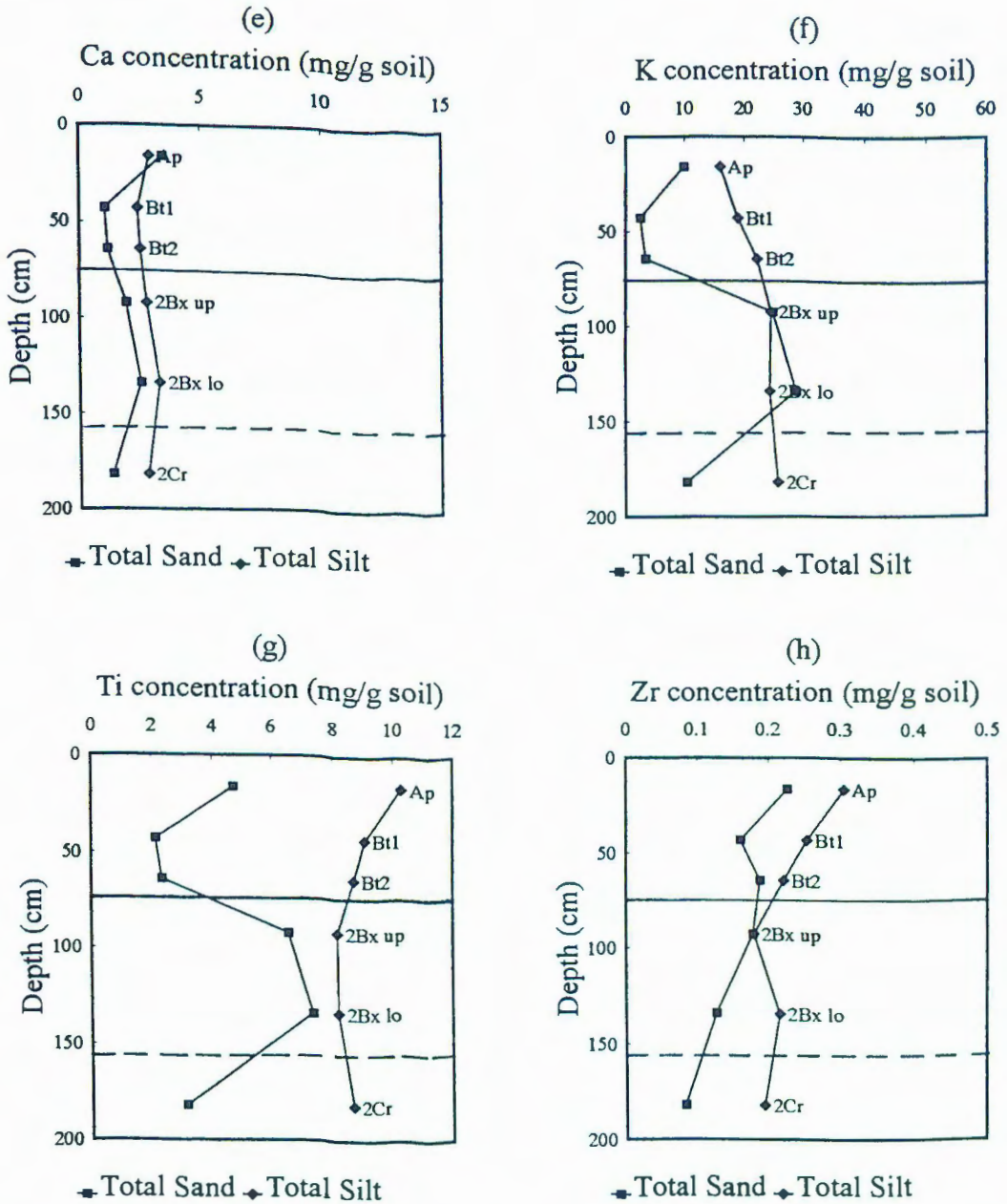

Figure 3-2. Depth distributions for pedon FC1A of e) % Ca, f) % K, g) % Ti, and h) % Zr. Discontinuities shown as solid horizontal lines. Variations shown as dashed horizontal lines.

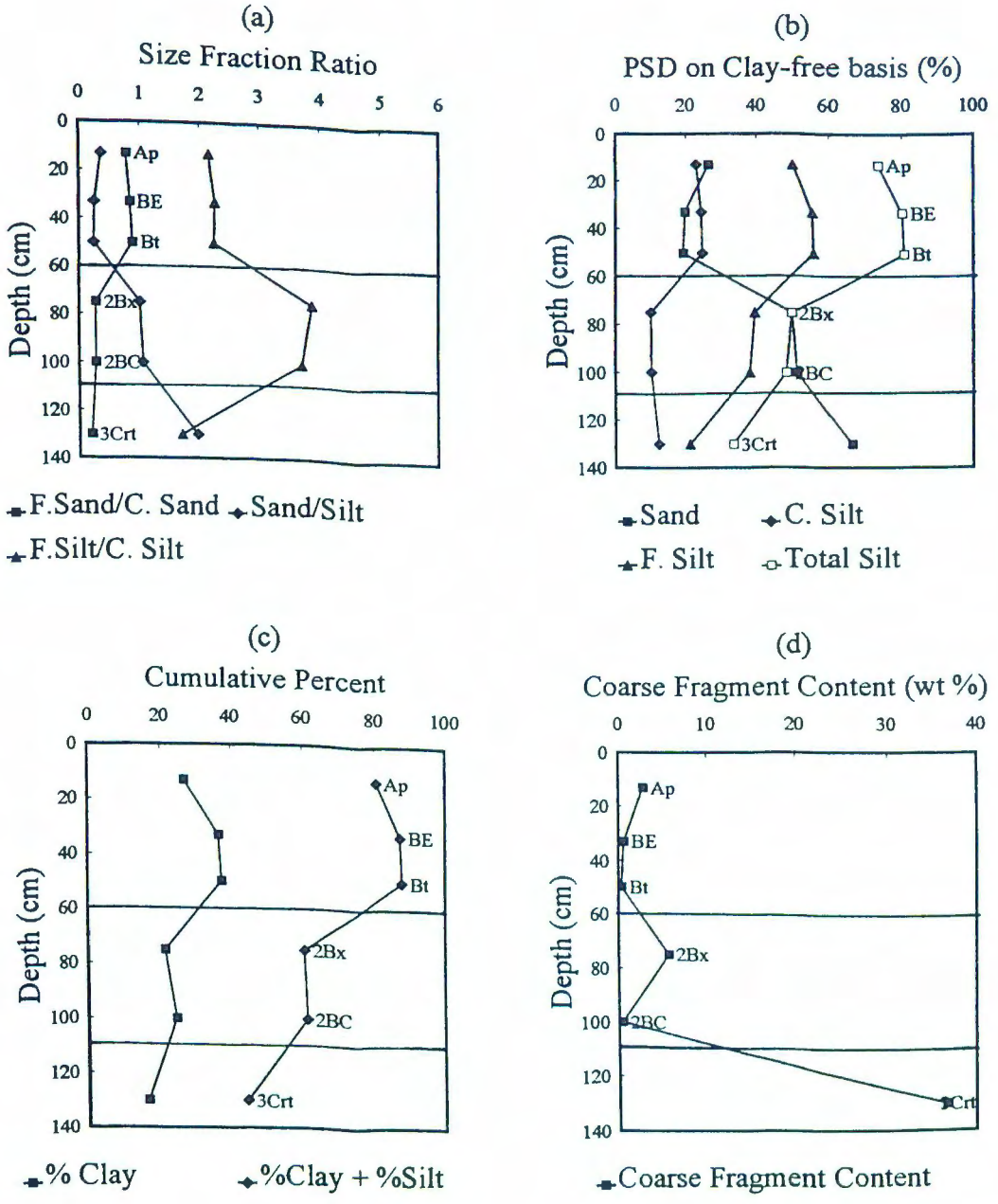

Figure 3-3. Depth functions for pedon FC2 of a) selected particle size ratios, b) PSD on clay-free basis, c) PSD with clay and d) coarse-fragment content. Discontinuities shown as solid horizontal lines. Variations shown as dashed horizontal lines.

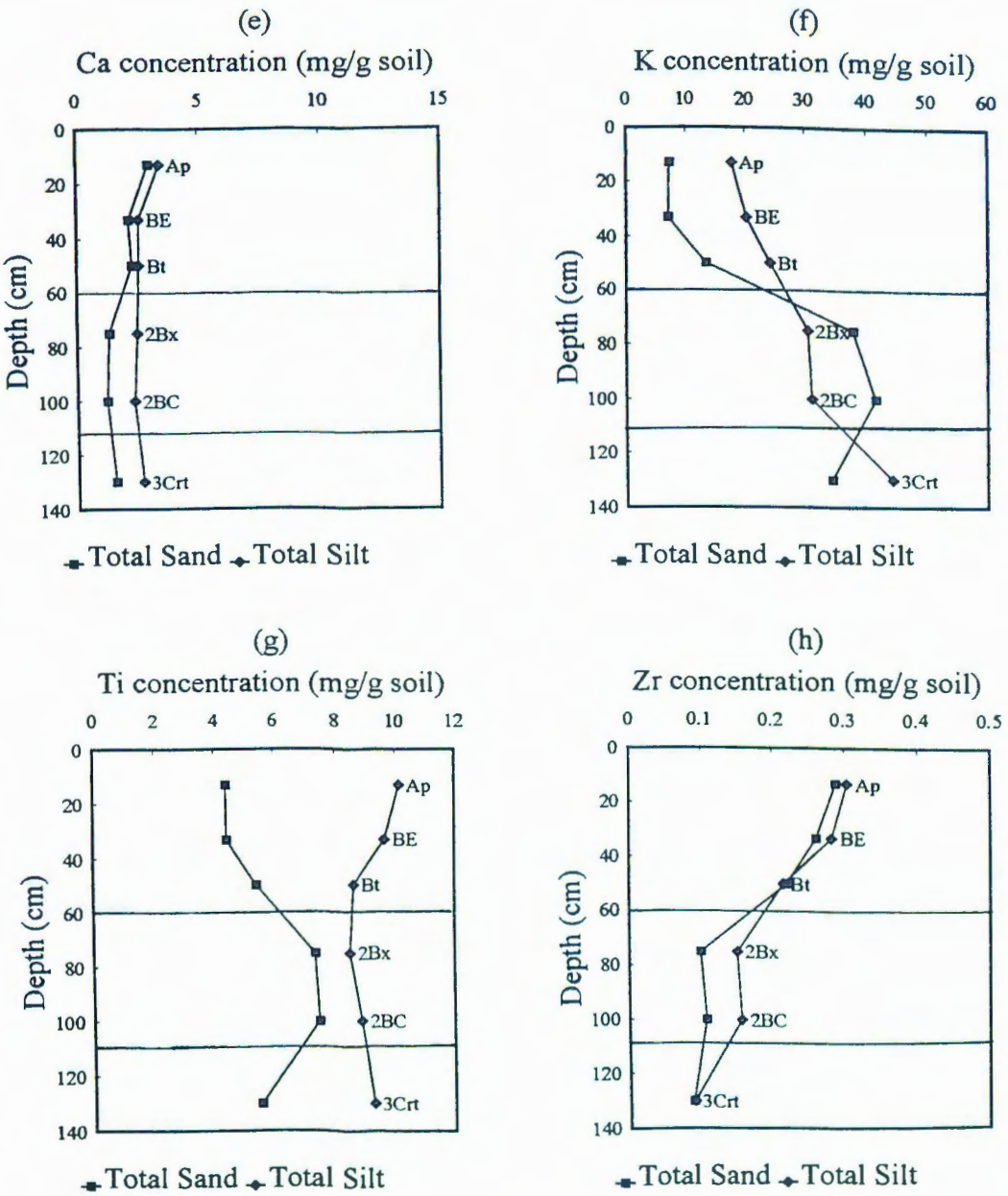

Figure 3-3. Depth distributions for pedon FC2 of e) % Ca, f) % K, g) % Ti, and h) % Zr. Discontinuities shown as solid horizontal lines. Variations shown as dashed horizontal lines.

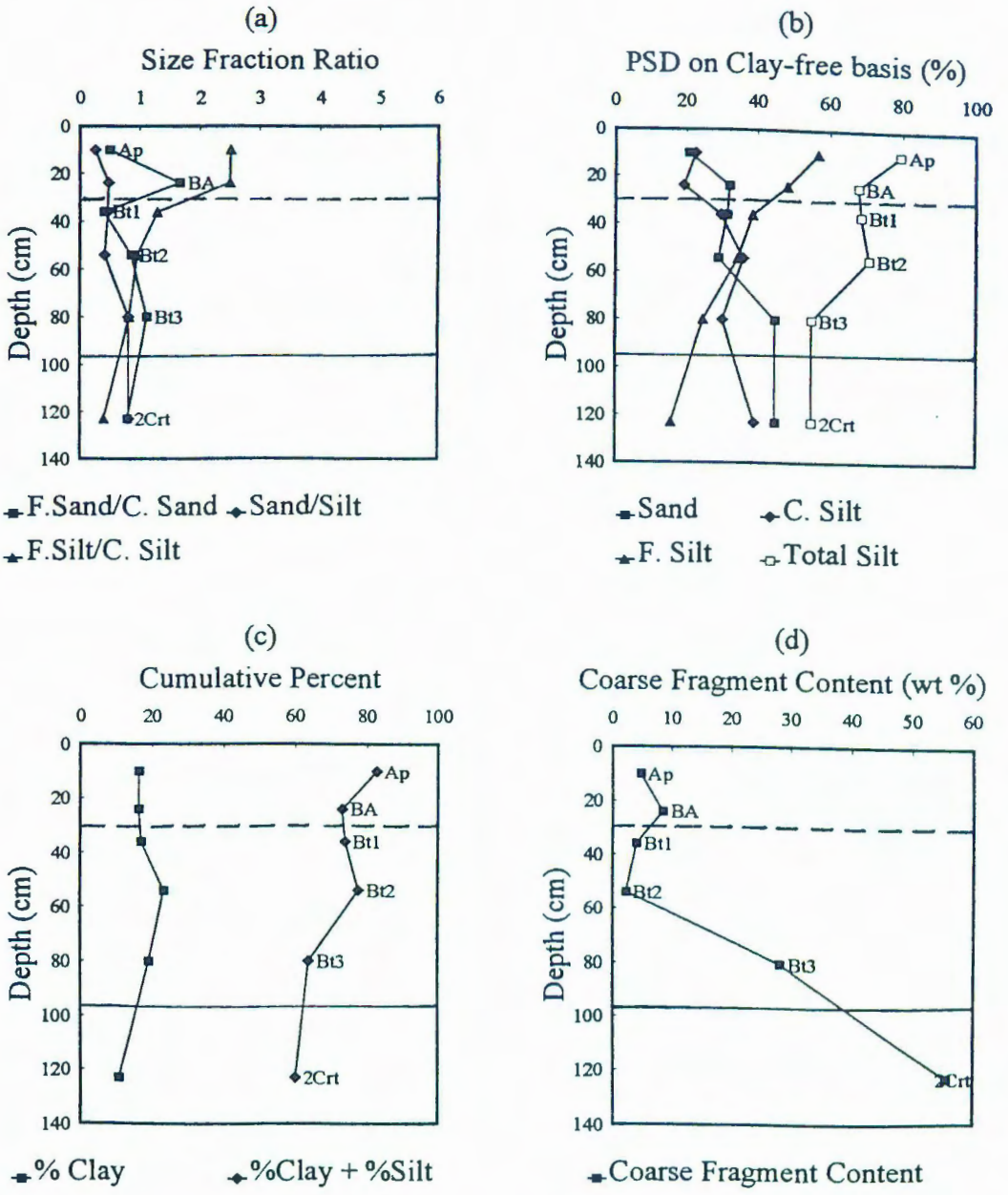

Figure 3-4. Depth functions for pedon FC3 of a) selected particle size ratios, b) PSD on clay-free basis, c) PSD with clay and d) coarse-fragment content. Discontinuities shown as solid horizontal lines. Variations shown as dashed horizontal lines.

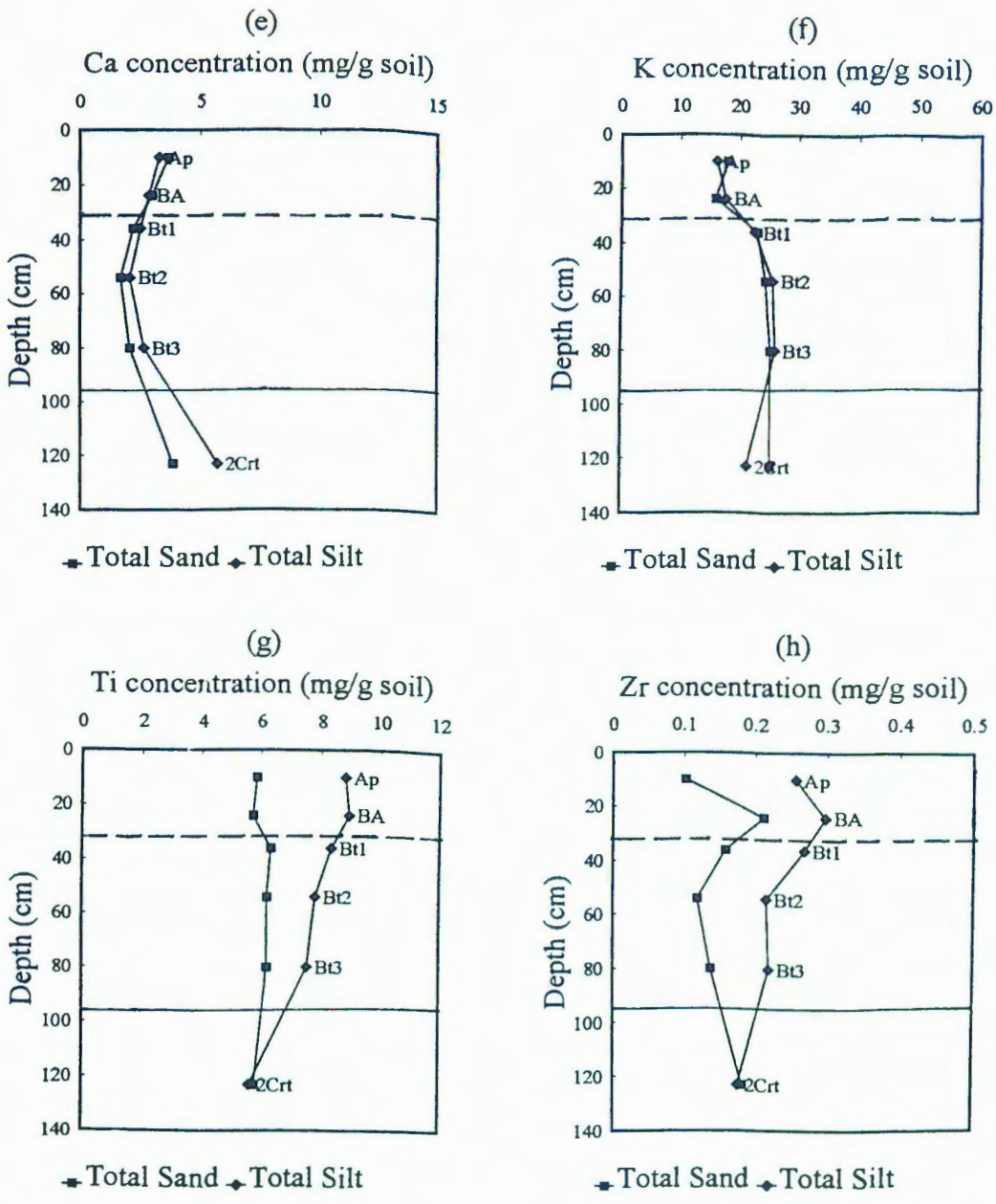

Figure 3-4. Depth distributions for pedon FC3 of e) % Ca, f) % K, g) % Ti, and h) % Zr. Discontinuities shown as solid horizontal lines. Variations shown as dashed horizontal lines.

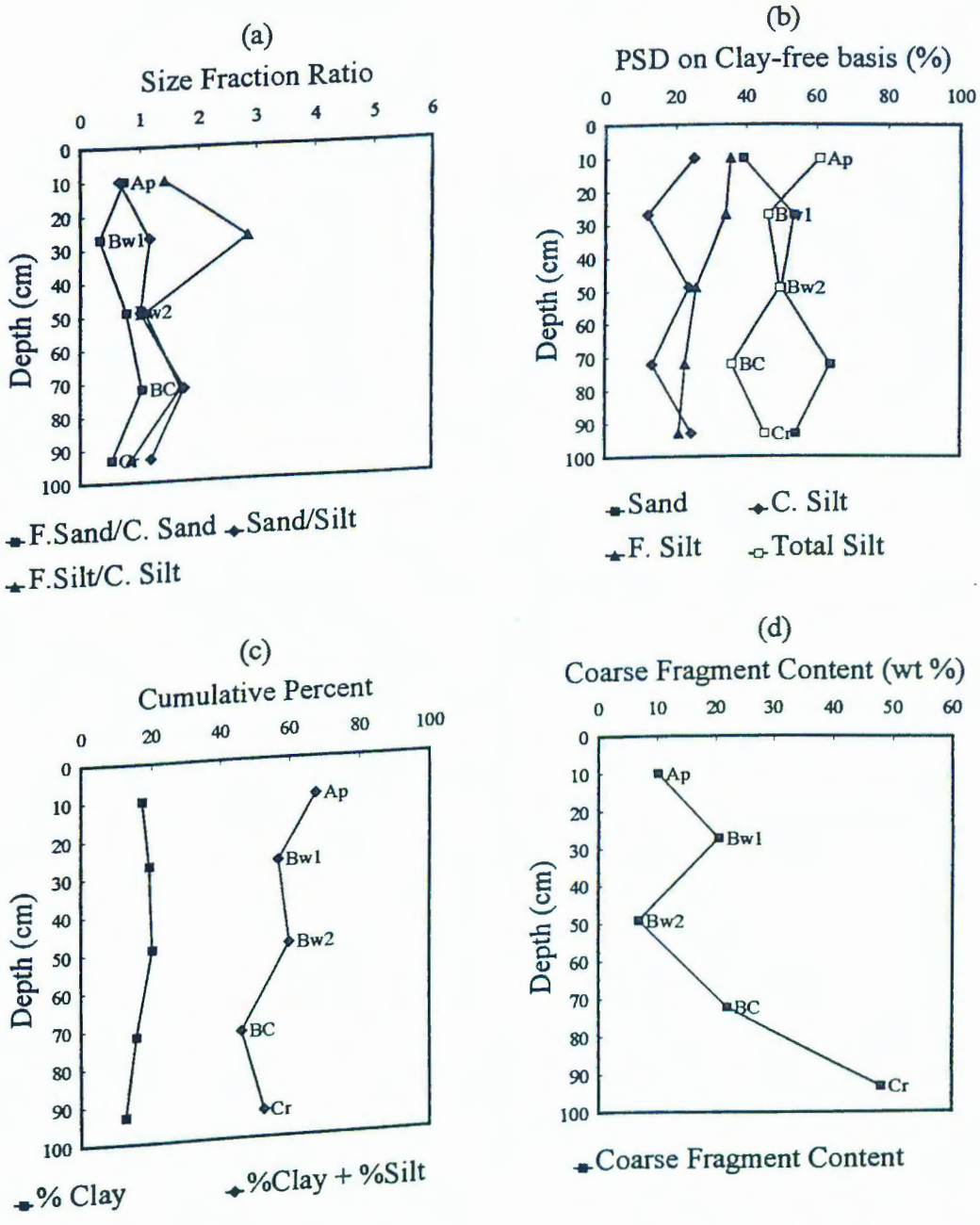

Figure 3-5. Depth functions for pedon FC4 of a) selected particle size ratios, b) PSD on clay-free basis, c) PSD with clay and d) coarse-fragment content. Discontinuities shown as solid horizontal lines. Variations shown as dashed horizontal lines.

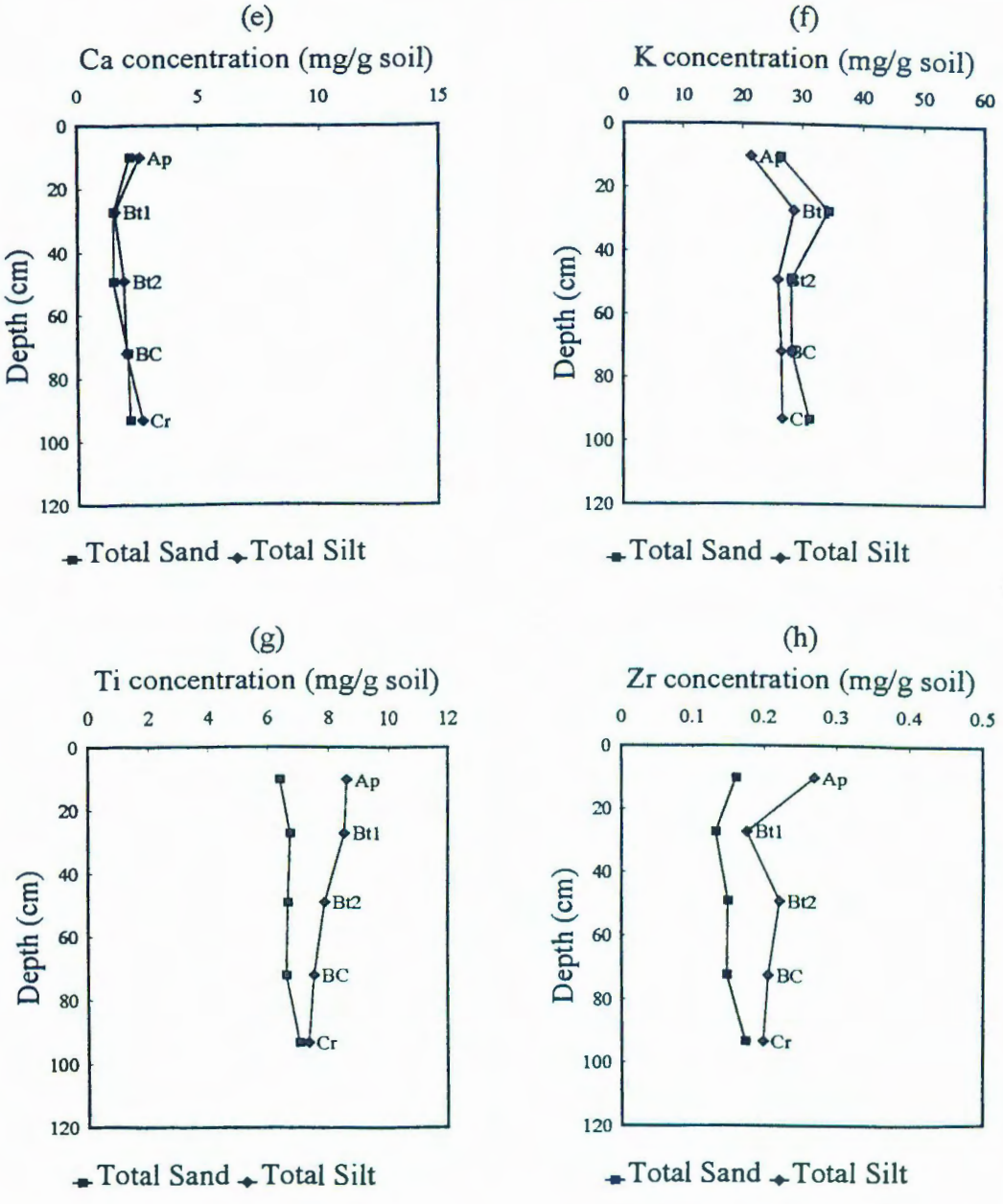

Figure 3-5. Depth distributions for pedon FC4 of e) % Ca, f) % K, g) % Ti, and h) % Zr. Discontinuities shown as solid horizontal lines. Variations shown as dashed horizontal lines.

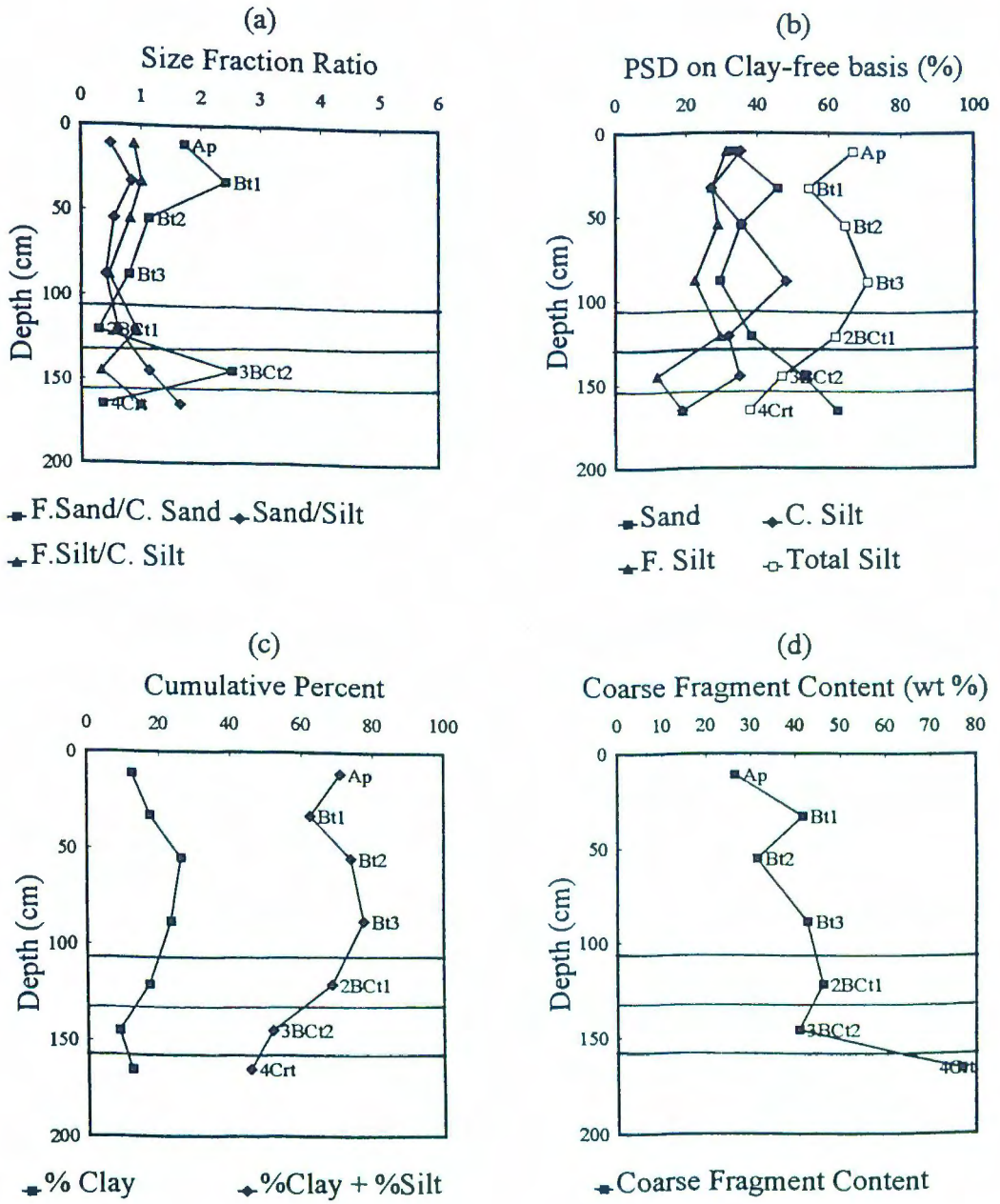

Figure 3-6. Depth functions for pedon FC5 of a) selected particle size ratios, b) PSD on clay-free basis, c) PSD with clay and d) coarse-fragment content. Discontinuities shown as solid horizontal lines. Variations shown as dashed horizontal lines.

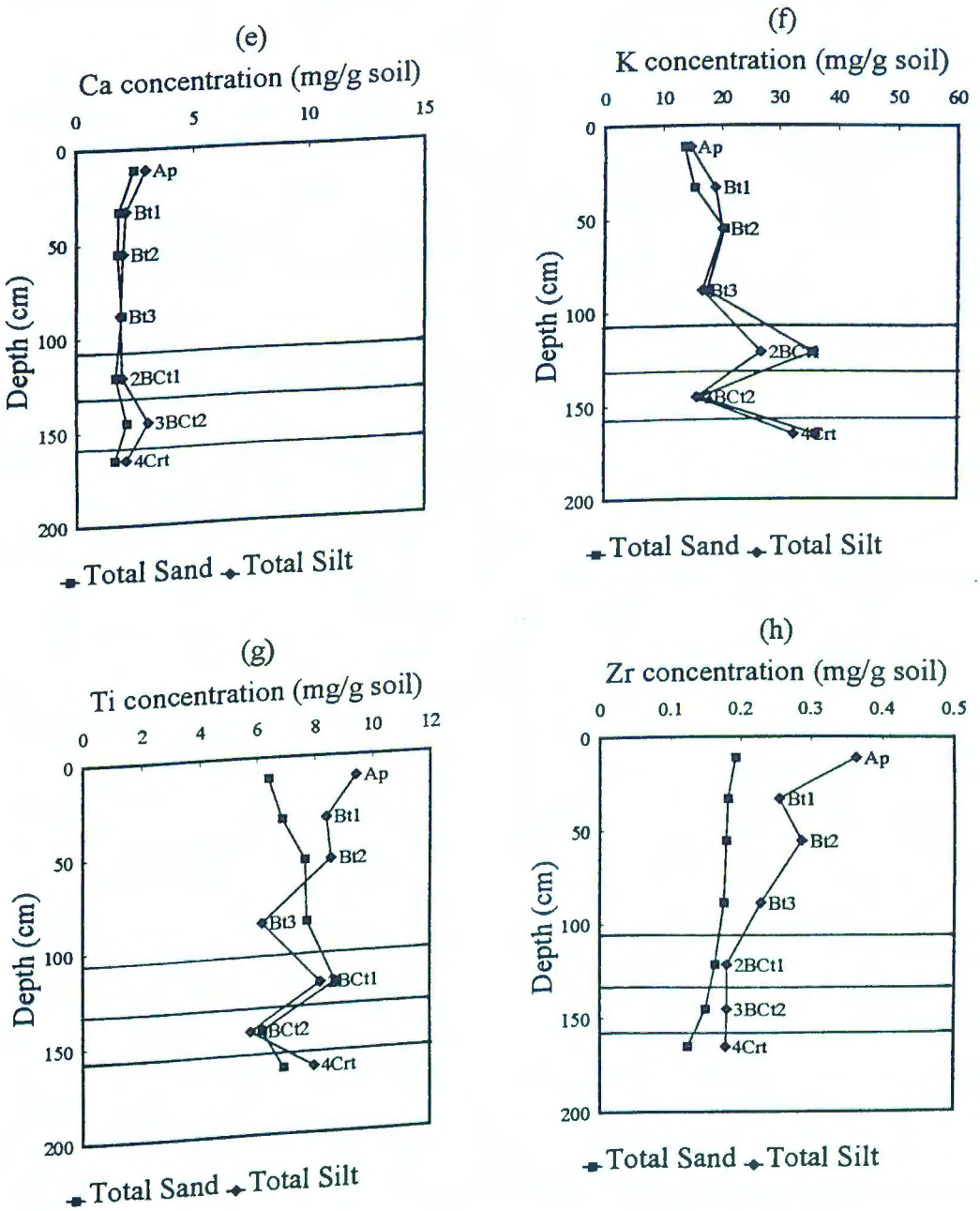

Figure 3-6. Depth distributions for pedon FC5 of e) % Ca, f) % K, g) % Ti, and h) % Zr. Discontinuities shown as solid horizontal lines. Variations shown as dashed horizontal lines.

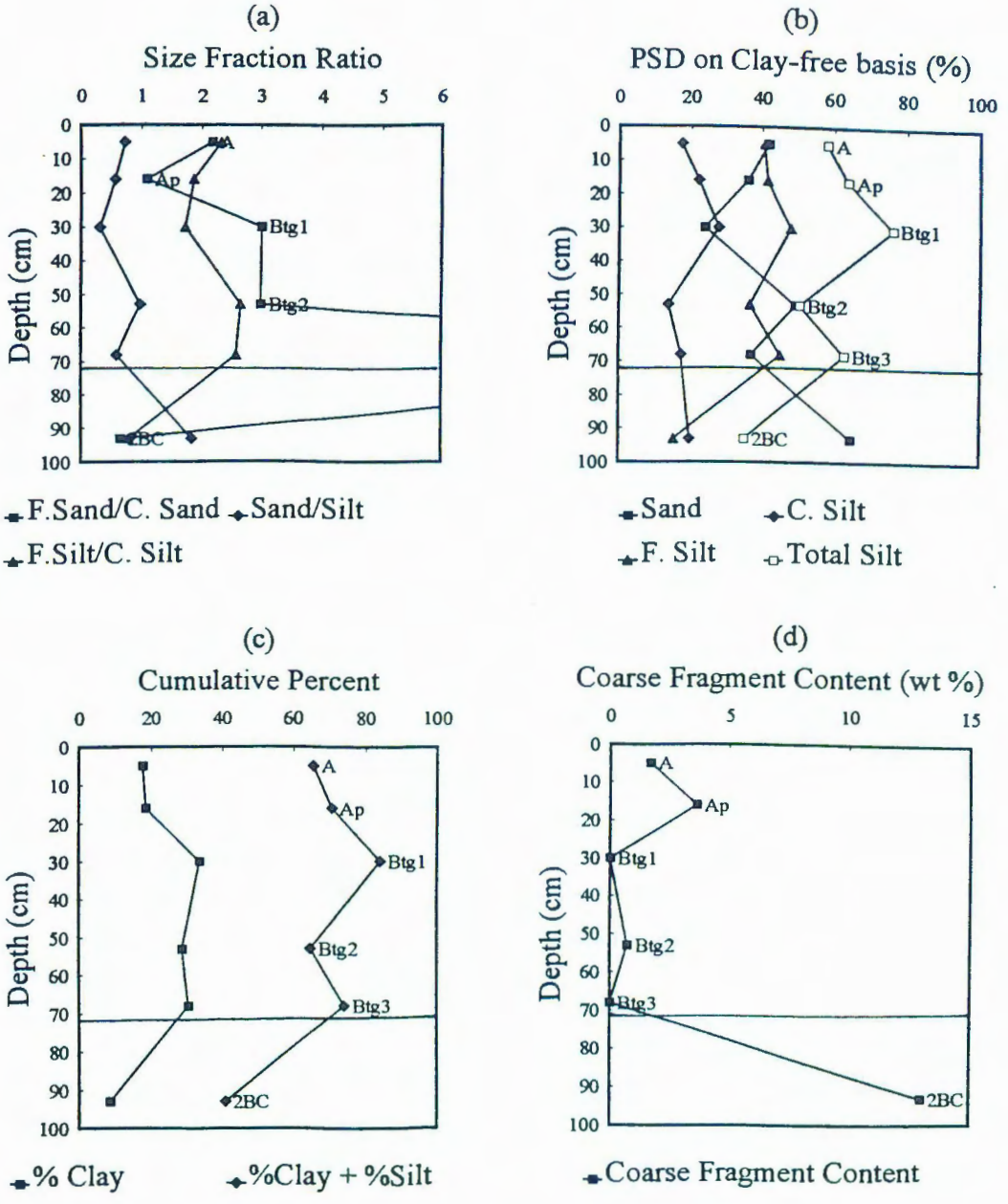

Figure 3-7. Depth functions for pedon MC1 of a) selected particle size ratios, b) PSD on clay-free basis, c) PSD with clay and d) coarse-fragment content. Discontinuities shown as solid horizontal lines. Variations shown as dashed horizontal lines.

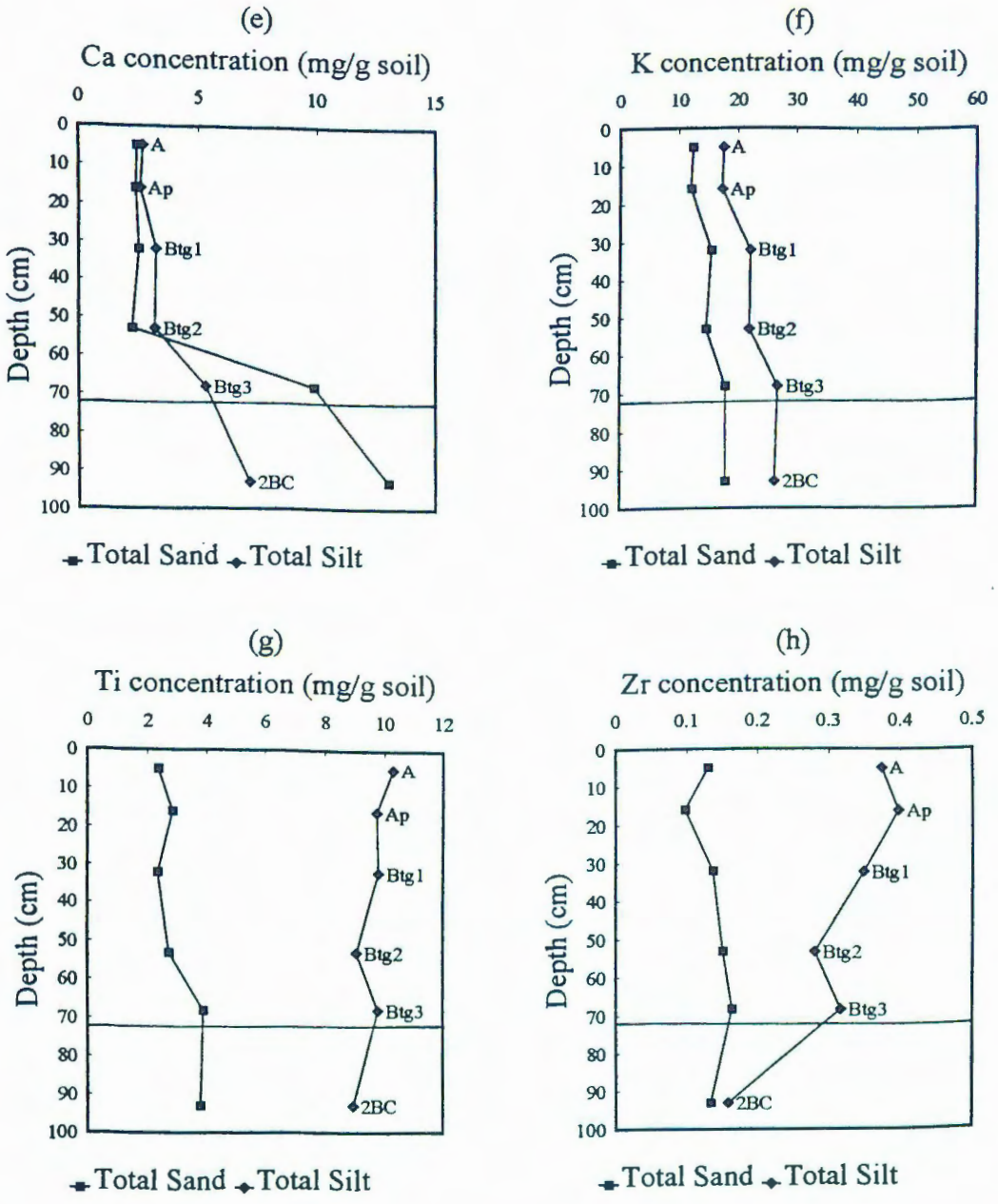

Figure 3-7. Depth distributions for pedon MC1 of e) % Ca, f) % K, g) % Ti, and h) % Zr. Discontinuities shown as solid horizontal lines. Variations shown as dashed horizontal lines.

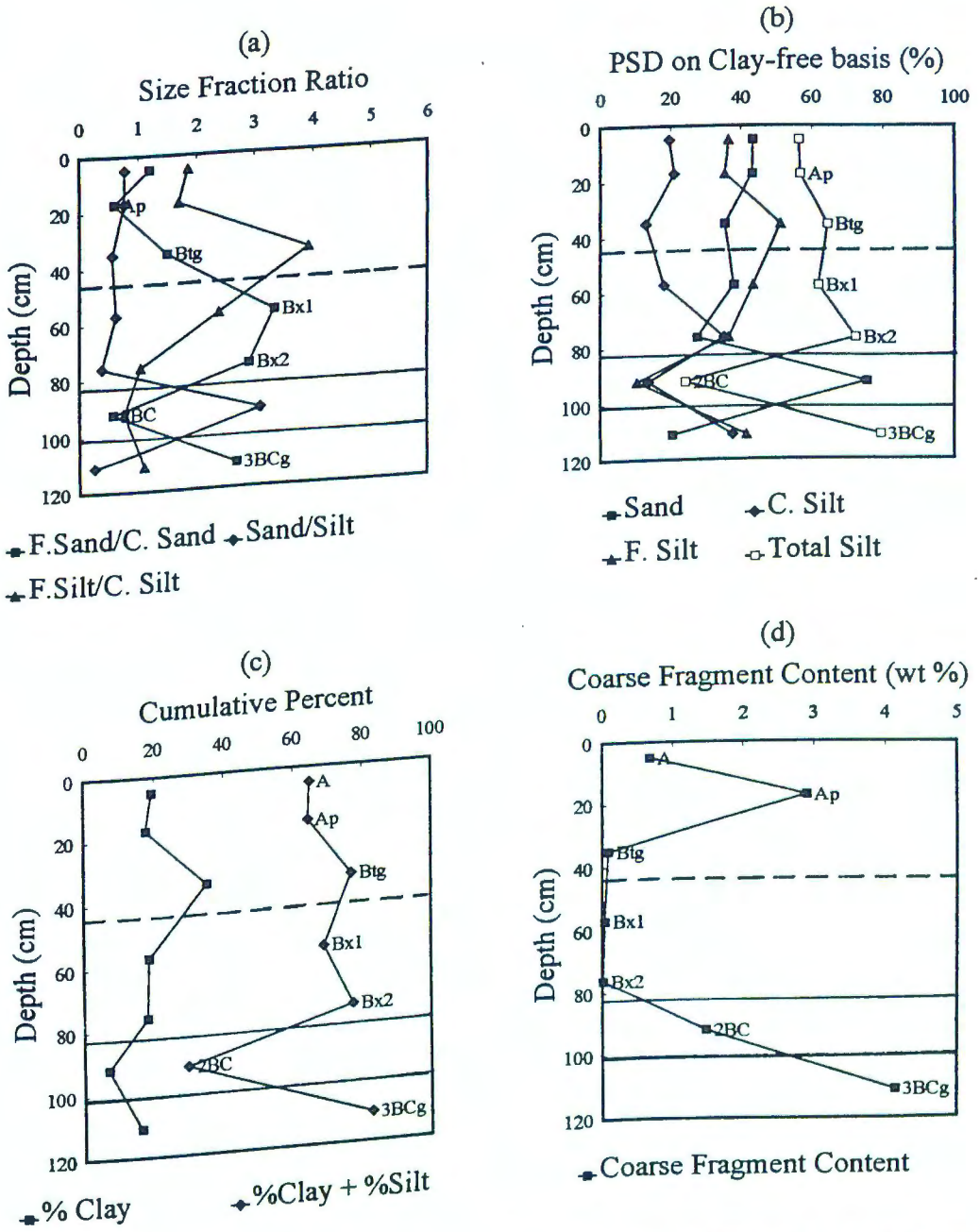

Figure 3-8. Depth functions for pedon MC2 of a) selected particle size ratios, b) PSD on clay-free basis, c) PSD with clay and d) coarse-fragment content. Discontinuities shown as solid horizontal lines. Variations shown as dashed horizontal lines.

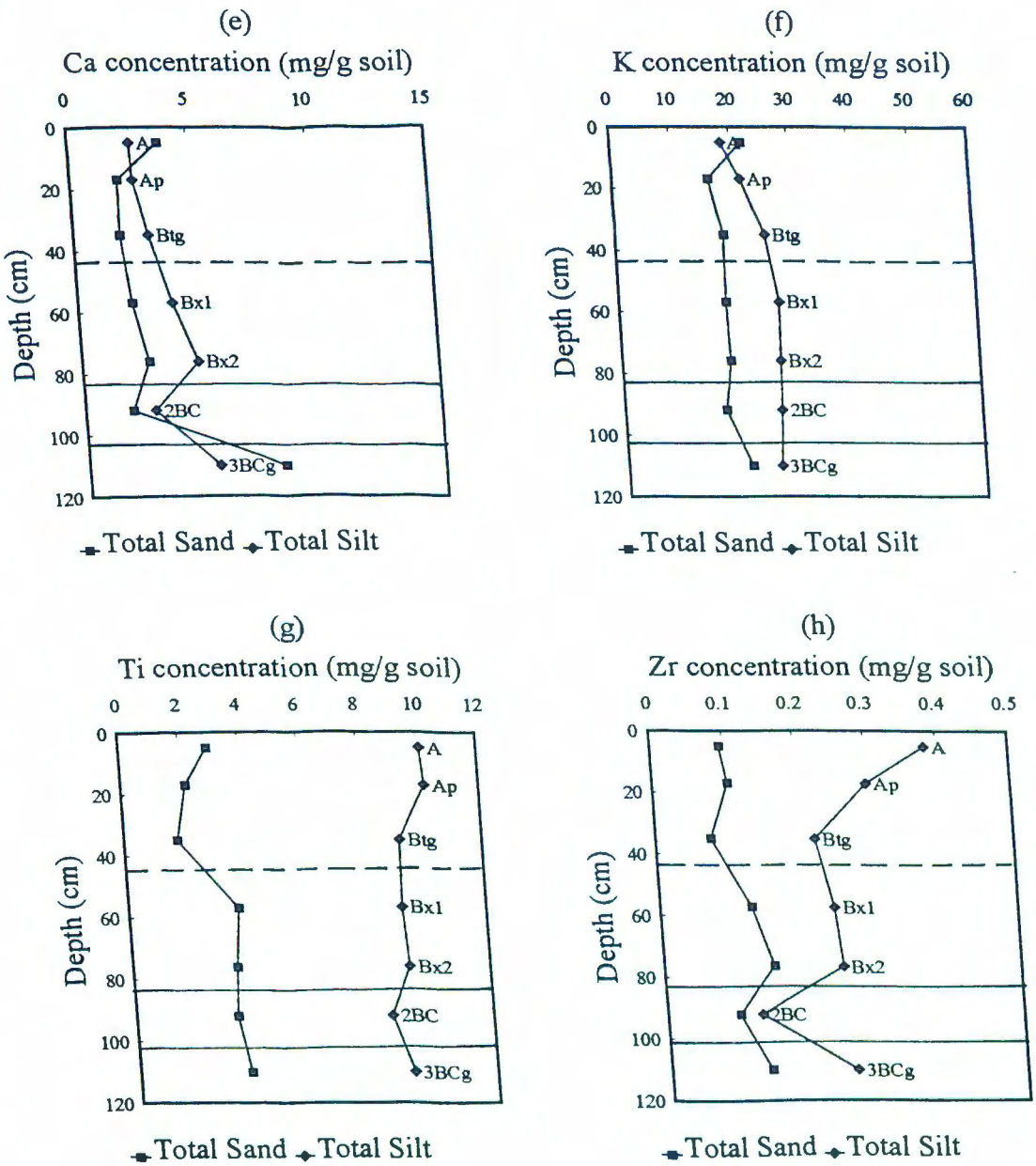

Figure 3-8. Depth distributions for pedon MC2 of e) % Ca, f) % K, g) % Ti, and h) % Zr. Discontinuities shown as solid horizontal lines. Variations shown as dashed horizontal lines.

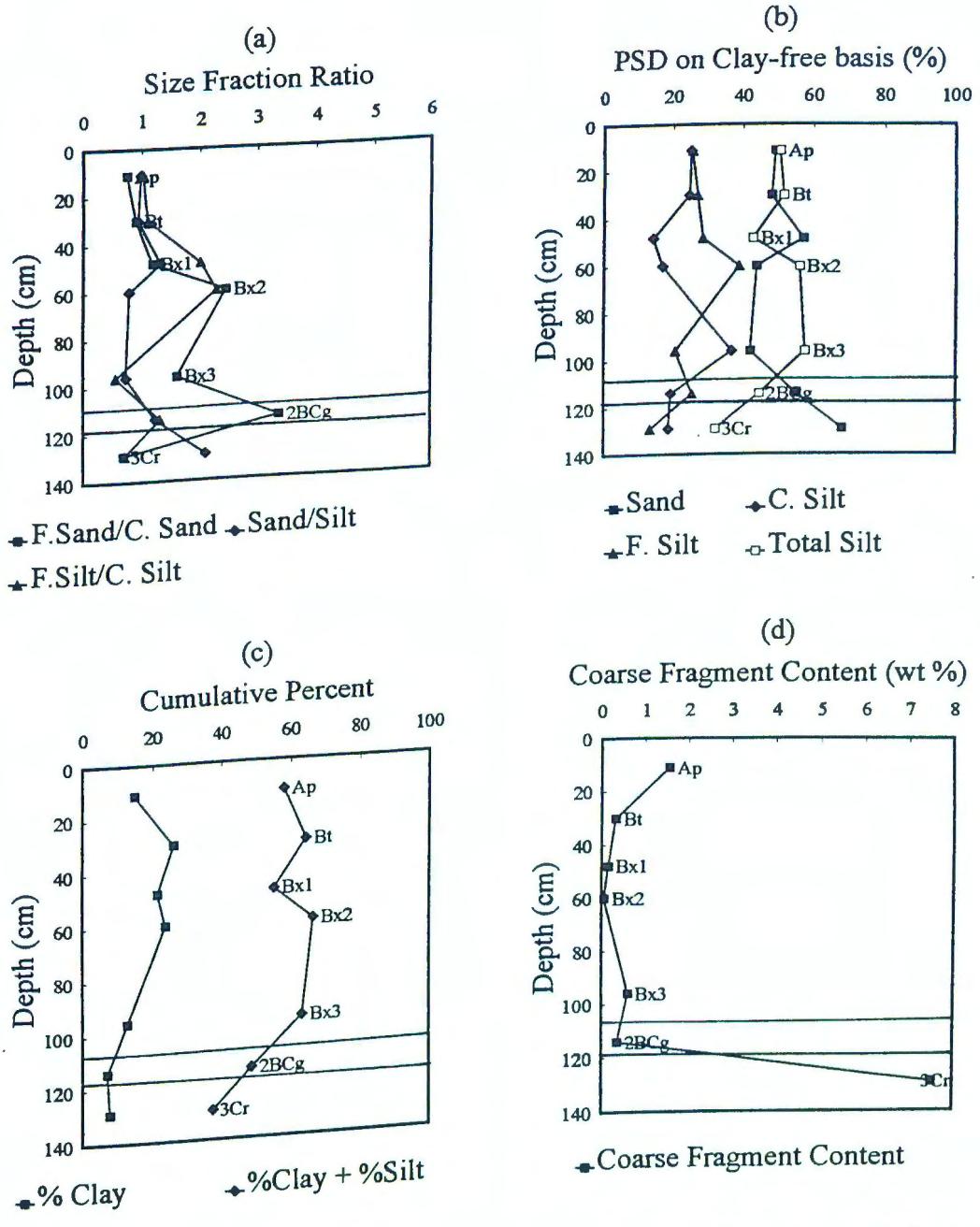

Figure 3-9. Depth functions for pedon MC3 of a) selected particle size ratios, b) PSD on clay-free basis, c) PSD with clay and d) coarse-fragment content. Discontinuities shown as solid horizontal lines. Variations shown as dashed horizontal lines.

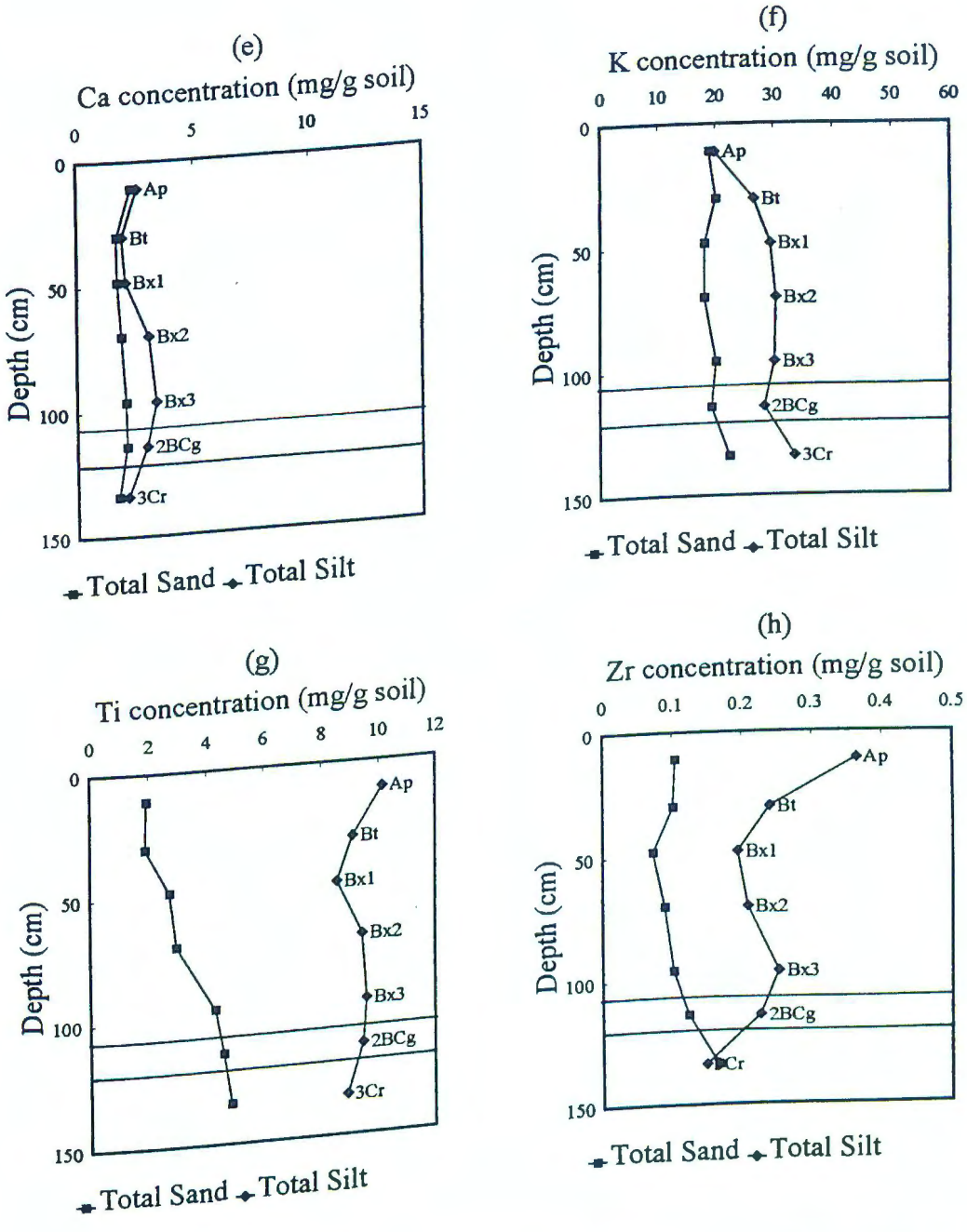

Figure 3-9. Depth distributions for pedon MC3 of e) % Ca, f) % K, g) % Ti, and h) % Zr. Discontinuities shown as solid horizontal lines. Variations shown as dashed horizontal lines.

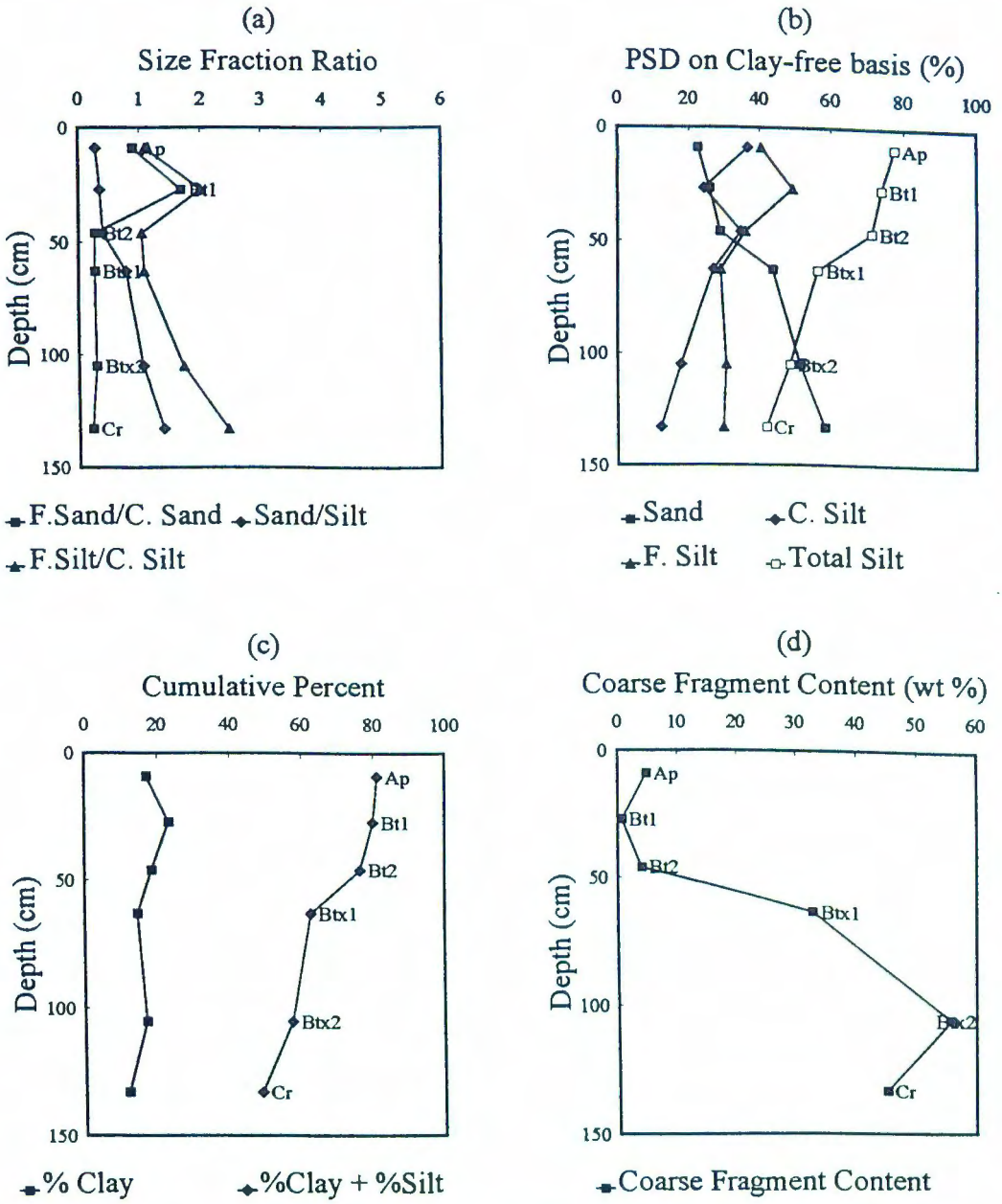

Figure 3-10. Depth functions for pedon MC4 of a) selected particle size ratios, b) PSD on clay-free basis, c) PSD with clay and d) coarse-fragment content. Discontinuities shown as solid horizontal lines. Variations shown as dashed horizontal lines.

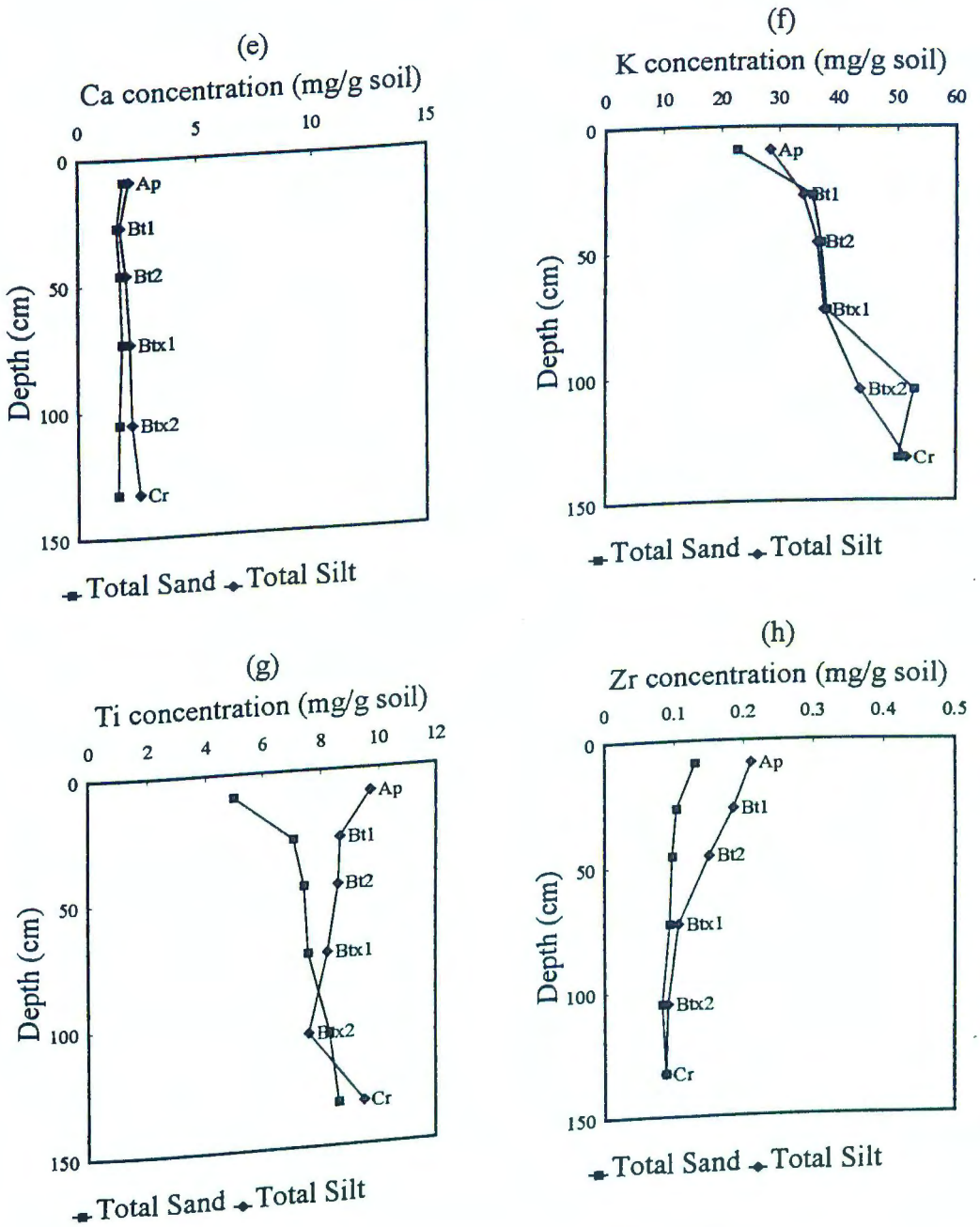

Figure 3-10. Depth distributions for pedon MC4 of e) % Ca, f) % K, g) % Ti, and h) % Zr. Discontinuities shown as solid horizontal lines. Variations shown as dashed horizontal lines.

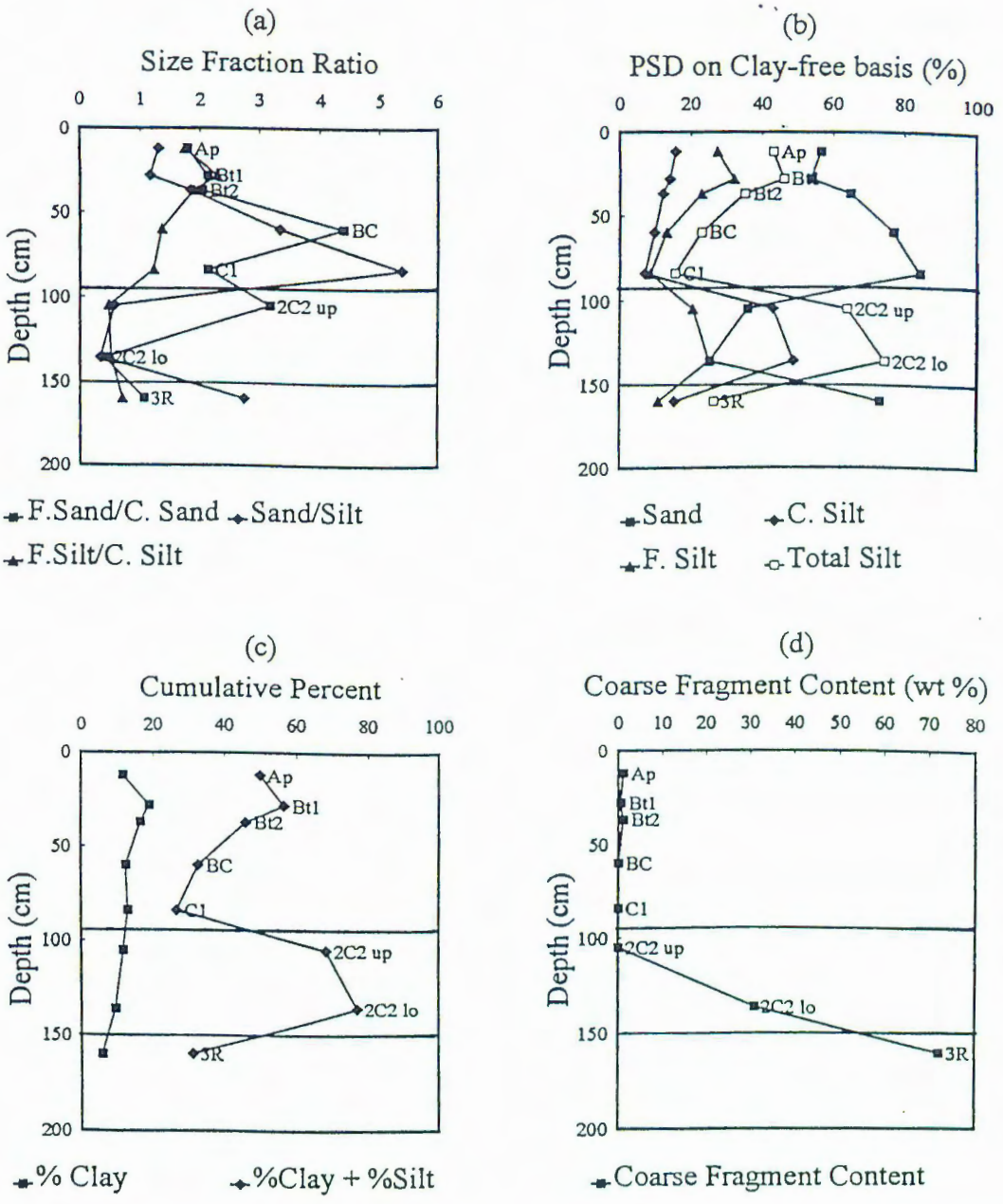

Figure 3-11. Depth functions for pedon MC5 of a) selected particle size ratios, b) PSD on clay-free basis, c) PSD with clay and d) coarse-fragment content. Discontinuities shown as solid horizontal lines. Variations shown as dashed horizontal lines.

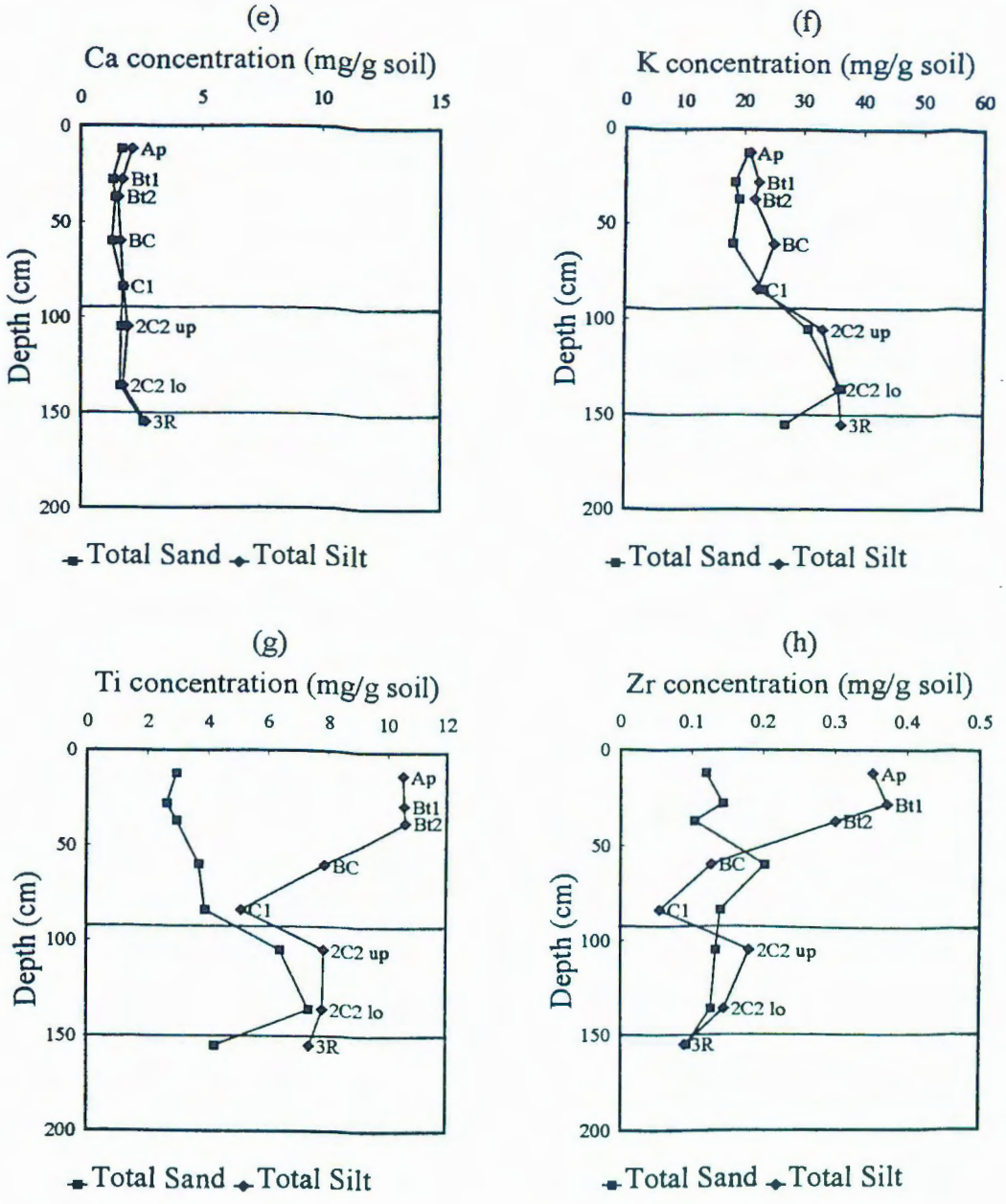

Figure 3-11. Depth distributions for pedon MC5 of e) % Ca, f) % K, g) % Ti, and h) % Zr. Discontinuities shown as solid horizontal lines. Variations shown as dashed horizontal lines.

residual soil.

Interpretation of Observed Lithologic Discontinuities

Overall, textural discontinuities believed to be due to loessal additions and/or mixing associated with colluvial activity occurred at a depth of 75 cm for pedon FC1, 74 cm for pedon FC1A, 60 cm for pedon FC2, and 71 cm for pedon MC1. A possible discontinuity occurs at 44 cm in pedon MC2. Thicker loess mantles have been reported in Maryland, such as 95 cm (Rabenhorst, 1978) and 120 cm (Darmody, 1980) in selected soils of the Piedmont physiographic province and 112 cm in selected soils of the Coastal Plain physiographic province (Wright, 1972). No such upper solum discontinuities were observed within the other upper pedons of either THS and these pedons are interpreted to be residual soils. Loess deposition may have occurred on these upper pedons; however, this deposition has been subject to both erosional and colluvial activity. Movement of this mixed material down to the lower landscape positions may account for the observed loessal and colluvial\alluvial additions to these soils. A schematic representation regarding the distribution of loess, colluvium/alluvium, and residuum for both THS are shown in Figure 3-12a and 3-12b.

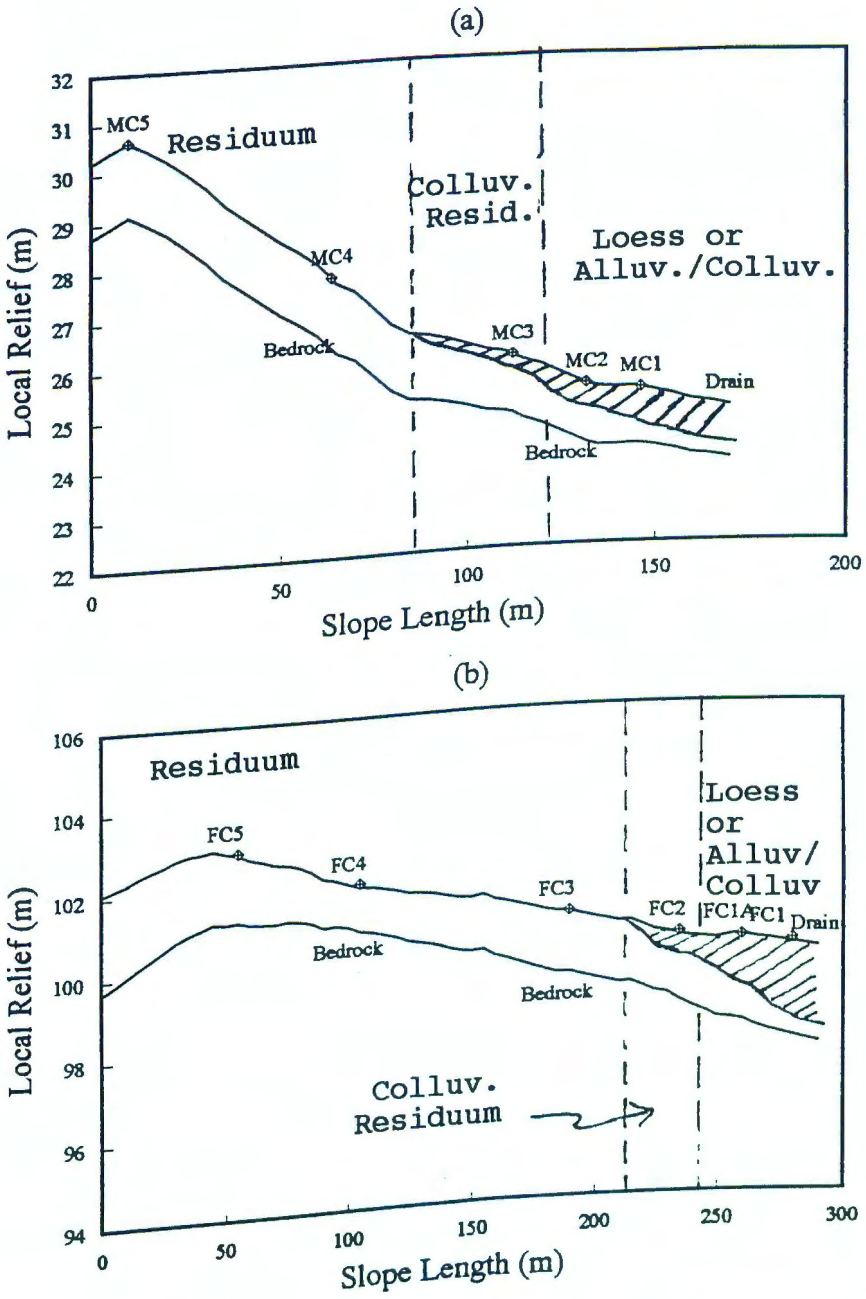

Figure 3-12. Schematic showing location of non-residuum materials in relation to residuum for a) the MC site (vert. exag = 13X and b) the FC site (vert. exag = 17X).

Conclusions

Pedons in the Triassic Culpeper Basin of Maryland which occupy the lower backslope to the toeslope landscape positions have developed from loessal or colluvial/alluvial additions to their upper sola. The pedons occupying the mid to upper backslope, shoulder, or summit landscape positions have developed from residuum or residuum-derived parent materials and therefore are interpreted as residual soils. These results confirmed our initial hypothesis that the upper solum of the lower landscape soils were affected by surficial additions which caused a) a more yellow/less red upper solum, b) the presence of rounded quartz cobbles in the solum, and c) a greater expression of the argillic horizon as compared to the higher landscape members of each topohydrosequence (Chapter 4). Because of these loessal or colluvial/alluvial additions to these landscape positions, interpretations regarding the soil morphology of these soils may need to include the influence of these additions upon the soil morphology. These features are formed by redox processes but the particular expression may be affected by the nature of the parent materials. The following chapter will describe the relationship, if any, between the morphology and hydrology of the soils along these two topohydrosequences and attempt to explain the degree of influence of such loessal and\or colluvial deposits on the morphological expression of these soils.

CHAPTER 4

FACTORS AFFECTING THE DEVELOPMENT OF REDOXIMORPHIC FEATURES

It has been reported by some that soils derived from red parent materials are problematic in terms of assessing their drainage class because the morphology of these soils is less apt to show their degree of wetness via the occurrence and distribution of redoximorphic features (gleying, low chroma mottling, Fe/Mn nodules) (Carl Robinnette, 1987, personal communication). The inhibition of gleying of red Triassic sediments was recently demonstrated in a three-month incubation study involving red C-horizon material derived from red shale and glucose even though incipient gley formation was observed in a gray shale after only eight days of incubation (Niroomand and Tedrow, 1991). The inhibition of such soils and sediments to form distinct redoximorphic features may lead to erroneous interpretations regarding both agricultural and engineering purposes. Faulty interpretations may result in septic tank failure, wet basements, erroneous wetland delineations, and so forth.

On the other hand, the Croton series (fine-silty, mixed, mesic Typic Fragiaqualf), which is believed to be partly colluvial in nature and underlain by these red Triassic sediments, has been traditionally delineated at the footslope topographic positions in Maryland (Matthews, 1960; Matthews et al., 1961). This delineation is based upon the observation of well expressed redoximorphic features (gleying) within the upper solum of these soils.

In Maryland, Triassic rocks are mainly found in the Culpeper Basin. This basin occupies a narrow belt through the central Piedmont of Maryland and is one of a series of Triassic basins which extend fairly continuously throughout the mid-Atlantic USA from North Carolina to Connecticut (Levin, 1978). Dusky red shales (2.5YR to 5YR 4/4 or 3/4) are the dominant parent material in this basin with lesser amounts of similarly colored and intimately associated fine-grained sandstones and siltstones (Fisher, 1964; Vokes and Edwards, 1974).

Besides the Croton series, two other soil series which are derived from these parent materials in Maryland have also been traditionally delineated according to landscape position and drainage class into a three-member topohydrosequence (THS) or catena. The Penn series (fine-loamy, mixed, mesic Ultic Hapludalf) has been generally mapped as the well-drained member and occurs mainly on the summit and upper backslope positions. The Readington series (fine-loamy, mixed, mesic Typic Fragiudalf) has been generally mapped as the moderately well-drained member on the lower backslopes and concave upland depressions.

Based upon the two conflicting observations over the development of redoximorphic features in these soils, the following three questions may be posed: 1) What soil properties other than hydrology may affect the coloration patterns of these soils?, 2) Is there an inhibitory effect

on the development of redox-related features due to the nature of the Triassic parent materials?, and 3) What is the relationship between the hydrology and the location of redoximorphic features in the soils derived from these rocks?

The objectives of this project were therefore 1) to examine the relationship between the hydrology and the morphology of these soils in two topohydrosequences derived from these red sediments, and 2) to determine which factor(s) most strongly control the development of redoximorphic features in these soils.

Materials and Methods

Soil Examination and Site Characteristics

Eleven pedons located along two topohydrosequences were examined in this study. One site was located in northern Frederick County (FC site) near the city of Emmittsburg and the other site was located in western Montgomery County (MC site) near the city of Boyds (Figure 4-1).

Along these two topohydrosequences, pedons were described and sampled using standard techniques from either back-hoe or hand-dug soil pits at selected points along each sequence. Five pedons were examined along the transect at the MC site and six pedons were examined along the transect at the FC site. Each pedon was classified by Soil Taxonomy (Soil Survey Staff, 1990). Field moist Munsell colors were

recorded for all matrices, mottles, and coatings.

Topographic surveying was performed along each transect to illustrate elevational and topographic relationships differences among the examined pedons (Figure 4-2a to 4-2d). The MC site is characterized by a 4% slope and an ephemeral drain cross-cutting the 170 m long transect between the third and fourth pedon (Figure 4-2a and Figure 4-2c). The current vegetation of this site consists of forage species used for hay. The FC site is characterized by a more gentle slope (1%) along the 290 m long transect (Figure 4-2b and Figure 4-2d). This tract of land is actively farmed and plowed each spring for the growing of milo.

Precipitation for both sites is well distributed throughout the year in this region; however, a "wet" season is noted during late November to early June when precipitation exceeds evapotranspiration. As compared to the thirty-year average, above normal annual precipitation during the "wet" season has occurred at both sites for the period of study (September 1989 to September 1991). The growing season for both sites is April 15 to November 15 (Matthews, 1960; Matthews et al., 1961).

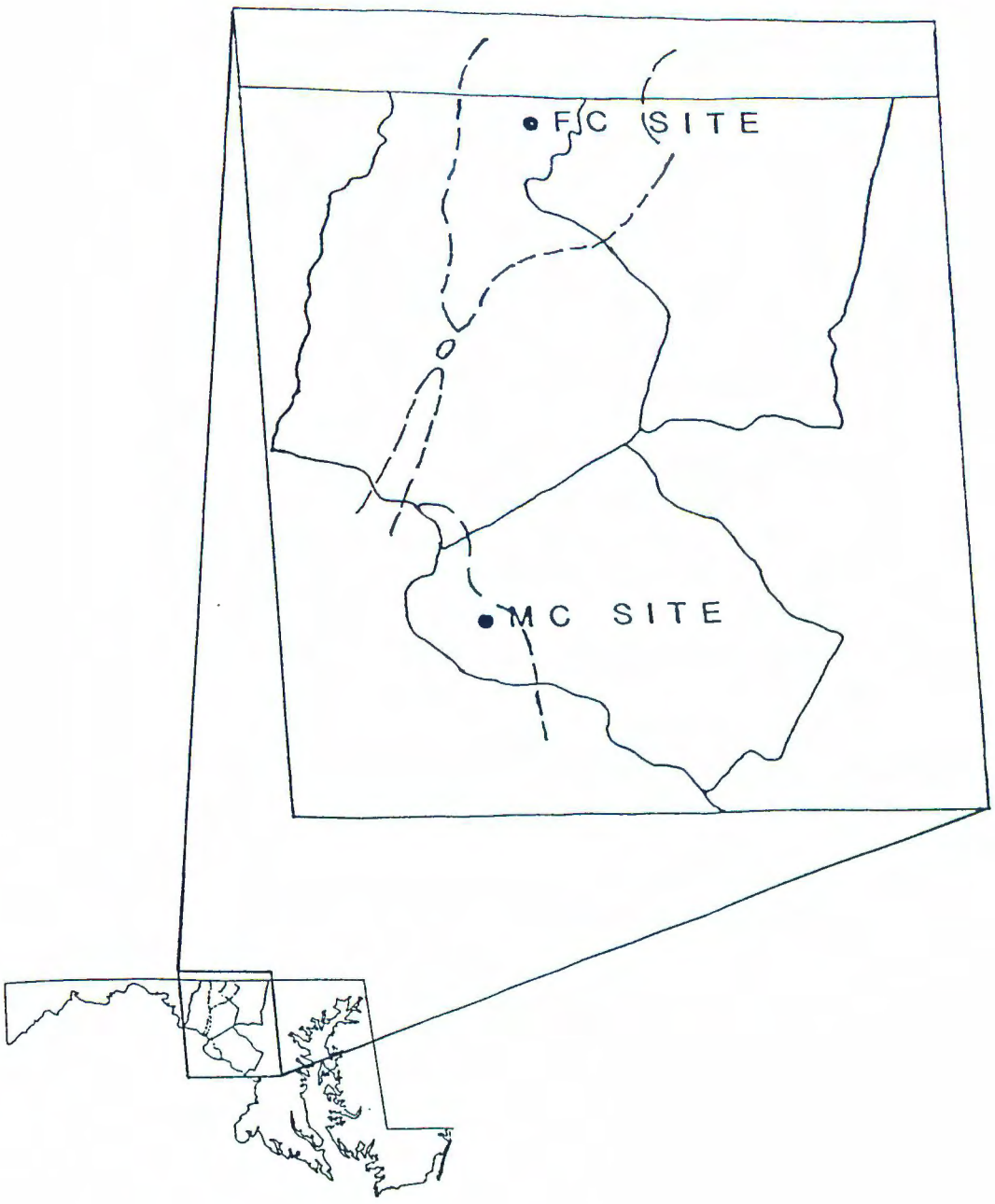

Figure 4-1. Location of study sites within the Triassic Culpeper Basin of Maryland.

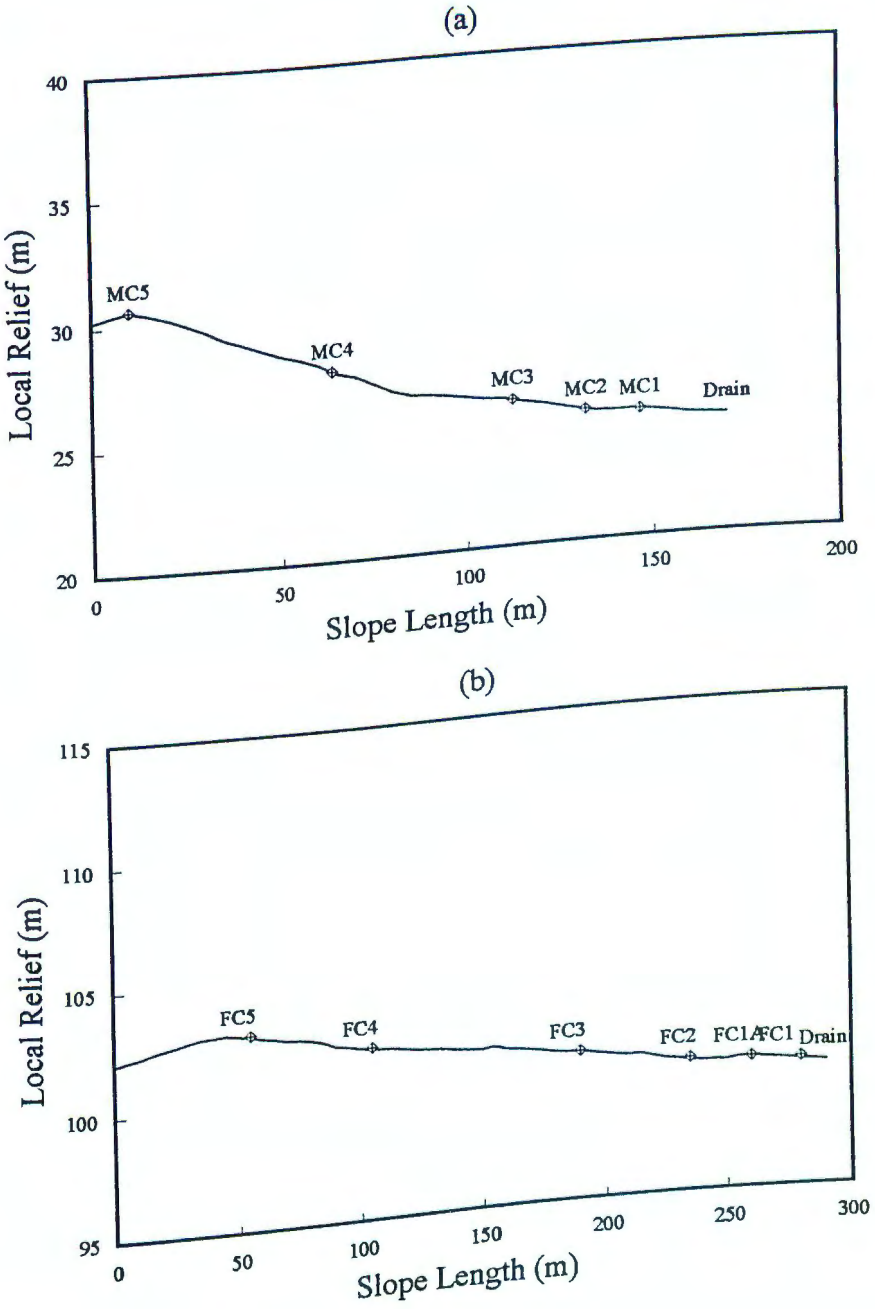

Figure 4-2. Topographic cross-section along the pedons examined at the a) MC site (vert exag.= 7x and b) FC site (vert exag. = 10x).

(c)

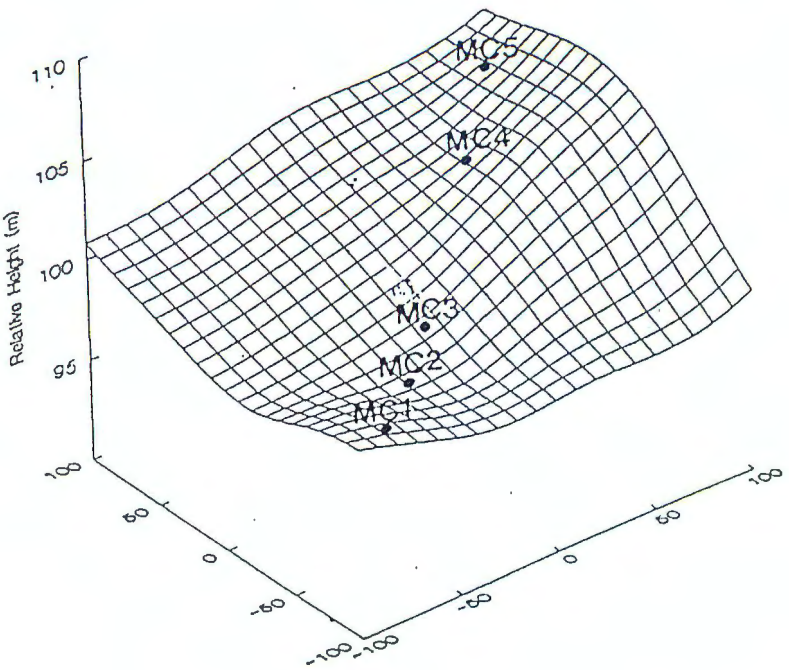

(d)

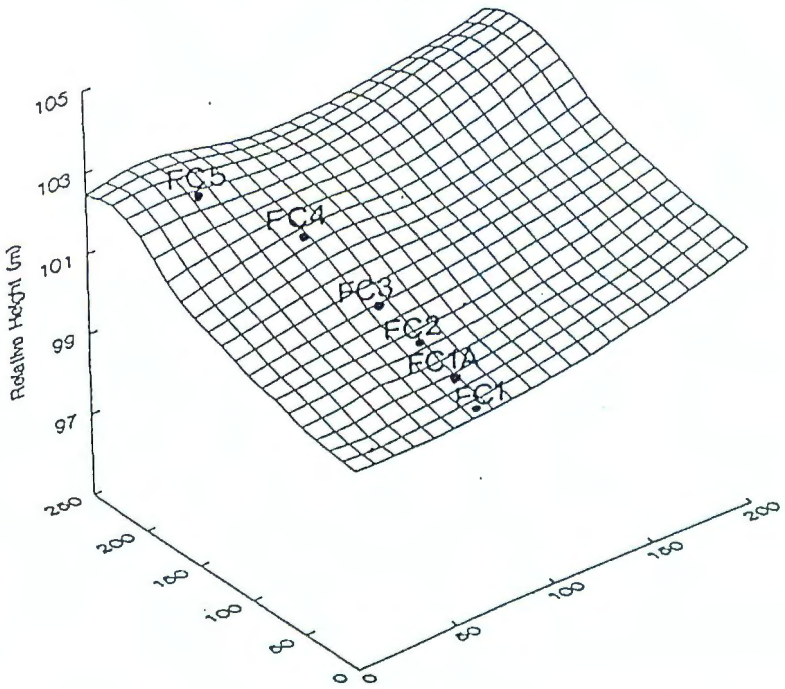

Figure 4-2. Overall site topography for c) the MC site and d) the FC site.

Hydrological Monitoring

To determine the hydrological status of each topohydrosequence, a combination of both open boreholes and water table wells was installed perpendicular to the transect axis and along the topographic contour at each pedon, except at pedon FC1A. For the water table well installation, two-inch diameter PVC pipes which were sequentially-slotted in 20-cm increments (i.e. first installed pipe - 20 cm long pipe and all slotted; second installed pipe - 40 cm long with the 20-40 cm area slotted; etc.) were placed until an auger-restricting layer was encountered. The purpose of the sequentially-slotted pipes was to test for the presence of a perched water table above water-restricting fragipans known to occur in these soils. Due to the presence of water-restricting layers (i.e. fragipans, impermeable bedrock) with 1 to 2 meters from the soil surface, epiaquic conditions as defined by ICOMAQ (1989) are expected to occur in these soils. Such hydrological conditions fit the pseudogley model as described by Fanning and Fanning (1989). Water table heights were recorded in each well on a biweekly basis from September 1, 1989 to August 31, 1991. When water was present in a well (i.e. during the "wet" season) that particular well was pumped dry following the measurement of the water height and allowed to recharge during the two-week period. All wells were used to analyze the actual water

table height at each pedon. During the wetter portions of the "wet" season, water table heights were nearly identical in all wells (i.e. within 1-2 cm). For each observation date during this portion of the "wet" season, the average water table height was taken as the water table height existing within that pedon. During the drier portions of the "wet" season, a perched water table was evident in the varying water table heights among the wells. For each observation date during this portion of the "wet" season, the water table height in the open borehole was then taken as the water table height for that pedon. Consecutive daily water table heights were interpolated between successive biweekly measurements and used in the construction of Figures 4-3, 4-4a to 4-4e, 4-5, and 4-6a to 4-6e.

Characterization of Soil Properties

Laboratory determinations included particle-size analyses by the pipette method (Gee and Bauder, 1986) and bulk density (at 40° C) by the clod method and corrected for coarse fragment content (Blake and Hartge, 1986). Cation exchange capacity by sum of cations using 1M NH_4OAc at pH 7.0 for soils with argillic horizons, CEC by replacement of NH_4^+ with Na^+ for soils without argillic horizons, and $BaCl_2$-TEA exchangeable acidity by titration were also performed (Soil Conservation Service, 1984). The replaced ammonium was determined colorimetrically using the indophenol method

(Dorich and Nelson, 1983). Extraction for CEC and exchangeable acidity was performed by the vacuum extraction method (Holmgren et al., 1977). The Soil Testing Laboratory at the University of Maryland performed % C on all horizons using a LECO model furnace[1] (Tabatabai and Bremner, 1970). Exchangeable bases were analyzed using atomic absorption spectroscopy.

Complete detailed soil descriptions are found in appendix A. Additionally, complete sets of data for pH, cation exchange capacity, and base saturation are located in appendix B.

Results

FC Site Hydrology/Morphology Relations

Pedons FC1 and FC2 have nearly identical cumulative frequency curves for their hydrology (Figure 4-3). In both pedons, the water table was observed within 40 cm of the soil surface for approximately 325 days of the two year study period and within 10 cm for approximately 200 days. These two pedons also show very similar curves for consecutive daily water heights (Figure 4-4a and 4-4b). In general, the water table is initially observed during December, rises towards the soil surface in January, and persists within 40 cm from the soil surface until June. The

[1] CHN-600 Elemental Analyzer for Macrosamples System 785-500. LECO Corp., 3000 Lakeview Ave., St. Joseph, MI 49085-2396.

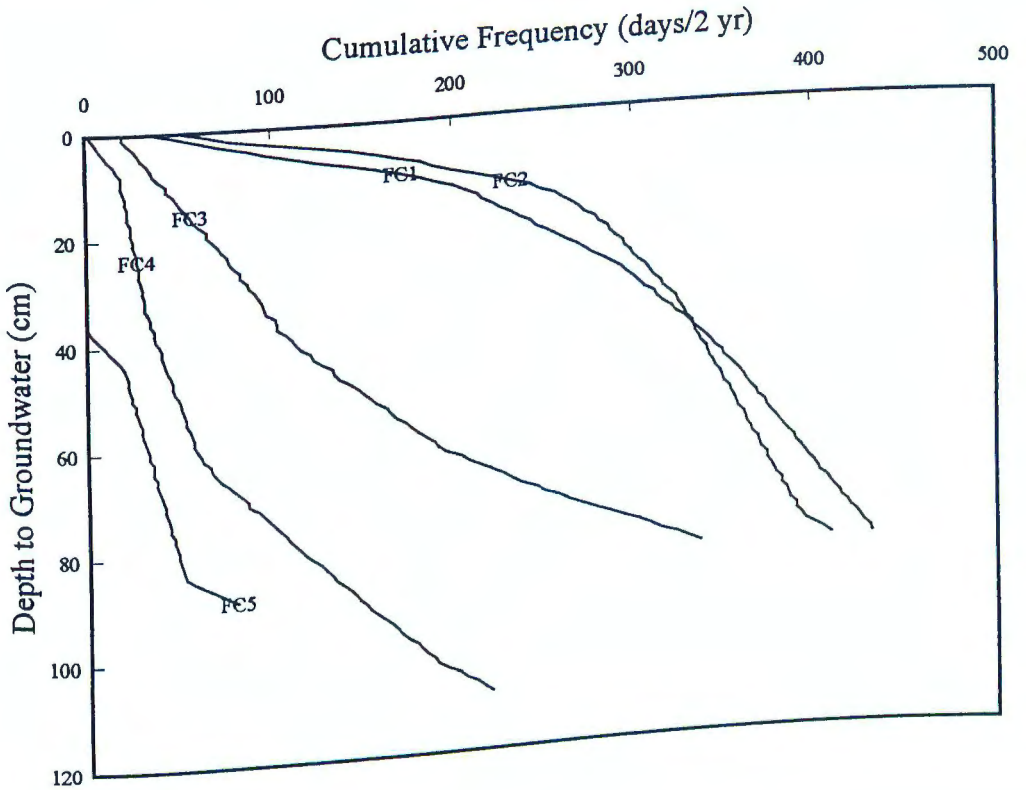

Figure 4-3. Cumulative frequency curve of the hydrology associated with the pedons of the FC site.

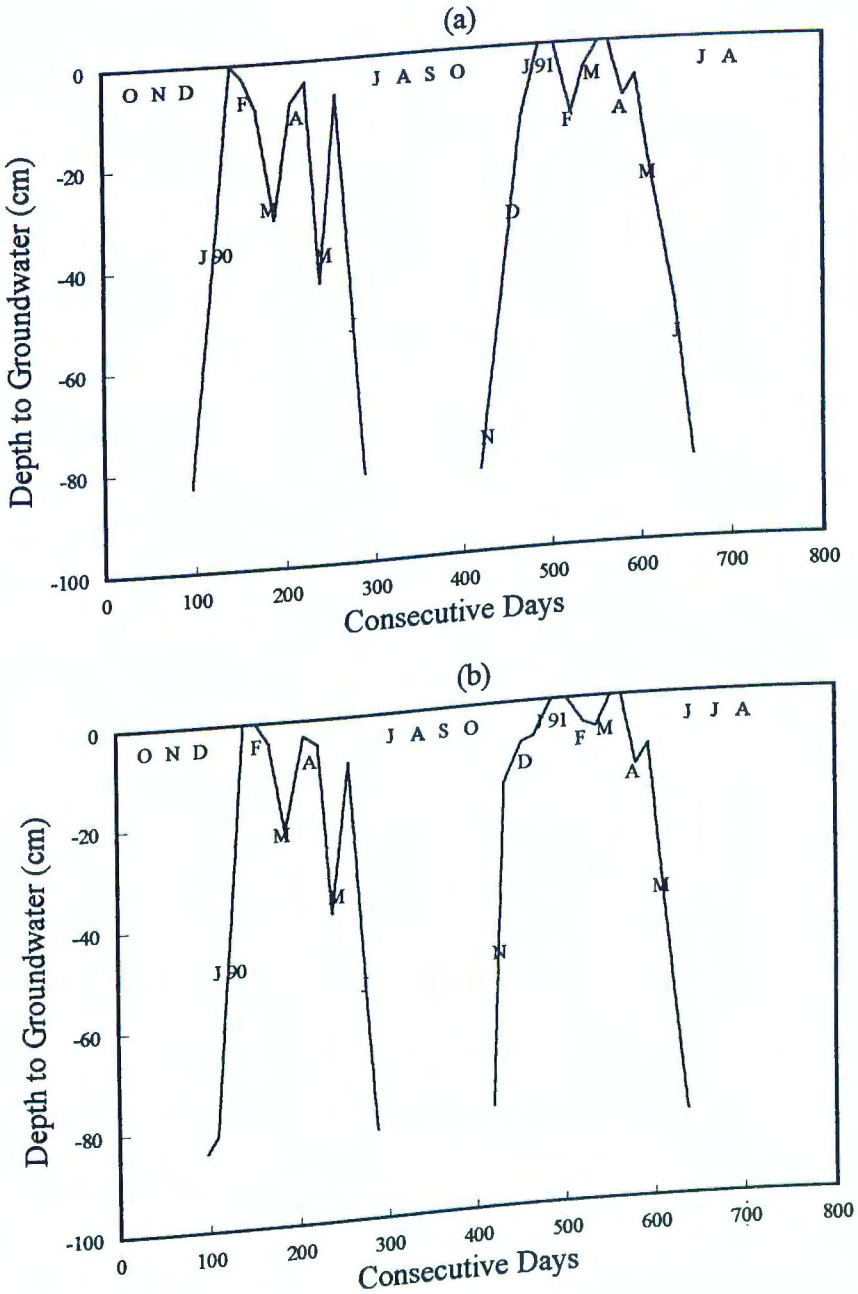

Figure 4-4. Consecutive water table heights of a) pedon FC1 and b) pedon FC2.

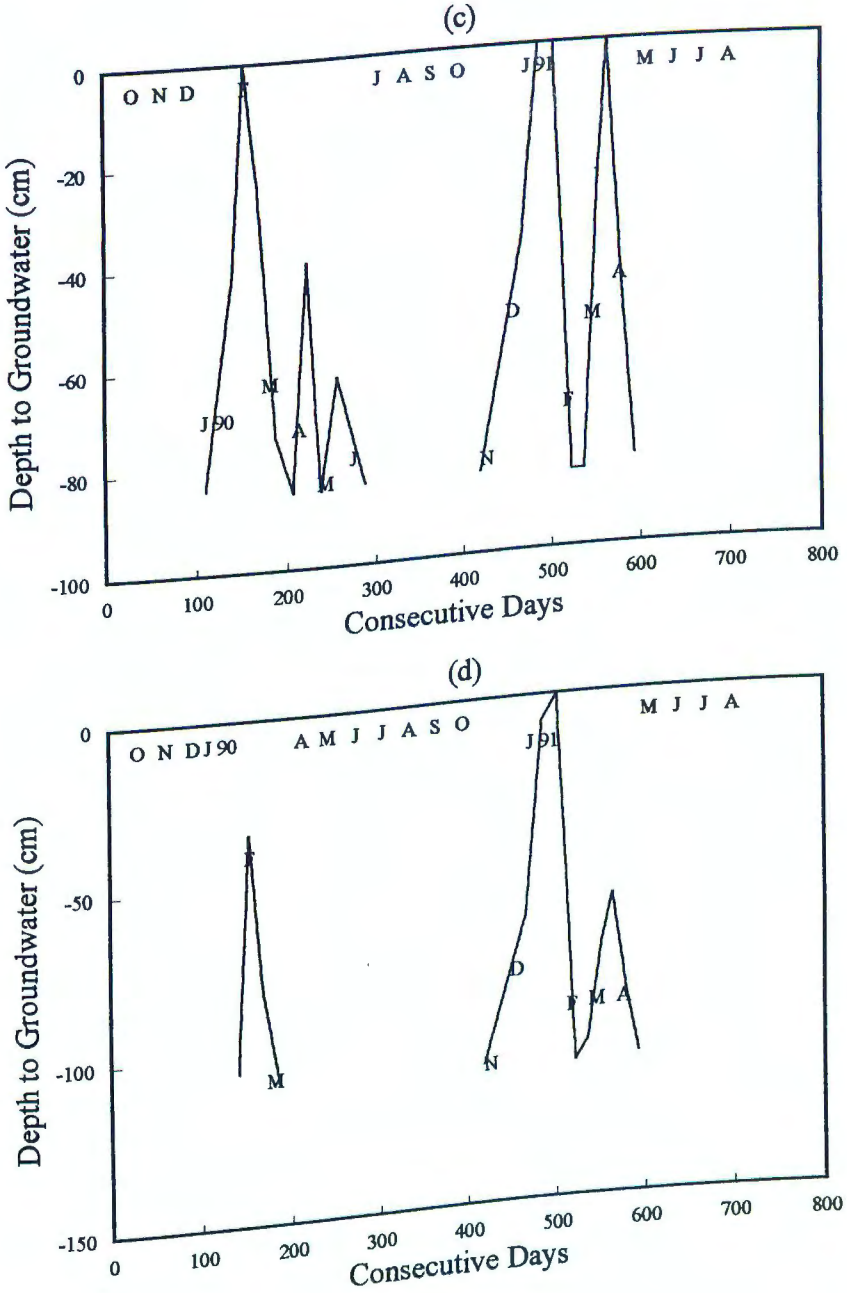

Figure 4-4. Consecutive water table heights for c) pedon FC3 and d) pedon FC4.

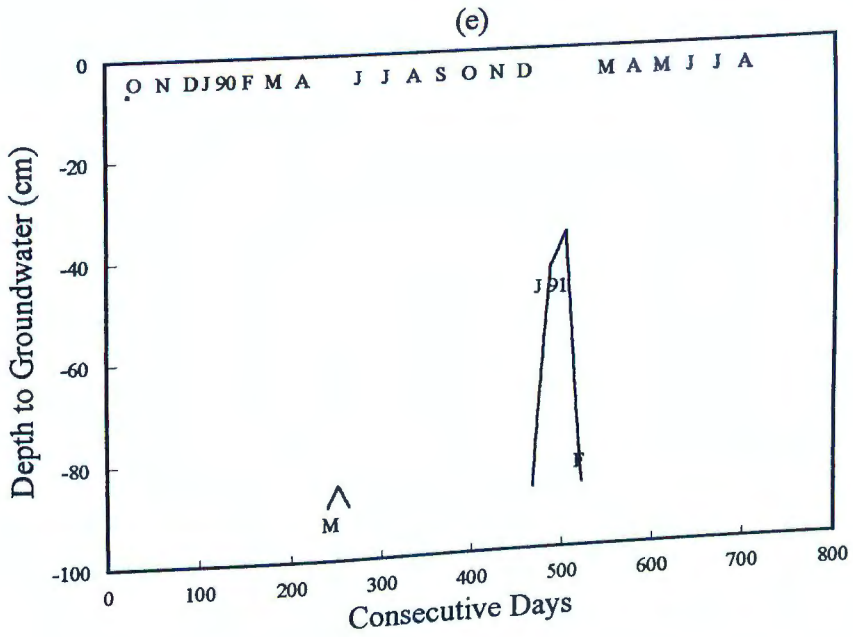

Figure 4-4. Consecutive water table heights for e) pedon FC5.

Table 4-1. Abbreviated Soil Descriptions for both sites.

Horizon	BD	Org C	Matrix Color	Mottle 1 Color	Mottle 2 Color	Mottle 3 Color
	Mg/m3	%				
			MC1---Typic Ochraqualf			
A	1.37	1.62	10YR 4/3			
Ap	1.64	0.85	10YR 4/4	2.5Y 6/3	10YR 5/6	
Btg1	1.82	0.39	2.5Y 6/2	7.5YR 6/6	10YR 5/4	
Btg2	1.87	0.25	2.5Y 5/3	5YR 5/6	7.5YR 5/8	2.5Y 5/2
Btg3	nd	0.21	2.5Y 6/2	7.5YR 5/4	7.5YR 5/8	
2BC	1.79	0.32	2.5YR 4/4	5YR 7/3	7.5YR 6/3	7.5YR 4/6
			MC2---Typic Fragiaqualf			
A	1.54	2.04	10YR 4/3			
Ap	1.73	0.73	10YR 4/4	10YR 5/6		
Btg	1.82	0.28	10YR 5/3	7.5YR 5/8	5YR 5/6	10YR 5/2
Bx1	1.89	0.15	2.5YR 4/6	5YR 5/8	7.5YR 5/2	7.5YR 5/4
Bx2	1.77	0.19	2.5YR 4/6	5YR 5/8	7.5YR 5/2	7.5YR 5/4
2BC	1.86	0.10	5YR 4/6			
3BCg	1.79	0.18	10YR 7/1			
3BCg			2.5YR 4/4	10YR 6/1	7.5YR 5/6	
			MC3---Aeric Fragiaqualf			
Ap	1.55	1.51	10YR 4/3			
Bt	1.70	0.35	10YR 5/3	7.5YR 5/6	5YR 5/8	
Bx1	1.87	0.20	5YR 3/4	7.5YR 6/8	10YR 6/2	
Bx2	1.91	0.18	5YR 4/6	10YR 5/6	5Y 6/1	
Bx3	1.82	0.13	5YR 3/4	10YR 6/8	5Y 6/1	
2BCg	1.80	0.17	2.5Y 7/2	7.5YR 5/8	5YR 5/4	
			MC4---Aquic Fragiudalf			
Ap	1.47	1.23	5YR 4/4			
Bt1	1.77	0.26	2.5YR 3/6			
Bt2	1.88	0.15	2.5YR 3/6	7.5YR 5/6	7.5YR 5/4	N 2/0
Btx1	1.75	0.09	2.5YR 3/6	5YR 6/2	7.5YR 5/6	
Btx2	2.18	0.10	2.5YR 3/6	7.5YR 5/6	10YR 7/2	N 2/0
Cr	nd	0.06	2.5YR 3/6	2.5Y 6/2		
			MC5---Alfic Hapludult			
Ap	1.61	0.79	10YR 4/4			
Bt1	1.79	0.43	7.5YR 4/6	10YR 5/4		
Bt2	1.76	0.30	7.5YR 4/4	7.5YR 5/8		
BC	1.80	0.11	5YR 3/4	7.5YR 5/6	5YR 6/4	
C1	1.82	0.12	5YR 4/3	5YR 5/8	5YR 5/4	
2C2up	1.87	0.09	5YR 5/4	7.5YR 5/8	10YR 7/3	
2C2lo	1.75	0.06	2.5YR 3/6	5YR 6/6		
3R	nd	0.16	2.5YR 3/6			

Table 4-1 (cont). Abbreviated soil descriptions for both sites.

Horizon	BD	Org C	Matrix Color	Mottle 1 Color	Mottle 2 Color	Mottle 3 Color
	Mg/m3	%				
			FC1---Ultic Ochraqualf			
Ap	1.57	1.55	10YR 4/3			
Btg1	1.60	0.50	10YR 6/2	7.5YR 5/6		
Btg2	1.62	0.33	10YR 5/2	7.5YR 5/6		
2BC	1.78	0.16	5YR 4/3	7.5YR 5/8	10YR 6/1	10YR 4/1
3BC	1.80	0.10	5Y 5/2	2.5Y 5/2	2.5YR 4/6	
4BCg1	nd	0.07	5Y 5/2	2.5Y 6/2	5YR 4/4	5YR 5/8
4BCg2	nd	0.02	5Y 6/2	2.5Y 6/2	5YR 4/4	5YR 5/8
4BCg3	nd	0.13	5Y 6/2	2.5Y 6/2	5YR 4/4	5YR 5/8
5Cr	nd	0.08				
			FC1A---Aeric Fragiaqualf			
Ap	1.45	1.29	10YR 4/3			
Bt1	1.58	0.38	7.5YR 5/8	10YR 6/3	7.5YR 6/4	10YR 6/3
Bt2	1.70	0.19	2.5YR 3/4	7.5YR 5/2	5YR 4/6	2.5YR 5/8
2Bxup	1.83	0.10	2.5YR 3/4	2.5Y 5/2	10YR 4/1	N 2/0
2Bxlo	1.85	0.05	2.5YR 3/4	2.5Y 5/2	10YR 4/1	N 2/0
wh sm	nd	0.12	2.5Y 7/2			
2Cr	nd	0.06	2.5YR 3/4	7.5YR 6/2	N 2/0	
			FC2---Aquic Fragiudalf			
Ap	1.46	1.44	5YR 4/4			
BE	1.56	0.36	5YR 5/3	5YR 5/6		
Bt	1.69	0.23	2.5YR 4/4	5YR 5/8		
2Bx	1.74	0.09	2.5YR 3/4	5YR 7/1		
2BC	1.86	0.06	2.5YR 3/4	5YR 7/2	10YR 5/2	
3Crt	1.78	0.07	2.5YR 3/4	5YR 8/2		
wh sm	1.82	0.15	5YR 7/1			
3R	nd		2.5YR 3/4	5YR 8/2		
			FC3---Aquic Hapludult			
Ap	1.37	1.45	2.5YR 4/3			
BA	1.45	0.58	2.5YR 3/4			
Bt1	1.62	0.22	2.5YR 3/4			
Bt2	1.70	0.15	2.5YR 3/4			
Bt3	1.86	0.09	2.5YR 3/4	5YR 4/6		
2Crt	2.13	0.06	2.5YR 3/4	5YR 5/1	5YR 7/1	N 2/0
			FC4---Typic Eutrochrept			
Ap	1.47	1.22	5YR 3/3			
Bw1	1.56	0.27	2.5YR 3/4			
Bw2	1.64	0.13	2.5YR 3/6	10YR 5/6		
BC	1.75	0.15	5YR 4/3	7.5YR 6/6	N 3/0	
Cr	2.02	0.08	5YR 4/3	N 3/0		

Table 4-1 (cont). Abbreviated soil descriptions for both sites.

Horizon	BD	Org C	Matrix Color	Mottle 1 Color	Mottle 2 Color	Mottle 3 Color
	Mg/m3	%				
		FC5---Ultic Hapludalf				
Ap	1.39	1.26	5YR 3/3			
Bt1	1.71	0.16	5YR 3/3			
Bt2	1.67	0.11	5YR 3/4			
Bt3	1.77	0.09	5YR 3/4			
2BCt1	1.85	0.05	2.5YR 3/4			
3BCt2	1.71	0.04	2.5YR 3/4			
4Crt	nd	0.07	2.5YR 3/4			

water table level drops beneath the deepest well by July in both pedons. The duration of the water table within 40 cm of the soil surface during a portion of the growing season for both pedons would be expected to create redoximorphic features in this portion of the profile.

It is important to observe that while the hydrology is very similar between pedons FC1 and FC2 (and presumably similar in FC1A), a strikingly different morphology is expressed in each of these pedons (Table 4-1). Gleying occurs directly below the Ap (10YR 4/3, brown to dark brown) and predominantly throughout the profile in pedon FC1 and only occurs in a thin seam directly above the parent materials in pedons FC1A and FC2. The color of the Ap horizon is 10YR 4/3 (brown to dark brown) for pedons FC1 and FC1A and 5YR 4/4 (reddish brown) for pedon FC2. The color of the underlying argillic horizon is 10YR 6/2 (light brownish gray) in pedon FC1, 7.5YR 5/8 (strong brown) in the upper part and 2.5YR 3/4 (dark reddish brown) in the lower part in pedon FC1A, and 2.5YR 4/4 (reddish brown) in pedon FC2. The predominant hue of the horizons underlying the argillic horizon is 5Y for pedon FC1 and 2.5YR for pedons FC1A and FC2. Additionally, the abundance of iron oxide concentrations (i.e high chroma mottling) or depletions (i.e. low chroma mottling) decreases from pedon FC1 to pedon FC2. Manganese oxide concentrations (i.e. neutral hue stains) occur only in the lower solum of pedon FC1A.

Generally, pedon FC1 is predominantly gray with brownish mottles whereas pedon FC2 is predominantly reddish brown with low chroma mottles.

The hydrology/morphology relations of pedons FC3 to FC5 are described in a later section.

MC Site Hydrology/Morphology Relations

Nearly identical curves for both the cumulative frequency (Figure 4-5) and consecutive daily water heights occur for pedons MC1, MC2, and MC3 (Figures 4-6a to 4-6c). All three pedons have the water table present within 40 cm of the surface approximately 300 or more days of the two-year study period. Additionally, the water table in these three pedons is initially observed in November, rises towards the surface in January, and begins to recede in late April. The water table completely recedes by July in these three pedons. Within these three pedons, the water table remains within 60 cm of the surface from the start of the growing season until the water table level recedes below the deepest well.

Because of the similar hydrological status of these three pedons, the morphological expressions might also be expected to be similar. The morphologies of these pedons, however, are strikingly different. Pedon MC1 shows a greater degree of iron mobilization and segregation than pedons MC2 and MC3 (Table 4-1). Gleyed or near gleyed

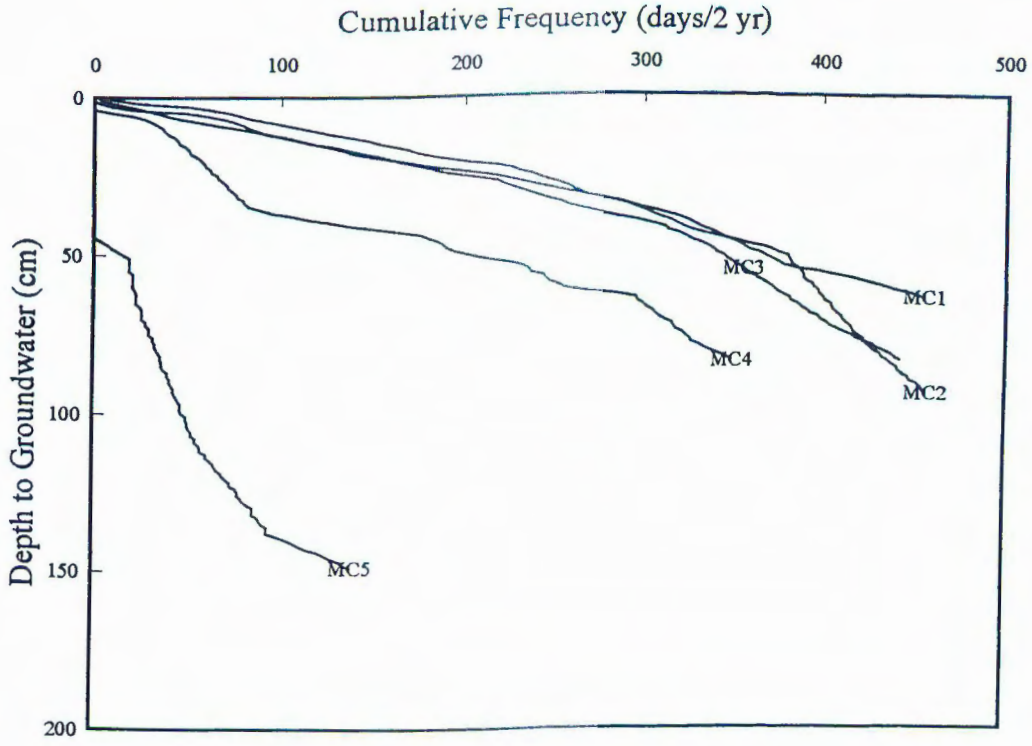

Figure 4-5. Cumulative frequency curves of the hydrology associated with the pedons of the MC site.

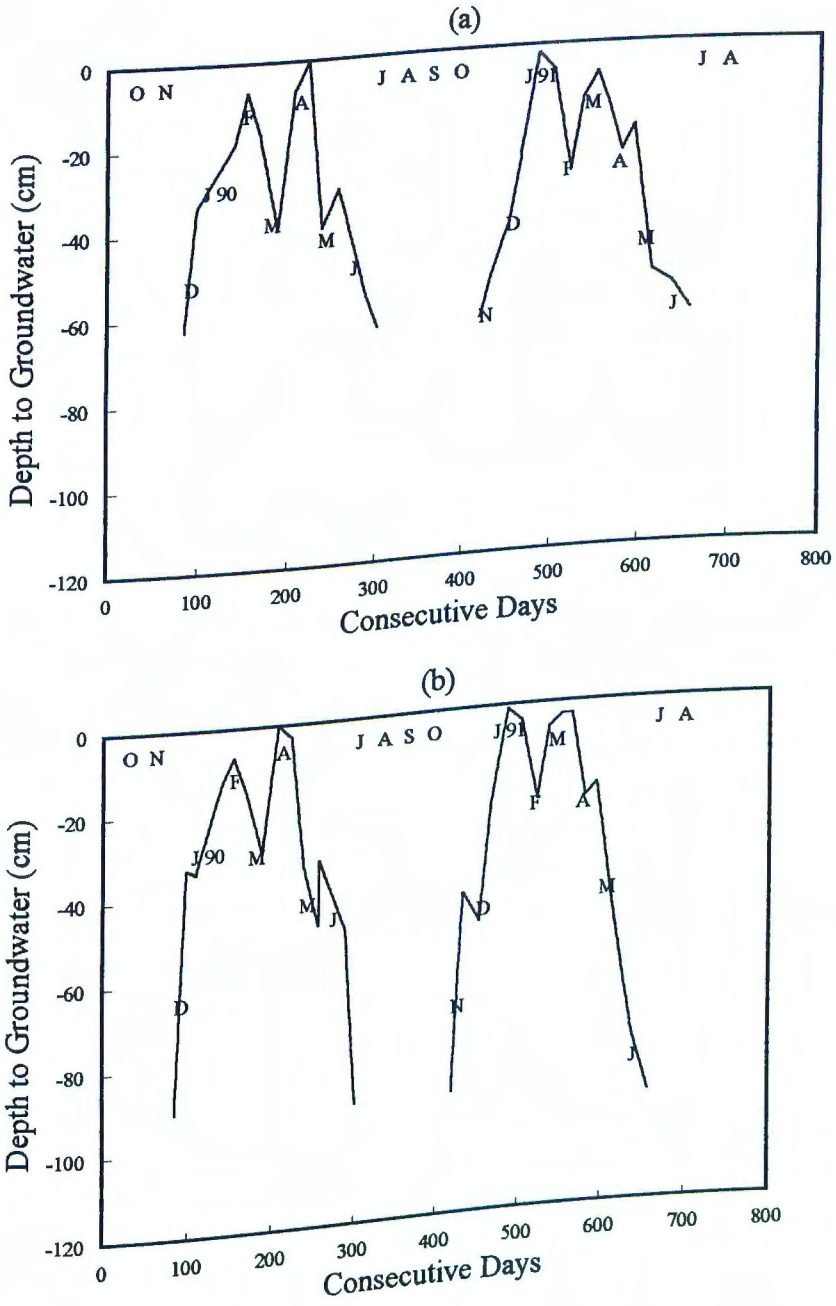

Figure 4-6. Consecutive water table heights for a) pedon MC1 and b) pedon MC2.

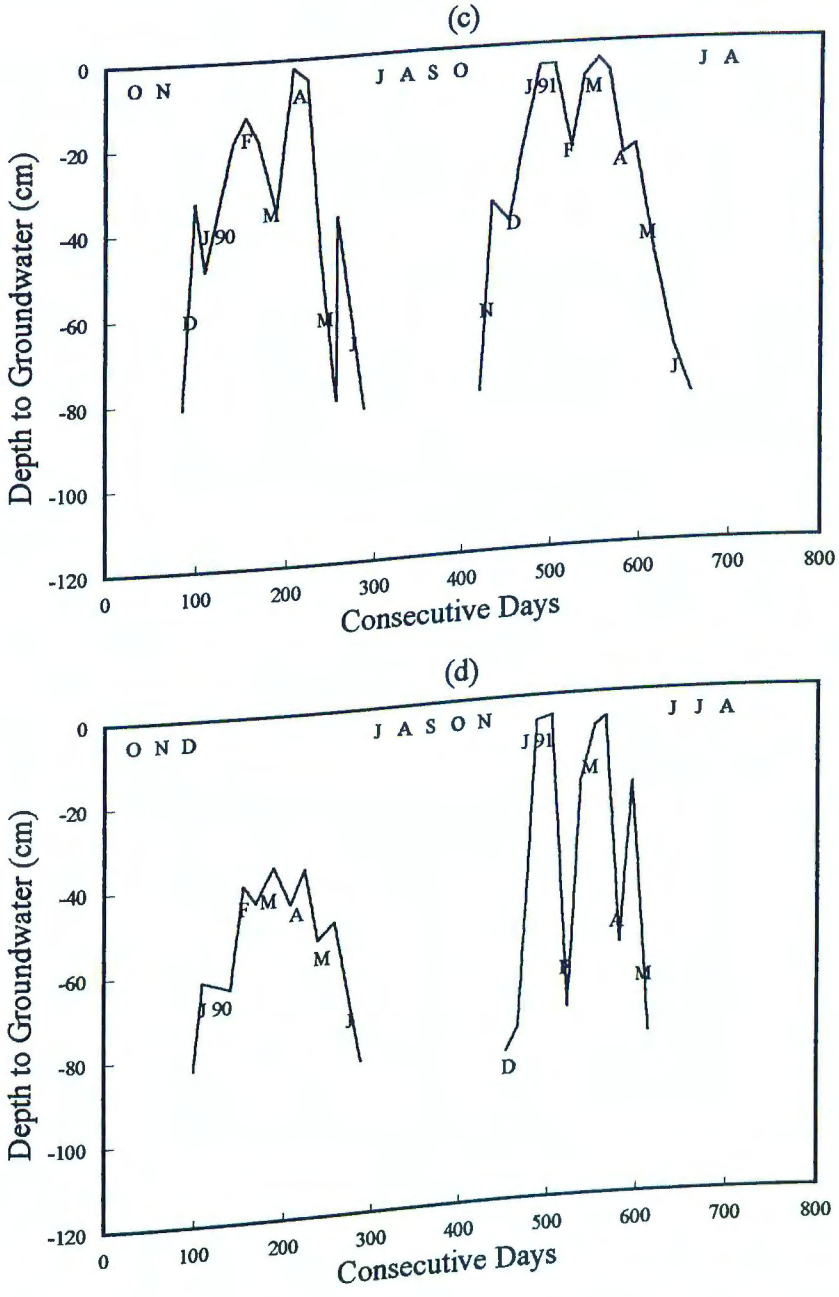

Figure 4-6. Consecutive water table heights for c) pedon MC3 and d) pedon MC4.

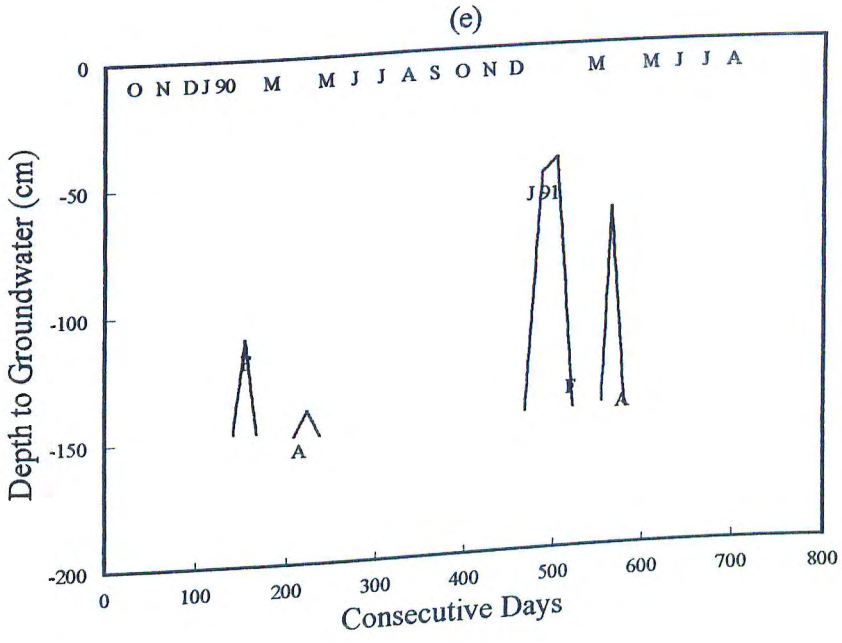

Figure 4-6. Consecutive water table heights for e) pedon MC5.

conditions occur beneath the Ap horizon of pedon MC1 until the reddish brown (2.5YR 4/4) BC horizon is encountered. Gley conditions occur only at depth in pedons MC2 (upper 3BCg) and MC3 (2BCg). High chroma mottling also occurs within the Ap horizon of pedons MC1 and MC2, but not pedon MC3. Distinct low chroma coatings occur along prism faces in pedons MC2 and MC3 but are absent in pedon MC1. Reddish hues were observed within the fragipan in pedons MC2 and MC3, but only occurred in the 2BC horizon of pedon MC1. Generally, pedon MC1 is predominantly gray beneath the Ap horizon with brownish mottles, pedon MC2 has a brown argillic horizon overlying the predominantly red lower solum with yellowish red, strong brown, or low chroma mottles, and pedon MC3 is predominantly red beneath the Ap horizon with low chroma mottles in the lower solum.

The hydrology/morphology relations of pedons MC4 and MC5 are described in a later section.

Discussion

Factors Responsible for the Hydrology/Morphology Contrast

In both locations (FC and MC sites) the lower three pedons of each THS demonstrated very similar hydrology yet very different morphology with respect to redox-related features. Four alternative hypotheses will now be addressed concerning soil properties which may explain the contrast in the development of redoximorphic features in these soils

which have very similar hydrology.

The first hypothesis concerns the distribution of organic carbon content throughout each pedon. Because organic carbon is required as an energy source for the microbially-mediated reduction of the Fe/Mn oxides, the occurrence of the seasonally-high water table in organic carbon-rich horizons may induce the development of redoximorphic features within these saturated horizons.

The organic carbon (OC) data for the soils are shown in Table 4-1. The OC levels for the Ap horizons of pedons FC1, FC1A, and FC2 are 1.55%, 1.29%, and 1.44%, respectively. The OC levels for the argillic horizons (weighted average) of pedons FC1, FC1A, and FC2 are 0.43%, 0.26%, and 0.23%, respectively. The OC levels for the Cr horizons for these three pedons are 0.08%, 0.06%, and 0.07%. For the MC site, the OC levels for the entire A and/or Ap horizons for pedons MC1, MC2, and MC3 (weighted average) are 1.20%, 1.20%, and 1.51%. The OC levels for the argillic horizons (weighted average) of pedons MC1, MC2, and MC3 are 0.31%, 0.28%, and 0.35%, respectively. The OC levels for the BC horizons for these three pedons are 0.32%, 0.18%, and 0.17%. Due to the similarity of the OC levels among the three pedons of each THS, it does not appear that the contrast in morphology can be explained on the basis of differences in the quantity and/or distribution of OC in these soils.

The second hypothesis is that the soil temperature during periods of saturation will affect the development of redoximorphic features. Because temperatures above biologic zero stimulate microbial activity and the reduction of Fe/Mn oxides is microbially-mediated, differences in the actual number of days above biologic zero when a seasonally-high water table is present may account for differences in the development of redox-related morphology among otherwise similar soils.

While some slight temperature differences might be expected between the two locations (approximately 40 miles between the MC and FC sites), minimal to no differences with respect to soil temperature would be expected between pedons of one location given the close proximity (approximately 100 feet apart) and similar slope and aspect among these pedons. Therefore, it does not appear that the contrast in soil morphology can be explained on the basis of differences in soil temperature during saturation episodes in these soils.

The third hypothesis is that differences in the nature and amount of vegetation may affect the development of redoximorphic features. The vegetation acts an energy source for the microorganisms and the population of the microorganisms may then be related to the nature and amount of vegetation. Therefore, differences in the type or quantity of vegetation among otherwise similar pedons might account for redox-related morphological differences in

soils.

At each THS, however, the vegetation was uniform across the sites. At the FC site, milo has been grown over the whole site for the past two years. At the MC site, timothy hay has been grown over the whole site for the past 3 years. Therefore, it appears that this hypothesis can not explain the contrast in soil morphology among these pedons.

The fourth hypothesis is that differences in the nature of the parent materials from which these soils have formed are responsible for the redox-related morphological differences observed.

Based upon the results of Chapter 3, the upper sola of pedons FC1, FC1A, MC1, and MC2 were derived in part from local alluvium or downslope colluvial debris whereas pedons FC2 to FC5 and MC3 to MC5 were derived from residuum or colluviated residuum. Pedons FC2 and MC3, which are derived mainly from the red Triassic residuum failed to demonstrate gleying or a high degree of redoximorphic alterations. Pedons FC1, FC1A, MC1, and MC2, which have their upper sola mainly derived from loess and/or colluvial/alluvial additions, show a predominance of gleying and a high degree of redoximorphic feature development in the upper part of their sola. Therefore, it appears that the contrast in the soil morphology among these hydrologically-similar pedons can be attributed to differences in the nature of the parent differences. It is believed that although redoximorphic

features are created by redox processes, the nature of the parent materials mediates their development.

Inhibition of Redoximorphic Features in Triassic Parent Materials

As described above, pedons principally derived from Triassic parent materials failed to develop a high degree of redox-related morphology (i.e. gleying), while soils derived principally from local alluvium/colluvium with a similar hydrology produced substantial gleying and mottling. This indicates that there is a factor associated with the red Triassic parent materials which inhibits the development of redoximorphic features. There are three hypotheses which may explain this inhibitory effect.

The first hypothesis is related to the degree of Al-substitution in the iron oxides. Fey (1983) as stated in Schwertmann and Taylor (1989) has shown that increasing Al-substitution causes an increased thermodynamic stability of the iron oxide as compared to its pure end-member. The net effect is that, at a given pe and pH, Al-substituted iron oxides will be less easily reduced than their pure analogs and will therefore retard the development of redoximorphic features. For example, Al-substituted goethites in soils of Brazil were shown to be relatively redox stable as compared to the coexisting hematite which had a lower degree of Al-substitution (Macedo and Bryant, 1989).

Data presented in Chapter 2 has shown that an Al-

substituted hematite (7-8 mole % Al_2O_3 in Fe_2O_3) does occur in these parent materials which is inherited in the soils derived from these rocks. These levels of Al-substitution may account for the increased stability of the hematite against reduction in these soils. Therefore, this hypothesis may explain the weak expression of redox-related features in the residually-derived pedons (FC2 and MC3).

The second hypothesis is related to the quantity of iron oxides within the parent materials. Because gleyed or near gleyed features require the absence or near absence of soil coloring agents, higher levels of iron oxides may inhibit the expression of redox-related morphology by requiring longer reduction episodes to develop gleyic features.

The iron oxide content of these soils is shown in Table 5-1. Dithionite extractable iron (Fe_d) levels for the upper argillic horizon ranges from 1.2 to 3.8% with an average of 2.5%. Wright (1972) observed similar Fe_d ranges in the upper argillic horizons for other loess-affected Coastal Plain soils (i.e. Magnolia series range from 1.6 to 2.0% Fe_d with average of 1.8%; Caroline series range from 1.4 to 1.7% Fe_d with average of 1.6%). Darmody (1980) also observed similar Fe_d ranges in the upper argillic horizons for other loess-affected Piedmont soils (i.e. Chester series range from 1.6 to 3.3% Fe_d with an average of 2.5%; Elioak series range from 2.9 to 4.3% with an average of 3.6%). The wetter

soils assoicated with these display a greater expression of redoximorphic features than those derived from red Triassic residuum. Therefore, it does not appear that the iron oxide content of the residually-derived soils can explain their inhibition of redoximorphic feature development.

The third hypothesis is that redoximorphic features are slow to develop because iron oxides are occluded within both sand and silt-sized grains. This occlusion would cause these grains, following reduction episodes, to continue to display a reddish or pinkish cast but not a greyish cast even though all prior coatings were removed.

Munsell colors of both dithionite treated and untreated whole soils and their sand fractions are listed in Table 4-2. The samples used in this experiment were red horizons from residually-derived soils. Results show that while the whole soil colors of extracted samples are low chroma colors (chroma of 1 or 0), the sand-size grains in these extracted samples still retain reddish or pinkish colors. Therefore, while low chroma colors can apparently form in these materials, this hypothesis does have some merit in the stabilization of the red color in these soils and sediments.

The inhibitory effect on the development of redoximorphic features in soils derived from red Triassic rocks is thus believed to be due to the increased stability associated with the Al-substituted hematite and the occlusion of Fe oxides within sand and silt-sized grains.

Table 4-2. Munsell Colors of dithionite treated and untreated for selected whole soils and sand fractions derived from red Triassic parent materials.

Sample	Whole Soils Dithionite		Sand Fraction Dithionite	
	Untreated	Treated	Untreated	Treated
	<----------Munsell Color---------->			
MC4 Cr	2.5YR 3/6	5Y 5/1	2.5YR 3/4	5YR 4/3
MC5 2C2lo	2.5YR 3/6	5Y 4/1	2.5YR 3/4	5YR 5/2
MC5 3R	2.5YR 3/6	5Y 4/1	2.5YR 3/4	5YR 6/2
FC4 Cr	2.5YR 3/4	N 5/	2.5YR 3/4	5YR 5/2
FC5 3BCt2	2.5YR 3/4	5Y 4/1	2.5YR 3/4	5YR 5/2
FC5 4Crt	2.5YR 3/4	N 5/	2.5YR 3/4	5YR 4/2

Hydrology/Soil Morphology Relations

Because field soil scientists have long relied upon the location of low chroma features to discern soil drainage classes, one general hypothesis for the second question states that the height and the duration of the seasonally-high water table may be correlated with the location of redoximorphic features in these soils. In order to address the impact of hydrology upon the morphology of these soils, uniformity of parent materials of the examined pedons is necessary. Because the impact of the hydrology on the morphologies of the pedons affected by loess and/or colluvial/alluvial additions has been presented above, this section will therefore only address the impact of hydrology upon the development of redoximorphic features in the pedons principally derived from residuum.

Within pedons FC2-FC5, hydrological differences are observed between these pedons. The cumulative frequency curves of the hydrology associated with pedons FC2, FC3, FC4, and FC5 show, respectively, a decrease in the total number of days the water table was observed in the upper solum of each pedon (Figure 4-3). The water table was observed within 40 cm of the surface for 329 d in pedon FC2, 111 d in pedon FC3, 39 d in pedon FC4, and only 10 d in pedon FC5 for the two-year period. For consecutive daily water heights in these four pedons, both the persistence within the upper solum and the overall duration of the water

table decreases from pedon FC2 to pedon FC5 (Figures 4-4b to 4-4e). Generally, the water table for pedons FC3 to FC5 is initially observed in late December, rises towards the soil surface in January, and begins to recede in late January or early February. In contrast to the other pedons, the water table in pedons FC3 to FC5 does not persist at a given depth for a long duration (i.e. greater than 3 weeks) and undergoes many short wetting/drying cycles throughout the "wet" season. The net effect is the appearance of "spikes" in their consecutive water table heights data (Figures 4-4c to 4-4e). For pedons FC3 and FC4, the water table level usually drops below the deepest well by May and by March for pedon FC5. The duration of the water table in pedons FC3 and FC4 within a portion of the growing season may allow for the formation of redoximorphic features in these soils. The recession of the water table prior to the growing season for pedon FC5 will probably favor the stability of the inherited hematite in this pedon. Also, the progressively lower OC levels from pedons FC2 to FC5 should adversely affect the development of redoximorphic features as the summit is approached (Table 4-1).

Morphologically, high chroma mottles occur to within 25 cm of the soil surface and low chroma mottles below 60 cm in pedon FC2. The percentage of the time that the water table level occurred at these two depths are 40% and 49%. In pedons FC3 to FC5, no gleying was observed within any of

these three pedons (Table 4-1). Segregation of iron oxides did occur but only as low chroma mottles in the 2Crt horizon of pedon FC3 was observed. The dominant redoximorphic feature observed within pedons FC3 and FC4 was manganese stains in the BC and/or saprolitic horizons. Apparently in these landscape positions, the reduction of manganese is possible but not iron. The percentage of the time that the water table level occurred where these manganese stains were formed in pedon FC4 is 8.4%.

The cumulative frequency curves for the water table associated with pedons MC4 and MC5 show an expected lesser degree of upper solum wetness than the downslope MC1, MC2, and MC3 pedons (Figure 4-5). For pedon MC4, the water table was within 40 cm of the soil surface for 126 days over the two-year observation period. For pedon MC5, the water table was never observed within 40 cm of the soil surface. The curve for consecutive daily water heights for pedon MC4 shows the water table is initially observed in December, rises towards the soil surface in January, persists as high as 5 cm below the soil surface, and begins to recede in May (Figure 4-6d). The water table level drops below the deepest well by late May to mid June. The curve for consecutive daily water heights for pedon MC5 shows the water table is initially observed in mid December to January, occurs as high as 45 cm, and begins to recede in April (Figure 4-6e). The ephemeral nature of the water

table associated with pedon MC5 produces the "spikes" observed in the consecutive water table height data (Figure 4-6e). The water table level for pedon MC5 drops below the deepest well by May.

Because of the short duration of the water table within the upper solum of pedons MC4 and MC5, their morphologies would be expected to lack redoximorphic feature development. These expected morphologies are observed for these pedons. No gleying was observed within these two pedons (Table 4-1). Low chroma mottling associated with iron mobilization and segregation was observed only within the Cr horizon of pedon MC4. Coatings of manganese were also observed in this pedon, in both the lower argillic horizon and fragipan. No such low chroma mottling or manganese coatings were observed within pedon MC5. High chroma mottles occur from the lower argillic horizon throughout the lower solum but these mottles are not interpreted as drainage mottles and probably represent weathered shale and/or sandstone fragments.

The lower incidence of redoximorphic feature development in the pedons MC4, MC5, FC3, FC4, FC5 may be attributed to the short duration of the water table in the upper solum of these five pedons, particularly within the growing season. This short duration combined with frequent aeration of the soil and low OC levels (Table 4-1) favors the stability of the iron oxides in these pedons. As found for the wetter MC3 and FC2 pedons, stabilization of the red

color in these five pedons is also enhanced by the presence of the Al-substituted hematite and the occlusion of the iron oxides within both sand and silt-sized grains.

It is important to note that the impact of hydrology upon the development of redoximorphic features is shown to a much lesser degree in the soils derived principally from residuum than the soils whose upper sola were affected by local alluvium/colluvium additions. Therefore, the nature of the parent materials mediates the development of redox-related features of the soils in these landscapes.

Conclusions

While several factors are known to affect redox processes in wet soils, including OC content, vegetation, and soil temperature, these factors were insufficient to explain differences in morphology observed among hydrologically-similar soils.

Redoximorphic feature development in soils of Triassic basins appears mediated by the nature of the parent materials. Within pedons whose upper sola are influenced by loessal or colluvial/alluvial additions, substantial development of redoximorphic features was observed in those which had persistent seasonally-high water tables. Gleying and high chroma mottling occurred directly beneath the plow layer. Within hydrologically-similar pedons derived mainly from Triassic residuum, no gleying was observed in the zone

directly under the Ap horizon and they were dominantly red or brown in color. The development of three chroma matrices having high chroma mottling may be indicative of the depth to the seasonally-high water table in these soils derived principally from residuum. The weak expression of redoximorphic feature development in these pedons is due primarily to the presence of Al-substituted hematite and to a lesser degree by the occlusion of iron oxides within sand and silt-sized grains.

Among pedons derived principally from residuum, hydrological factors are responsible for the development of redoximorphic features. However, this relationship between the hydrology and the redox-related morphology is different from soils derived from other parent materials. The increased duration of the water table in the upper solum, during the growing season, caused a gradual increase in the incidence of redoximorphic features downslope. These effects were markedly affected by downslope accumulations of contrasting soil materials.

The morphology/hydrology relationship observed in these red soils appear to fit the secondary pseudo-gley model as described by Fanning and Fanning (1989) and the epiaquic conditions as determined by ICOMAQ (1989). Meteoric water, during times when precipitation exceeds evapotranspiration demands, is believed to create a seasonally-high water table within these pedons and assist in the coloration patterns of

these soils.

Future research on the development of redoximorphic features in soils derived from similar red sediments should assess the degree of parent material uniformity existing within those soils due to the mediating effect that the nature of the parent materials has upon the formation of these features.

CHAPTER 5

IRON OXIDE CHEMISTRY AND MINERALOGY OF THE SOILS

Previous investigations have shown the importance of the iron oxide mineralogy in determining soil color. Bigham et al. (1978) observed a higher proportion of hematite (α-Fe_2O_3) relative to goethite (α-FeOOH) in the soils having reddish hues than in the soils having yellowish hues. Schwertmann et al. (1982) also observed hematite to be responsible for the color of soils having hues ranging from 7.5YR to 5YR whereas goethite was solely responsible for the color of the soils having yellower hues. Davey et al. (1975) and Schwertmann et al. (1982) have also noted that 10YR or yellower hues are due solely to goethite but that reddening to 5YR hue is possible even with the addition of minor amounts of hematite. Furthermore, Fitzpatrick et al. (1985) has shown lepidocrocite (γ-FeOOH) to be commonly associated with 7.5YR 6-7/4-8 colors. Soil color, particularly for B and C horizons, therefore appears to be primarily related to the iron oxide mineralogy, but the purity, crystallinity, and particle size affects the resulting color of each iron oxide (Schwertmann and Taylor, 1989).

Along topohydrosequences (THS), coloring patterns often reflect the color of the strongest pigmenting iron oxide at each point along the sequence. Macedo and Bryant (1987) observed reddish hues (2.5YR or 5YR) and a codominant hematite and goethite iron oxide mineralogy for the well-drained soils and yellowish hues (10YR or 7.5YR) and a

dominantly goethitic iron oxide mineralogy in the upper organic rich solum of the more poorly-drained soils along a topohydrosequence of Oxisols in Brazil. Pedogenic yellowing of red soils is believed to be due to preferential microbial reduction of the hematite over the goethite. This is caused by increased stability of goethite via Al-substitution thereby resulting in the morphological expression of yellow hues and a dominantly goethitic iron oxide mineralogy (Fey, 1983; Macedo and Bryant, 1989). Similar morphological expressions along other topohydrosequences have also been observed (Simonson and Boersma, 1972; Karim and Adams, 1984; Pickering and Veneman, 1984).

In the present study, concern is focused upon the coloring patterns observed within two topohydrosequences derived from dusky red shales and sandstones (5YR and redder) in the Triassic Culpeper Basin of Maryland. This basin is one member of a series of Triassic-aged basins occurring along the Mid-Atlantic USA. Previous results have shown that an Al-substituted hematite (7-8 mole% Al_2O_3 in Fe_2O_3) is the only iron oxide within these red parent materials and is responsible for its color (Chapter 2). Goethite and hematite often coexist in warmer climates (particularly in warm temperate, tropical, and subtropical regions) but pedogenic hematite forms only rarely relative to goethite in cooler climates (Schwertmann and Taylor, 1989). Therefore, the monomineralic iron oxide parent

material provides an opportunity in the present study to examine possible iron oxide transformations in the soils derived from these parent materials as a function of hydrological differences along topohydrosequences.

Materials and Methods

Eleven pedons located along two topohydrosequences in the Triassic Culpeper Basin of Maryland were examined. One site was located in northern Frederick county (FC site) near the town of Emmittsburg and the other site was located in western Montgomery county (MC site) near the town of Boyds. Site descriptions, including the topographical cross-sections for both sites, are given in Chapter 3. All pedons were examined by either backhoe or hand-dug pits representing the major hillslope elements along each topohydrosequence. Each pedon was described using standard soil description techniques and was classified using Soil Taxonomy (Soil Survey Staff, 1990). Moist Munsell colors were reported for all matrices, mottles, and coatings. A composite sample for each horizon was collected for basic soil characterization data (i.e. particle-size analyses, CEC, pH, mineralogy, etc.) and chemical analyses (i.e. selective dissolution of the Fe/Mn oxides). In those pedons having redoximorphic features, large undisturbed clods were collected for mineralogical/chemical examination of the redoximorphic features present.

Bulk samples were air-dried and then lightly ground prior to sieving through a 2 mm sieve. This light grinding was performed so as to minimize the crushing of any gravel-sized Fe/Mn nodules. A subfraction of the <2 mm fraction of each horizon was then ground in a ball mill mixer for five minutes for sample homogenization and the disintegration of any sand-size Fe/Mn nodules. These ground samples were then oven-dried at 105° C and stored in a desiccator prior to use in selected chemical analyses. A 1.000 g subfraction of the oven-dried ground soil was also fractionated (using 5% Na_2CO_3 as the dispersing agent) into its clay and nonclay fractions without prior removal of Fe cements in order to determine the size partitioning of the iron oxide(s). Redoximorphic features (mottles, nodules, and coatings) as well as the matrix from two horizons per pedon which contained such features were hand-separated, based upon differences in color, from the large field moist clods. Because sufficient amounts were required for the analyses, each feature is a composite of that colored mottle, matrix, nodule, or coating. These features were air-dried, crushed in an agate mortar and pestle for sample homogenization, oven-dried at 105°C, and stored in a desiccator prior to chemical and mineralogical analyses.

Chemical analyses on the ground soils were performed to quantify the amount, and to determine the crystallinity, of the iron oxide(s) present. These analyses included a)

sodium dithionite citrate buffer (DCB) on the ground whole soils, the clay fraction, and redoximorphic features (Kittrick and Hope, 1963), and b) acid ammonium oxalate in the dark (Schwertmann, 1964) on the whole ground soils and redoximorphic features. Dithionite-extractable iron (Fe_d) is a measure of the total free iron oxide content of a sample, independent of its crystallinity, whereas oxalate-extractable iron (Fe_o) is considered to measure the poorly-crystalline or amorphous form of iron oxides. For DCB analyses, duplicate 1.000 g samples of ground oven-dried soil or 0.100 g samples of each redoximorphic feature were used with approximately 0.8 g of sodium dithionite and 100 ml final volume of the citrate buffer at pH 7.3. For oxalate analyses, duplicate 1.000 g of oven-dried ground soil or 0.100 g of each redoximorphic feature was used in a 1:100 soil weight to oxalate solution volume. This suspension was then shaken in the dark for two hours and immediately centrifuged and filtered. Additionally, total digestion of the ground whole soils was performed to determine the total iron content of each sample (Fe_t) following a modification of Lim and Jackson's (1982) procedure involving nitric, sulfuric, and hydrofluoric acids but using 30% hydrogen peroxide in place of perchloric acid. Duplicate 0.100 g samples of air-dried ground soil were dissolved in a 100 ml final volume of 6N HCl. All extracts were stored in a refrigerator (< 5°C) prior to analyses. Iron, Mn, and Al

were determined in all extracts by atomic absorption spectroscopy.

For mineralogical analyses, x-ray diffraction (XRD) of the sand, silt, and clay fractions for each pedon was performed with no prior removal of the iron oxides. This was done to document the occurrence of the iron oxides as a function of particle size in these soils. Both the sand and silt fractions were ground in an agate mortar and pestle and slides were prepared using a slurry of the ground sand or silt and 95% ethanol. For the clay fraction, oriented slides of K-saturated and Mg-saturated clays (using 1 M KCl and 0.5 M $MgCl_2$) were prepared using the filter-membrane peel technique of Drever (1973). Approximately, 50 to 100 mg of clay was used in the preparation of these slides. All clay slides were examined by XRD following these treatments: a) Mg-saturation followed by ethylene glycol solvation at room temperature, b) K-saturation followed by air-drying at room temperature, c) K-saturation followed by a heat treatment of 300°C for two hours, and d) K-saturation followed by a heat treatment of 550°C for two hours. To determine the iron oxide mineralogy of the redoximorphic features, XRD following 5M NaOH treatment of the clay fraction from each feature was performed in order to concentrate the iron oxides via silicate dissolution (Norrish and Taylor, 1961). Approximately 50 to 100 mg of clay was used for this analysis.

All XRD was performed using CuKα radiation from a Norelco diffractometer equipped with a graphite monochromator and a theta-compensating slit. Scans were run from 2-45° 2θ using a scan rate of 2° 2θ per minute.

Results and Discussion

Sand and Silt Mineralogy

Based upon peak height analysis, quartz and muscovite were the two most dominant silicate minerals in the sand and silt-size fractions (Appendix C). Sand-size muscovite content appeared to decrease toward the soil surface, probably as a result of disintegration of sand size muscovitic shale fragments due to increased physical weathering nearer the soil surface. Both potassium feldspar and sodium-rich plagioclase feldspar were minor constituents in these two size fractions throughout all horizons. Sand-size kaolinite and chlorite occurred only at depth within pedons MC4 and MC5. Silt-size kaolinite, however, occurred in nearly every horizon and tends to increase with depth. Silt-size chlorite occurred at minor levels either sporadically with depth in the more poorly-drained soils (pedons MC1 MC2, FC1, FC1A, FC2) or throughout nearly all horizons in the other better-drained pedons.

In terms of the iron oxides associated with the sand and silt-size soil material, hematite was observed mainly in the reddish-hued horizons of all pedons (Figures 5-1a and 5-

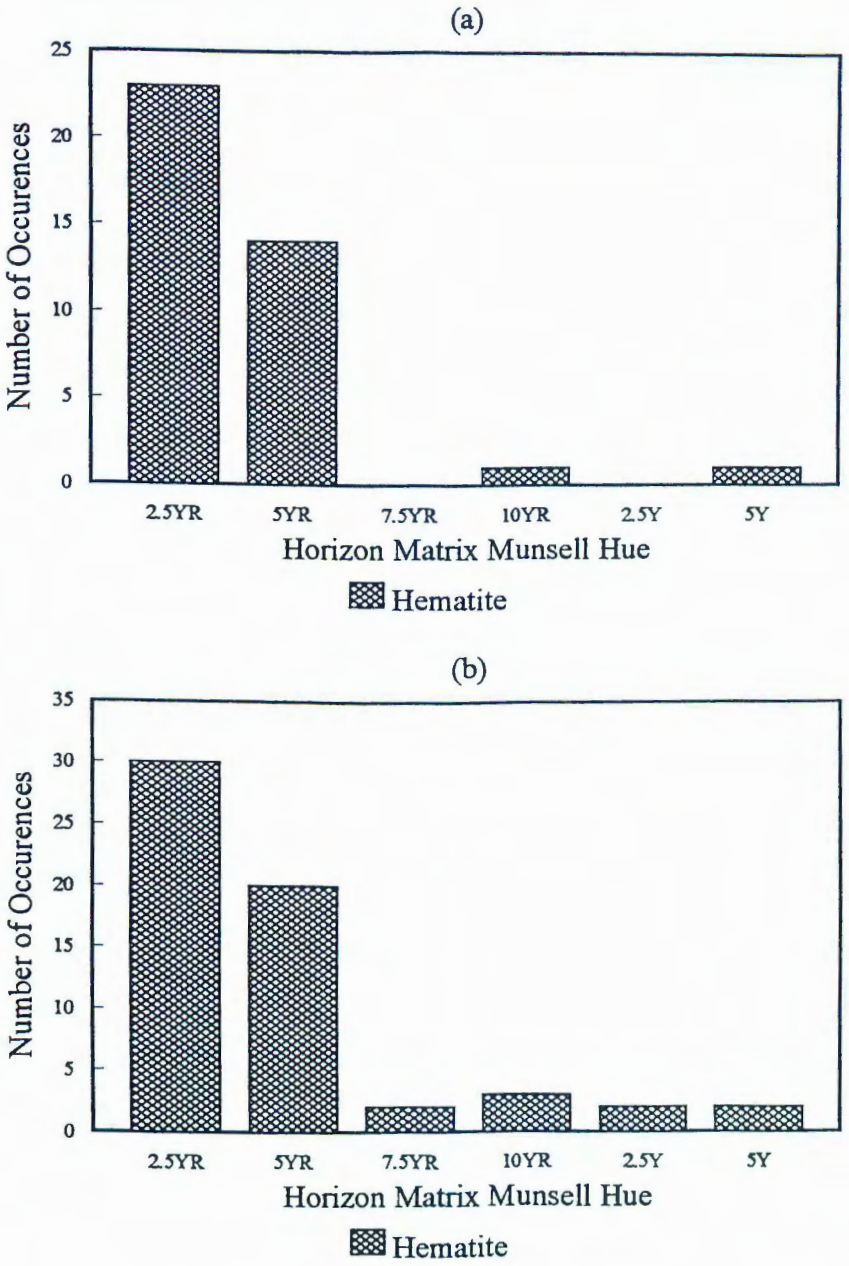

Figure 5-1. Distribution of iron oxide occurrence versus Munsell hue of the horizon matrix associated with the a) sand-size fraction and b) the silt-size fraction of both topohydrosequences.

1b). Along these topohydrosequences, reddish-hued horizons occur below water-restricting layers in the more poorly-drained soils and throughout in the better-drained soils. The limited occurrence of hematite within horizons having yellow coloration (7.5YR or yellower hues) is probably due to either a small amount of residual hematite persisting in these horizons which experience seasonal reduction episodes or the occlusion of hematite within fragments of these horizons. No other iron oxide minerals were observed in association with the sand or silt-size soil material in any of the soils.

Clay Mineralogy

Based upon peak height analysis, mica and kaolinite were the two most abundant silicate minerals throughout all the soils examined (Appendix C). Vermiculite tends to increase with depth whereas both quartz and chlorite are minor throughout all pedons.

In terms of the iron oxides, hematite occurred nearly exclusively within the reddish-hued horizons whereas goethite was observed mainly in the yellow-hued horizons (7.5YR and yellower) associated with the upper solum of the more poorly-drained soils (Figure 5-1c). In those occurrences in which hematite was the sole iron oxide, the Munsell matrix of the horizon exhibited red hues (5YR or redder). However, where hematite coexisted with goethite,

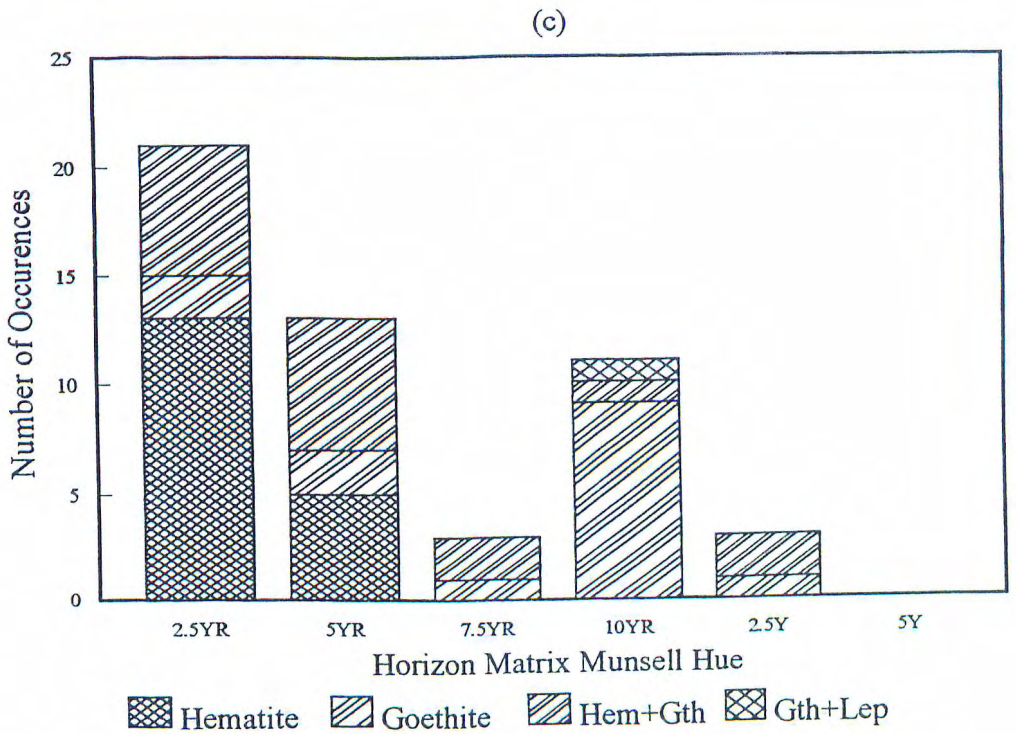

Figure 5-1c. Distribution of iron oxide occurrence versus Munsell hue of the horizon matrix associated with the clay fraction of both THS.

the Munsell matrix had hues of 2.5YR to 10YR hues with the resulting color probably dependent upon the goethite/hematite ratio. The four occurrences of goethite as the sole iron oxide within reddish-hues (5YR and redder) is probably due to the concentration of co-existing hematite being below the limit of detection by XRD ($\leq$ 2 wt%) in these samples. Lepidocrocite was also found coexisting with goethite in the Btg horizon of pedon FC1.

Interpretation of Mineralogical Results

The mineral suite for these soils is principally composed of minerals extremely resistant towards weathering. Quartz, muscovite, chlorite, kaolinite, and iron oxides are all very stable minerals in a well-drained soil environment. The weatherable minerals which do occur in these soils (i.e. the feldspars) occur in such low amounts that their effect upon the pedogenic development of these soils is minimal. This highly resistant mineralogy is quite possibly the dominant factor in the weak development of the argillic horizon and shallow solum depths of these soils, particularly the well-drained soils. Similar soils from more southern Triassic basins have greater pedogenic development (Griffin and Buol, 1988), due to either greater weatherable mineral content or warmer temperature regime.

The occurrence of iron oxides other than hematite (i.e goethite and lepidocrocite) in these soils is of major

importance. From previous work (Chapter 2), hematite is known to be the only iron oxide present in the parent materials for these soils. Because goethite and lepidocrocite were not inherited from the parent material, these two iron oxides represent transformation products either from hematite reduction or chlorite weathering and reprecipitation in the clay fraction.

Both lepidocrocite and goethite mainly occur in the yellow-hued horizons of the pedons associated with the footslope or toeslope positions. The higher levels of organic carbon associated with these yellow-hued upper sola horizons may also inhibit hematite formation in favor of lepidocrocite formation as suggested by Cornell (1985).

Two mechanisms may be causing the yellowing of these soils. The first mechanism is the occurrence of transformed goethite and lepidocrocite via hematite reduction or chlorite weathering and reprecipitation of goethite and lepidocrocite in these wetter horizons. This mechanism is at odds with the current concepts of pedogenic yellowing (Macedo and Bryant, 1989). Their concept states that goethite and hematite coexist in the red well-drained soils but that in the yellow poorly-drained soils goethite is the dominant iron oxide due to preferential reduction of the hematite. The pedogenic yellowing in the soils of the Triassic Culpeper Basin in Maryland is the result of pedogenic goethite and lepidocrocite at the expense of the

inherited hematite or chlorite and not due solely to preferential reduction of hematite.

The second mechanism of pedogenic yellowing of these soils is the introduction of loessal or colluvial/alluvial materials within these yellow horizons (Chapter 3). The degree of redoximorphic feature development was found to be well correlated to the presence or absence of loessal or colluvial/alluvial additions among these pedons. These materials may be more easily altered by redox processes than the residuum and result in an enhanced yellowing of these affected horizons. Quite possibly, these two mechanisms are operating together to cause the yellowing of these soils.

Whole Soil Iron Oxide Chemistry

Dithionite-extractable iron (Fe_d) levels in these soils ranged from 3 to 44 g Fe/kg soil (Table 5-1). The lowest levels were associated with the gleyed horizons and thin white seams due to reductive dissolution and loss of the iron oxides from these horizons through leaching. Elevated iron levels within the A and Ap horizons of the more poorly-drained soils (MC1, MC2, FC1) as compared to their B horizon counterparts may reflect an incorporation and crushing of Fe/Mn nodules present in the <2 mm size fraction during analytical procedures. No other significant trends in the total free iron oxide data were observed within or among the various pedons.

Table 5-1. Fe Chemistry of Whole Soils of Both Topohydrosequences.

Pedon	Horizon	Munsell Color	Fe_d	Fe_o	Fe_t	AlOOH in FeOOH	Fed in Clay	$\frac{Fe_o}{Fe_d}$
			<--g/kg soil->			<----%--->		
MC1	A	10YR 4/3	19.1	3.3	4.3	19.6	23.3	0.17
	Ap	10YR 4/4	26.3	3.9	5.9	12.4	21.8	0.15
	Btg1	2.5Y 6/2	12.2	0.9	0.0	29.3	69.6	0.07
	Btg2	2.5Y 5/3	7.9	0.6	14.2	14.6	58.0	0.08
	Btg3	2.5Y 6/2	3.5	0.6	17.0	26.2	60.5	0.17
	2BC	2.5YR 4/4	13.3	1.2	15.1	8.6	41.1	0.09
MC2	A	10YR 4/3	16.3	3.3	8.3	17.3	20.5	0.20
	Ap	10YR 4/4	24.5	3.6	15.3	17.2	22.3	0.15
	Btg	10YR 5/3	12.4	0.8	13.4	22.1	51.4	0.06
	Bx1	2.5YR 4/6	8.5	0.5	0.0	16.6	37.8	0.05
	Bx2	2.5YR 4/6	16.1	0.9	15.8	11.9	32.7	0.05
	2BC	5 YR 4/6	19.3	0.7	5.7	8.8	26.9	0.04
	3BCg	2.5YR 4/4	6.2	0.6	14.7	14.3	34.8	0.09
MC3	Ap	10YR 4/3	15.0	1.7	5.3	15.2	17.3	0.11
	Bt	10YR 5/3	20.3	0.9	8.9	21.6	48.7	0.04
	Bx1	5YR 3/4	26.0	1.2	10.4	10.0	32.8	0.05
	Bx2	5YR 4/6	6.8	0.6	15.1	13.2	39.7	0.08
	Bx3	5YR 3/4	14.9	1.1	13.5	8.3	26.0	0.07
	2BCg	2.5Y 7/2	11.8	1.5	11.5	9.5	21.2	0.13
	3Cr		22.1	2.2	13.5	6.7	20.7	0.10
MC4	Ap	5YR 4/4	23.8	2.6	22.7	14.4	22.7	0.11
	Bt1	2.5YR 3/6	37.8	1.8	23.6	10.1	30.3	0.05
	Bt2	2.5YR 3/6	37.6	2.0	19.3	7.2	23.3	0.05
	Btx1	2.5YR 3/6	25.5	1.4	30.2	7.5	26.2	0.05
	Btx2	2.5YR 3/6	31.6	2.3	37.8	5.0	17.6	0.07
	Cr	2.5YR 3/6	32.4	1.5	41.4	4.0	14.7	0.05
MC5	Ap	10YR 4/4	8.5	0.6	11.1	25.5	35.9	0.07
	Bt1	7.5YR 4/6	14.5	0.8	10.1	19.6	43.6	0.06
	Bt2	7.5YR 4/4	15.5	1.1	9.2	20.7	33.5	0.07
	BC	5YR 3/4	12.3	0.6	13.4	13.1	25.6	0.04
	C1	5YR 4/3	12.3	0.8	14.6	18.5	24.8	0.06
	2C2 up	5YR 5/4	22.8	0.9	28.9	6.8	21.7	0.04
	2C2 lo	2.5YR 3/6	27.7	0.6	29.7	3.6	18.8	0.02
	3R	2.5YR 3/6	14.7	0.6	20.1	4.1	25.4	0.04

Table 5-1 (cont). Fe Chemistry of Whole Soils of Both Topohydrosequences.

Pedon	Horizon	Munsell Color	Fe_d	Fe_o	Fe_t	AlOOH in FeOOH	Fe_d in Clay	$\frac{Fe_o}{Fe_d}$
			<--g/kg soil->			<----%--->		
FC 1	Ap	10YR 4/3	34.1	11.8	4.9	15.0	18.4	0.35
	Btg1	10YR 6/2	16.9	3.4	14.0	20.4	81.9	0.20
	Btg2	10YR 5/2	13.8	2.2	24.0	24.7	89.1	0.16
	2BC	5YR 4/3	20.6	3.2	21.3	10.0	38.4	0.15
	3BC	5Y 5/2	12.7	3.4	19.6	10.9	34.1	0.26
	4BCg1	5Y 5/2	4.2	1.2	10.0	14.9	31.6	0.29
	4BCg2	5Y 6/2	3.5	1.3	10.5	24.5	58.2	0.37
	4BCg3	5Y 6/2	11.7	2.9	17.4	12.4	34.7	0.24
	5Cr		39.4	3.7	32.9	5.5	16.3	0.09
FC 1A	Ap	10YR 4/3	26.8	6.8	10.2	19.3	19.3	0.25
	Bt1	7.5YR 5/8	35.3	2.6	14.9	21.3	64.2	0.07
	Bt2	2.5YR 3/4	27.4	2.4	17.7	14.0	48.6	0.09
	2Bxup	2.5YR 3/4	27.8	2.8	20.4	7.6	30.1	0.10
	2Bxlow	2.5YR 3/4	24.1	2.4	23.0	5.7	28.9	0.10
	wh. sm.	2.5Y 7/2	3.4	0.6	19.6	34.1	53.5	0.16
	2Cr	2.5YR 3/4	30.3	1.8	29.0	5.2	22.4	0.06
FC2	Ap	5YR 4/4	27.5	5.3	9.0	16.2	21.4	0.19
	BE	5YR 5/3	36.8	2.8	8.9	12.4	42.7	0.08
	Bt	2.5YR 4/4	33.5	3.0	15.8	10.8	41.9	0.09
	2Bx	2.5YR 3/4	40.1	2.5	19.1	4.9	16.9	0.06
	2BC	2.5YR 3/4	27.8	2.4	25.5	6.9	23.8	0.09
	wh. sm.	5Y 7/1	12.7	1.0	22.3	12.2	10.6	0.08
	3Crt	2.5YR 3/4	35.3	1.7	23.6	5.0	18.8	0.05
FC3	Ap	2.5YR 4/3	24.5	4.2	6.0	17.0	27.0	0.17
	BA	2.5YR 3/4	23.2	3.0	11.5	13.2	31.9	0.13
	Bt1	2.5YR 3/4	31.3	2.3	12.5	11.0	24.4	0.07
	Bt2	2.5YR 3/4	37.4	5.0	9.7	7.2	24.7	0.13
	Bt3	2.5YR 3/4	34.1	2.6	9.3	6.8	24.9	0.08
	2Crt	2.5YR 3/4	26.9	3.5	9.8	11.6	21.0	0.13
FC4	Ap	5YR 3/3	25.6	1.6	16.1	13.0	22.7	0.06
	Bw1	2.5YR 3/4	37.9	2.0	13.0	9.0	31.4	0.05
	Bw2	2.5YR 3/6	27.4	2.9	14.3	10.6	33.5	0.11
	BC	5YR 4/3	26.1	3.1	6.7	10.0	25.0	0.12
	Cr	5YR 4/3	31.7	2.9	3.9	9.2	18.3	0.09

Table 5-1 (cont). Fe Chemistry of Whole Soils of Both Topohydrosequences.

Pedon	Horizon	Munsell Color	Fe_d	Fe_o	Fe_t	AlOOH in FeOOH	Fe_d in Clay	$\frac{Fe_o}{Fe_d}$
			<--g/kg soil->			<----%--->		
FC5	Ap	5YR 3/3	19.5	1.6	6.2	11.2	13.3	0.08
	Bt1	5YR 3/3	31.9	1.6	4.4	9.7	25.0	0.05
	Bt2	5YR 3/4	43.8	2.6	2.1	4.7	32.4	0.06
	Bt3	5YR 3/4	31.8	2.3	9.4	5.2	40.6	0.07
	2BCt1	2.5YR 3/4	41.7	2.0	15.6	2.2	26.6	0.05
	3BCt2	2.5YR 3/4	23.4	1.5	14.8	7.7	25.2	0.06
	4Crt	2.5YR 3/4	39.6	1.8	21.0	5.7	23.3	0.05
	R	2.5YR 3/4	36.3	2.8	0.0	0.0	17.7	0.08

In terms of the degree of Al-substitution in the iron oxides, levels between 15 and 25% Al-substitution (from Al measured in DCB extracts) commonly occurs in the goethite-containing horizons of the more poorly-drained pedons. In contrast, 5 to 10% Al-substitution commonly occurs in deeper red horizons and is very similar to that reported for the hematite within the red shales of this basin (Chapter 2). The ranges of Al substitution observed are intermediate in comparison to the maxima reported for goethite (approximately 33%) and hematite (approximately 17%) (Schwertmann and Taylor, 1989). The maximum extent of Al-substitution in lepidocrocite is not currently known (Schwertmann and Taylor, 1989). This degree of Al-substitution will stabilize the goethite and lepidocrocite more than their pure end-members (Fey, 1983). The Al-substitution would, in effect, tend to lower the redox potential necessary for reduction of iron oxides at a given pH. According to the pe-pH diagram shown in Figure 1-2, the overall effect of Al-substitution in any iron oxide would be to move the lower boundary of the FeOOH stability field to a slightly lower pe. The actual shift would be dependent upon the thermodynamic data of such Al-substituted iron oxides.

Acid ammonium oxalate extractable iron (Fe_o) levels were low throughout all the pedons, ranging from 0.4 to 11.8 g Fe/kg soil (Table 5-1). The highest levels of Fe_o were

always associated with the A or Ap horizons of each pedon. Among the A or Ap horizons of all the pedons, the highest levels of Fe_o were observed in the lowest landscape positions which may reflect the presence of poorly-crystalline iron oxides in this near surface environment.

The low Fe_o/Fe_d ratio observed in all the pedons, ranging from 0.02 to 0.35, suggests that the iron oxides are rather crystalline (Table 5-1). In the summit soils, this ratio is always less than 0.10, probably reflecting the crystalline nature of the inherited hematite in these pedons.

In terms of the size partitioning of the iron oxides, a definite catenary effect is observed. In those horizons not affected by a seasonally high water table (i.e the reddish horizons beneath water-restricting layers in the poorly-drained soils and throughout the solum of the upper well-drained soils) of each topohydrosequence, 15-35% of the total free iron oxides occurs within the clay fraction of these horizons (Table 5-1). However, in those horizons overlying water-restricting layers in the more-poorly drained soils this percentage increases dramatically (42-89%). Two explanations may be offered for these size partitioning phenomena. In the first, because both goethite and lepidocrocite occur only within the clay fractions of these horizons, it is postulated that at times of a seasonally high water table the inherited hematite, which

may be associated with the silt and sand fractions, becomes unstable and undergoes reductive dissolution. Due to the restricted drainage in these pedons, the dissolved iron is not lost through leaching but is reprecipitated during the next cycle of oxidation as either clay-sized goethite, lepidocrocite, or amorphous iron oxides. In the second explanation, the observed loess or colluvial\alluvial additions to these yellow-hued horizons (Chapter 3) may have introduced either clay-sized iron-containing material or overall higher clay contents providing greater surface area for the adsorption of iron oxides onto their surfaces.

The residual iron (Fe_t) data generally shows depleted levels in the horizon(s) near the soil surface as compared to the horizons found at greater depths in all pedons (Table 5-1). Because residual iron may be considered the primary source for secondary iron oxide formation, the distribution of the Fe_t and Fe_d with depth (i.e $Fe_d >>> Fe_t$ near the surface than at depth) may indicate pedogenic iron oxide formation at the expense of the silicate-bound iron in those horizons having greater differentiation from the parent materials. From the mineralogical results, chlorite is the probable source of the Fe_t.

Fe and Mn Chemistry of Redoximorphic Features

Fe/Mn Nodules

Dithionite and oxalate extractable Fe and Mn data for

several Fe/Mn nodules found in the A or Ap horizons of both topohydrosequences are shown in Table 5-2. Dithionite extractable iron levels range from 36.1 to 134.1 g Fe/kg nodule, showing a concentration of Fe-oxides within these nodules as compared to the iron chemistry of the whole soils for these horizons (Table 5-2). Oxalate extractable iron levels are much lower than the Fe_d for each nodule, ranging from 10.6 to 43.7 g Fe/kg soil. The resulting Fe_o/Fe_d ratio ranges from 0.19 to 0.53 and approximates the ratio found in the whole soil for these same horizons. It is therefore probable that through the grinding of the soils, these sand and gravel-sized nodules became crushed and incorporated within the <2 mm fraction, resulting in a similar whole soil Fe_o/Fe_d ratio as found for the nodules within the same horizon. Dithionite extractable manganese levels range from 9.7 to 65.8 g Mn/kg nodule. Such levels are sufficient to mask the coloring due to the high levels of the associated iron and cause these features to be black in color (N 2/0).

Matrices, Mottles, and Coatings

Dithionite and oxalate extractable Fe and Mn data for the redox concentration features (generally chroma $\geq$ 4) for the MC and FC site are shown in Table 5-3a and Table 5-3b, respectively. Levels of Fe_d of these features for both sites range from 10.7 to 75.7 g Fe/kg soil. Generally, an

Table 5-2. Iron and Manganese Chemistry of Selected Nodules.

Horizon	Fe_d	Fe_o	Mn_d	Fe_o/Fe_d
	<------g/kg nodule------>			
MC1 A	128.2	31.6	35.2	0.25
MC1 Ap	87.0	29.5	46.7	0.34
MC2 A	123.4	23.8	40.0	0.19
MC2 Ap	121.5	26.7	45.7	0.22
MC3 Ap	82.2	32.4	27.5	0.39
FC1 Ap	134.1	43.7	46.4	0.33
FC1A Ap	100.1	32.3	39.3	0.32
FC2 Ap	68.7	36.6	65.8	0.53
FC3 Ap	36.1	10.6	9.70	0.29

Table 5-3a. Iron and Manganese Oxide Chemistry of Redox Concentration Features at the MC site, grouped by hue.

Redox Feature	Munsell Color	Fe_d	Fe_o	Mn_d	Fe_o/Fe_d	Fe Oxide Minerals
		<--g/kg soil->				
MC4 Btx2 Mn stn	N 2/0	38.3	4.6	9.2	0.12	
MC2 Btg Mn stn	N 2/0	17.8	2.1	4.2	0.12	GH
AVERAGE		28.1				
STD DEV		nd				
MC3 Bx2 mottle	10YR 5/6	18.7	1.0	0.0	0.05	GH
MC1 Btg1 mottle	10YR 5/4	11.9	0.5	0.0	0.04	H
MC2 Btg mottle	10YR 6/3	16.4	1.3	0.1	0.08	
AVERAGE		15.7				
STD DEV		2.9				
MC1 Btg1 mottle	7.5YR 6/6	22.1	1.4	0.0	0.06	G
MC1 Btg2 mottle	7.5YR 5/8	14.4	0.8	0.0	0.06	
MC2 Btg mottle	7.5YR 5/8	14.9	0.6	0.0	0.04	
MC5 Bt2 mottle	7.5YR 5/8	18.7	0.9	0.0	0.05	
MC5 2C2 mottle	7.5YR 5/8	18.0	0.6	0.0	0.03	
MC3 Bt mottle	7.5YR 5/6	24.3	1.4	0.0	0.06	GH
MC2 Bx1 mottle	7.5YR 5/4	23.0	1.0	0.0	0.04	GH
MC4 Bt2 mottle	7.5YR 5/4	17.7	0.8	0.0	0.05	H
MC5 Bt2 matrix	7.5YR 4/4	15.8	1.3	0.3	0.08	H
AVERAGE		18.8				
STD DEV		3.4				
MC2 Bx1 mottle	5YR 5/8	22.5	1.1	0.0	0.05	GH
MC1 Btg2 mottle	5YR 5/6	16.9	0.8	0.0	0.04	GH
MC2 Btg mottle	5YR 5/6	22.3	0.6	0.0	0.02	H
MC3 Bx2 matrix	5YR 4/6	15.9	0.6	0.0	0.04	GH
MC5 2C2 matrix	5YR 5/4	27.3	1.7	0.1	0.06	H
AVERAGE		21.0				
STD DEV		4.2				
MC2 Bx1 matrix	2.5YR 4/6	13.0	0.4	0.0	0.03	GH
MC4 Bt2 matrix	2.5YR 3/6	26.7	1.5	0.0	0.06	GH
MC4 Bt2 SST	2.5YR 3/6	37.6	1.8	0.1	0.05	GH
MC4 Btx2 matrix	2.5YR 3/6	36.4	0.8	0.1	0.02	H
AVERAGE		28.4		9.9		
STD DEV						

Note: H=Hematite, G=Goethite, and L=Lepidocrocite

Table 5-3b. Iron and Manganese Oxide Chemistry of Redox Concentration Features at the FC site, grouped by hue.

Redox Feature	Munsell Color	Fe_d	Fe_o	Mn_d	Fe_o/Fe_d	Fe Oxide Minerals
		<--g/kg soil->				
FC4 BC Mn stain	N 3/0	27.1	6.3	9.0	0.23	
FC3 2Crt stain	N 2/0	25.9	5.5	12.3	0.21	H
AVERAGE		26.5				
STD DEV		0.6				
FC4 Bw2 mottle	10YR 5/6	18.2	0.0	0.0	0.00	
FC1A Bt1 mottle	10YR 6/3	10.7	1.0	0.0	0.09	G
AVERAGE		14.5				
STD DEV		3.8				
FC1A Bx mottle	7.5YR 6/4	54.1	13.9	0.0	0.26	GH
FC1A Bt1 matrix	7.5YR 5/8	73.9	5.4	0.0	0.07	G
FC1 2BC mottle	7.5YR 5/8	43.0	9.6	0.0	0.22	
FC3 Bt3 mottle	7.5YR 5/6	16.7	3.2	0.0	0.19	
FC1 Btg2 mottle	7.5YR 5/6	40.9	4.0	0.0	0.10	G
AVERAGE		45.7				
STD DEV		18.6				
FC2 Bt mottle	5YR 5/8	45.7	5.1	0.0	0.11	H
FC4 BC matrix	5YR 4/3	26.3	2.3	0.9	0.09	H
FC1 2BC matrix	5YR 4/3	21.6	3.1	0.0	0.14	H
AVERAGE		31.2				
STD DEV		10.4				
FC1A Bt1 mottle	2.5YR 5/8	75.7	5.7	0.0	0.08	G
FC2 Bt matrix	2.5YR 4/4	21.6	1.9	0.0	0.09	H
FC4 Bw2 matrix	2.5YR 3/6	37.1	3.0	0.0	0.08	HLG
FC2 2BC matrix	2.5YR 3/4	41.8	1.7	0.0	0.04	H
FC1A Bx matrix	2.5YR 3/4	26.1	3.7	0.0	0.14	HL
FC3 2Crt matrix	2.5YR 3/4	22.9	3.0	1.7	0.13	H
FC3 Bt3 matrix	2.5YR 3/4	36.4	3.4	0.0	0.09	H
AVERAGE		37.4				
STD DEV		17.2				

Note: H=Hematite, G=Goethite, and L=Lepidocrocite

increase in the average levels of Fe_d is observed from 10YR hues to 2.5YR hues which may reflect increasing hematite content in the redder hues. Levels of Fe_o remain quite low in these features, ranging from 0.0 to 13.9 g Fe/kg soil. The highest Fe_o levels are typically associated with the manganese stains. The resulting Fe_o/Fe_d ratio also remains quite low, thereby confirming the high degree of crystallinity associated with these features. Dithionite extractable manganese levels greater than 1 g Mn/kg soil for these features from both sites occurred with the manganese coatings. These coatings either occurred in the upper sola of a more poorly-drained soil (pedon MC2) or at depth in the better-drained soils of each sequence (pedons MC4, FC3, FC4). Apparently, the redox potential of the water table in these better-drained soils is still low enough to accomplish reduction of ped interiors and segregation of the Mn oxides to the more oxidized ped faces. Conversely, these Mn stains may have been reduced in the organic carbon-rich upper sola, translocated to this depth, and reprecipitated on these features.

Dithionite and oxalate extractable Fe and Mn data for the redox depletion features (chroma $\leq$ 3) for the MC and FC site are shown in Table 5-4a and Table 5-4b, respectively. Levels of Fe_d for these features from both sites range from 2.2 to 27.6 g Fe/kg soil. The lowest levels are typically associated with those features having 10YR or yellower hues.

Table 5-4a. Iron and Manganese Oxide Chemistry of Redox Depletion Features associated with the MC site.

Redox Feature	Color	Fe_d	Fe_o	Mn_d	Fe_o/Fe_d	Fe Oxide Min
		<--g/kg soil->				
MC3 Bx2 coating	5Y 6/1	2.2	0.1	0.0	0.02	
MC1 Btg2 matrix	2.5Y 5/3	5.3	0.4	0.0	0.07	G
MC1 Btg1 matrix	2.5Y 6/2	5.1	0.3	0.0	0.06	
MC1 Btg2 mottle	2.5Y 5/2	7.4	0.5	0.0	0.07	G
AVERAGE		5.9				
STD DEV		1.0				
MC5 2C2 clay ctg	10YR 7/3	11.0	0.4	0.0	0.03	H
MC3 Bt matrix	10YR 5/3	7.5	0.5	0.0	0.06	
MC2 Btg matrix	10YR 5/3	14.8	0.8	0.0	0.05	GH
MC4 Btx2 mottle	10YR 7/2	27.6	2.5	0.1	0.09	H
MC2 Btg mottle	10YR 5/2	7.1	0.4	0.0	0.06	
AVERAGE		13.6				
STD DEV		7.5				
MC2 Bx1 mottle	7.5YR 5/2	9.1	0.3	0.0	0.03	G

Note: H=Hematite, G=Goethite, and L=Lepidocrocite

Table 5-4b. Iron and Manganese Oxide Chemistry of Redox Depletion Features associated with the FC site.

Redox Feature	Color	Fe_d	Fe_o	Mn_d	Fe_o/Fe_d	Fe Oxide Min
		<-g/kg soil->				
FC1A 2Bx mottle	2.5Y 5/2	7.4	5.0	0.0	0.68	H
FC2 2BC mottle	10YR 5/2	17.3	0.0	0.0	0.00	
FC1 Btg2 matrix	10YR 5/2	6.1	1.1	0.0	0.18	LG
FC1 2BC mottle	10YR 6/1	4.9	0.5	0.0	0.10	H
FC1A 2Bx mottle	10YR 4/1	5.9	6.2	0.0	1.05	L
FC1 2BC mottle	10YR 4/1	3.0	6.4	0.0	2.13	H
AVERAGE		7.4				
STD DEV		5.1				
FC2 2BC mottle	5YR 7/2	17.6	0.9	0.0	0.05	H
FC3 2Crt mottle	5YR 7/1	12.4	1.6	0.0	0.13	H
FC3 2Crt mottle	5YR 5/1	26.1	3.9	0.2	0.15	
AVERAGE		18.7				
STD DEV				5.6		

Note: H=Hematite, G=Goethite, and L=Lepidocrocite

The increase in Fe_d with increasing degree of redness which was observed for the redox concentration features is not observed for the redox depletion features. This poor correlation may be due to the difficulty in assessing the proper hue in low chroma materials. Levels of Fe_o remain low for these features, ranging from 0.0 to 6.4 g Fe/kg soil. For most of these features, the resulting Fe_o/Fe_d ratio is quite low (< 0.20) and suggests that these features have a high degree of crystallinity. However, several low chroma mottles have unusually high Fe_o/Fe_d ratios (0.68 to 2.13) which may be due to the presence of amorphous iron oxides associated with these features. Dithionite-extractable manganese (Mn_d) levels remained low throughout all these features ($\leq$ 0.2 g Mn/kg soil).

Fe Oxide Mineralogy of Redoximorphic Features

X-ray diffraction analyses of Fe/Mn nodules suggests amorphous iron oxides dominate these redoximorphic features. The only crystalline iron oxide which was observed was goethite, but only in one sample.

X-ray diffraction analysis of particular redoximorphic features was performed to determine the iron oxide mineralogy associated with each feature. Hematite, goethite, and lepidocrocite were the only iron oxide minerals observed in these features. Results showed that features may contain a single iron oxide (Figure 5-2a) or a

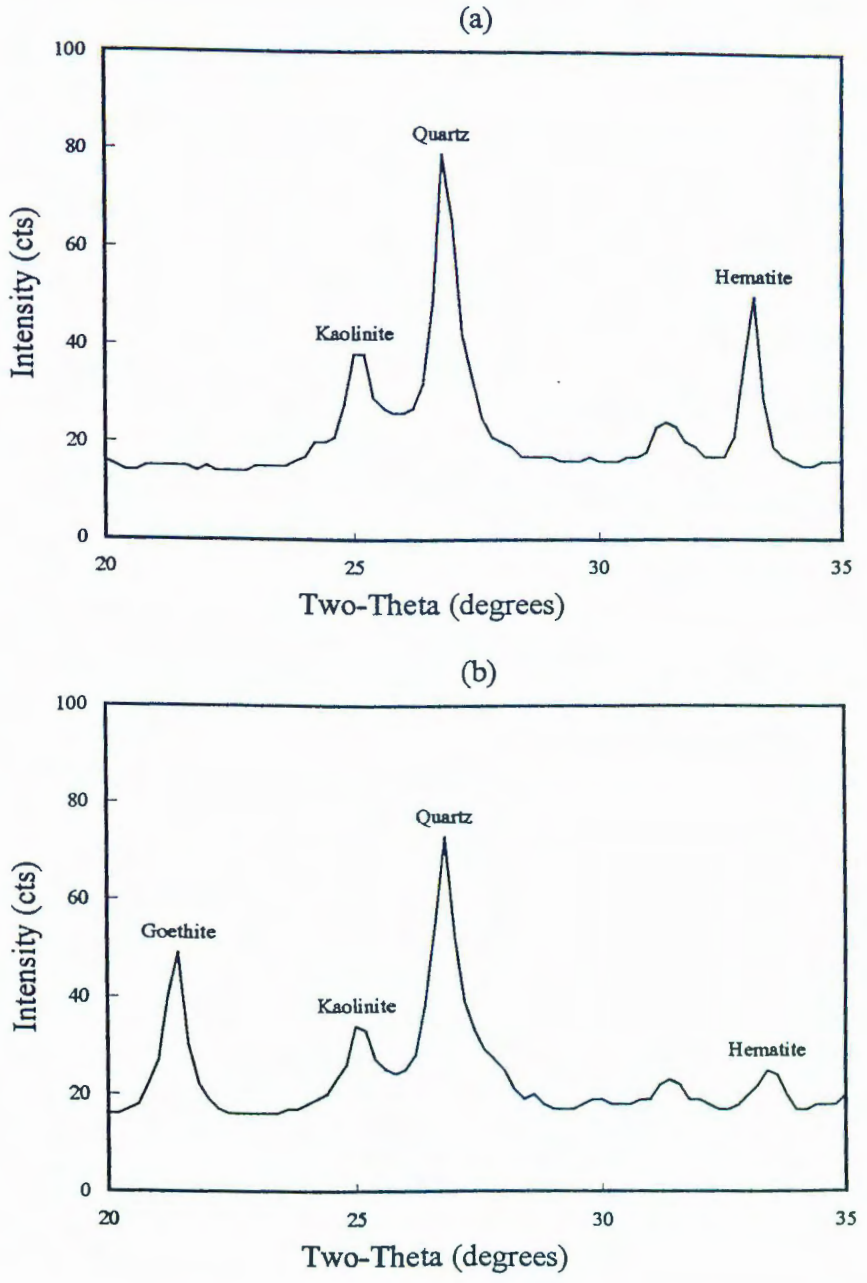

Figure 5-2. X-ray diffractograms showing a) sole occurrence of iron oxides and b) coexistence of iron oxides.

combination of iron oxides (Figure 5-2b). Various mixtures of all three crystalline iron oxides were observed in the features examined.

The relationship between the iron oxide mineralogy of the redox concentration features versus Munsell hue is shown in Figure 5-3a. This figure shows that hematite occurs mainly in the concentrations with redder hues (5YR or redder) whereas goethite occurs mainly in the concentrations with yellower hues (7.5YR or yellower). Hematite and goethite were also found to coexist in materials with all hues from 2.5YR to 10YR. The hue of these features is probably related to the actual proportion of goethite to hematite and their respective pigmenting powers. Lepidocrocite was found coexisting with hematite in the matrix of the upper Bx horizon of pedon FC1A (2.5YR 3/4) but the hematite apparently masked the presence of lepidocrocite. The occurrence of only hematite in three of the more-yellow hued features probably is due to residual hematite in the unreduced core of these features. The sole occurrence of goethite as the only iron oxide in a red-hued feature (a 2.5YR 5/8 mottle in the Bt horizon of pedon FC1A) is probably due to the concentration of coexisting hematite being below the detection limit of XRD. The relationship between the iron oxide mineralogy of the redox depletion features versus Munsell hue for both topohydrosequences is shown in Figure 5-3b. This figure shows that hematite can

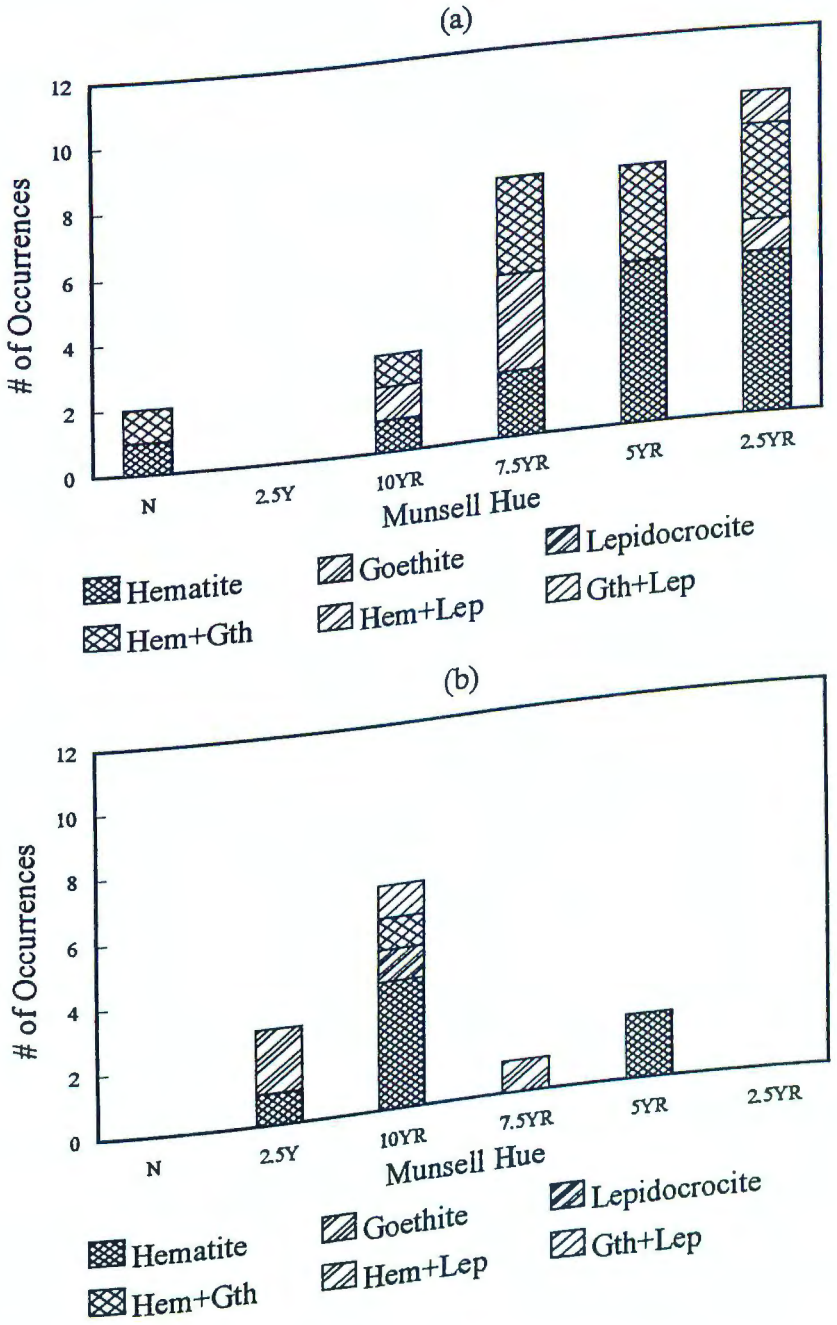

Figure 5-3. Iron oxide mineralogy versus Munsell hue of redox a) concentration features and b) depletion features for both topohydrosequences.

exist as the sole iron oxide in features having 5YR, 10YR, and 2.5Y hues. The occurrence of hematite in these yellower features either represents the presence of residual hematite in the unreduced core of these features or the difficulty in assessing the proper hue of these low chroma features. That the hematite is present in the unreduced core of these yellow features is substantiated by their reddening following the 5M NaOH treatment (i.e. 2.5Y 5/2 grayish brown mottle containing only hematite became 5YR 6/4 light reddish brown). Goethite existed as the sole iron oxide in the more yellow-hued features (7.5YR and yellower) but coexisted with hematite in a feature expressing goethitic colors (10YR 5/3 brown). Lepidocrocite was observed both as the sole iron oxide and together with goethite in depletion features having 10YR hues.

Figures 5-3a and 5-3b show that goethite and lepidocrocite are not restricted to only the more yellow-hued features, as expected, but also occur in the redder-hued (5YR or redder) features. Obviously, the coexisting hematite masks the goethite and lepidocrocite in these reddish features due to its stronger pigmenting effect. Goethite and lepidocrocite in these soils is therefore not well correlated with the Munsell hue of the redoximorphic feature.

The relationship between the iron oxide mineralogy and the pedon or landscape position is shown in Figures 5-4a and

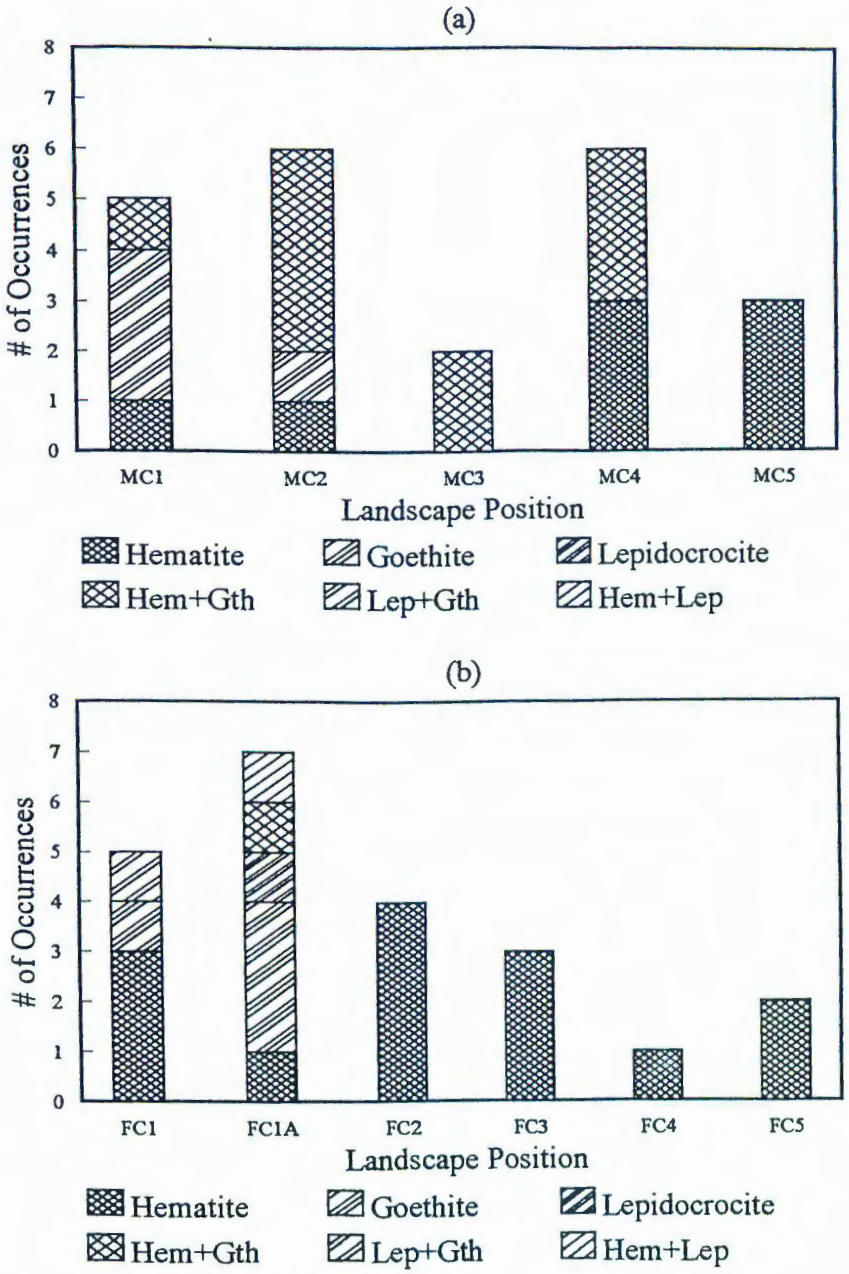

Figure 5-4. The number of occurrences of the various iron oxides identified in redoximorphic features from soils at various landscape positions; a) MC site and b) FC site.

5-4b, respectively. Both lepidocrocite and goethite appear to be better correlated with landscape position than Munsell hue (previous section). The incidence of lepidocrocite and goethite is greatest in the lower landscape positions and tends to diminish upslope.

Conclusions

The iron oxides associated with these soils, including the redoximorphic features, are rather crystalline as shown by the low Fe_o/Fe_d ratio. Inherited hematite occurred in those horizons relatively unaffected by alternating oxidizing/reducing conditions, such as horizons lying beneath water-restricting layers in the more poorly-drained horizons and in all horizons of the better-drained soils. Secondary clay-sized goethite and lepidocrocite formation via hematite transformation occurred in the upper sola of the more poorly-drained soils that overlie water-restricting layers and may be partly responsible for the pedogenic yellowing of these horizons. Because these horizons also experienced an introduction of loessal or colluvial/alluvial components, the nature of these components may also be partly responsible for the observed yellowing of these horizons.

CONCLUSIONS

Two topohydrosequences in the Triassic Culpeper Basin of Maryland were examined to determine the interrelationships between the morphology, mineralogy, and hydrology, particularly as these interrelationships pertain to the occurrence and distribution of redoximorphic features in these soils. These soil sequences are derived from dusky red shales and sandstones of the Newark Group. Mineralogical analysis of the shales indicate muscovite, kaolinite, quartz, chlorite, quartz, and hematite to be present with minor amounts of feldspars. The red color of the shales is due to the hematite. The fact that hematite is the only iron oxide occurring within these shales is important because it allows us to document iron oxide transformations during the pedogenesis of the soils derived from these parent materials. Such iron oxide transformations may be manifested as redoximorphic features within the solum of these soils, particularly in the more poorly-drained members of the sequence.

Initially, the degree of parent material uniformity within each of the pedons was examined. The pedons which occupy footslope and toeslope positions have had significant loessal or colluvial/alluvial additions to the upper portions of their sola and their origin is principally from these non-residual materials. These pedons also exhibit a yellow-hued upper solum which overlies, with sharp contrast, the red residuum. Additionally, a much higher clay content

was observed for these pedons as compared to the upslope red-colored pedons dominantly derived from residual materials.

The mechanism(s) responsible for the coloration patterns of these soils was then examined. Due to the similar hydrology yet highly contrasting morphologies in the three lowest pedons of each THS, the hydrological effect upon the morphology of these pedons was inconclusive. Although, organic carbon content, soil temperature, and vegetation may affect reduction and mobilization of iron, these factors were not sufficiently different to account for differences observed in the expression of redoximorphic features. Due to downslope accumulation of local alluvium/colluvium, differences in the nature of the parent materials were found to control the development of redoximorphic features in these soils. Soils whose upper sola were derived in part from non-residuum parent materials showed obvious redoximorphic features (i.e. gleying). Contrastingly, soils which were principally derived from the Triassic residuum failed to express redoximorphic features to the same degree. This inhibitory effect of the Triassic parent materials appears to be due to the occlusion of iron oxides within the sand and silt grains coupled with the increased stability of the Al-substituted hematite as compared to its pure end-member. Therefore, even though redoximorphic features are produced by redox processes, the

nature of the parent materials appear to mediate their degree of development.

In terms of the iron oxide mineralogy of the soils, goethite and lepidocrocite occurred mainly in the pedons occupying the footslope and toeslope positions. These minerals may result either from the reductive dissolution of hematite or goethite due to the seasonally high water table within the solum of these pedons, weathering of chlorite, or may have been transported into these pedons during the loessal or colluvial\alluvial deposition.

Overall, the coloring patterns of these soils are the result of the combined impacts of the nature of the parent material and the hydrological status. Future research dealing with the inhibition of red sediments to develop redoximorphic features should assess the degree of lithologic uniformity in the soils.

LITERATURE CITED

Bigham, J.M., D.C. Golden, S.W. Buol, S.B. Weed, and L.H. Bowen. 1978. Iron oxide mineralogy of well-drained Ultisols and Oxisols: II. Influence on color, surface area, and phosphate retention.

Blake, G.R., and K.H. Hartge. 1986. Bulk density. In A. Klute (ed.) Methods of soil analysis. Part 1. 2nd ed. Agronomy 9:363-376.

Bohn, H., B. McNeal, and G. O'Connor. 1985. Soil chemistry. Second edition. John Wiley and Sons, Inc. New York, New York.

Brewer, R. 1964. Fabric and mineral analysis of soils. Robert E. Krieger Publishing Co., Huntington, NY.

Bryant, R.B., and J. Macedo. 1990. Differential chemoreductive dissolution of Fe oxides in a Brazilian Oxisol. Soil Sci. Soc. Am. J. 54:819-821.

Cornell, R.M. 1985. Effect of simple sugars on the alkaline transformation of ferrihydrite into goethite and hematite. Clays Clay Miner. 33:219-227.

Cornell, R.M., and R. Giovanoli. 1987. Effect of manganese on the transformation of ferrihydrite into goethite and jacobsite in alkaline media. Clays Clay Miner. 35:11-20.

Cornell, R.M., R. Giovanoli, and P.W. Schindler. 1987. Effect of the silicate species on the transformation of ferrihydrite into goethite and hematite in alkaline media. Clays Clay Miner. 35:21-28.

Darmody, R.G. 1980. Geomorphic and pedologic relationships of Elioak and associated soils in the Piedmont of Maryland. Ph.D. diss. Univ. of Maryland, College Park.

Davey, B.G., J.D. Russell, and M.J. Wilson. 1975. Iron oxide and clay minerals and their relation to colours of red and yellow podzolic soils near Sydney, Australia. Geoderma 14:125-138.

Dorich, D.A., and D.W. Nelson. 1983. Direct colorimetric measurement of ammonium in potassium chloride extracts of soils. Soil Sci. Soc. Am. J. 47:833-836.

Drever, J.I. 1973. The preparation of oriented clay mineral specimens for x-ray diffraction analysis by a filter-membrane peel technique. Am. Mineral. 58:553-554.

Elless, M.P., and M.C. Rabenhorst. 1988. The occurrence of hematite in the shales of the Triassic Culpeper Basin of Maryland. Agronomy Abstracts p. 225.

Evans, C.V., and D.P. Franzmeier. 1986. Saturation, aeration, and color patterns in a toposequence of soils in North-central Indiana. Soil Sci. Soc. Am. J. 50:975-980.

Fanning, D.S., and M.C.B. Fanning. 1989. Soil morphology, genesis, and classification. John Wiley and Sons, New York, New York.

Fanning, D.S., R.F. Korcak, and C.B. Coffman. 1970. Free iron oxides: Rapid determination utilizing x-ray spectroscopy to determine iron in solution. Soil Sci. Soc. Am. Proc. 34:941-946.

Fey, M.V. 1983. Hypothesis for the pedogenic yellowing of red soil materials. Tech. Commun. S. Afr. Dep. Agric. Fish. 18:130-136.

Fisher, G.W. 1964. The Triassic rocks of Montgomery County. p. 10-17. In Maryland Geological Survey (ed.) The Geology of Howard and Montgomery Counties. Maryland Geological Survey, Baltimore, Maryland.

Fitzpatrick, R.W., R.M. Taylor, U. Schwertmann, and C.W. Childs. 1985. Occurrence and properties of lepidocrocite in some soil of New Zealand, South Africa, and Australia. Aust. J. Soil Res. 23:543-567.

Foss, J.E., D.S. Fanning, F.P. Miller, and D.P. Wagner. 1978. Loess deposits of the eastern shore of Maryland. Soil Sci. Soc. Am. J. 42:329-334.

Franzmeier, D.P., J.E. Yahner, G.C. Steinhardt, and H.R. Sinclair. 1983. Color patterns and water table levels in some Indiana soils. Soil Sci. Soc. Am. J. 47:1196-1202.

Gee, G.W., and J.W. Bauder. 1986. Particle-size analysis. In A. Klute (ed.) Methods of soil analysis. Part 1. 2nd ed. Agronomy 9:383-412.

Griffin, R.W., and S.W. Buol. 1988. Soil and saprolite characteristics of vertic and aquic Hapludults derived from Triassic basin sandstones. Soil Sci. Soc. Am. J. 52:1094-1099.

Hawley, J.W., and R.B. Parsons. 1980. Glossary of selected geomorphic and geologic terms. West Technical Service Center, SCS-USDA, Portland, OR

Holmgren, G.S., R.L. Juve, and R.L. Geschwender. 1977. A mechanically controlled variable leaching device. Soil Sci. Soc. Am. J. 41:1207-1208.

Hurst, V.J. 1977. Visual estimation of iron in saprolite. Geol. Soc. Am. Bull. 88:174-176.

International Committee on Aquic Moisture Regimes (ICOMAQ). 1989. Circular letter no. 9. 14p.

Jenny, H. 1980. The soil resource. Springer-Verlag, New York.

Kampf, N., and U. Schwertmann. 1982. The 5M NaOH concentration treatment for iron oxides in soils. Clays Clay Miner. 30:401-408.

Karim, M.I., and W.A. Adams. 1984. Relationships between sesquioxides, kaolinite, and phosphate sorption in a catena of Oxisols in Malawi. Soil Sci. Soc. Am. J. 48:406-409.

Kittrick, J.A., and E.W. Hope. 1963. A procedure for the particle size separation of soils for XRD analysis. Soil Sci. 96:319-323.

Langmuir, D., and D.O. Whittemore. 1971. Variations in the stability of precipitated ferric oxyhydroxides. In R.F. Gould (ed.) Nonequilibrium systems in natural water chemistry. Adv. Chem. Ser. 106:209-234.

Latshaw, G.J., and R.F. Thompson. 1968. Water table study verifies soil interpretations. J. Soil Water Cons. 23:65-67.

Levin, H.L. 1978. The earth through time. W.B. Saunders Co., Philadelphia, PA.

Lim, C.H., and M.L. Jackson. 1982. Dissolution for total elemental analysis. In A.L. Page, R.H. Miller, and D.R. Keeney (ed.) Methods of soil analysis. Part 2. Chemical and microbiological properties. Agronomy No. 9. ASA-SSSA, Madison, WI.

Macedo, J., and R.B. Bryant. 1987. Morphology, mineralogy, and genesis of a hydrosequence of oxisols in Brazil. Soil Sci. Soc. Am. J. 51:690-698.

Macedo, J., and R.B. Bryant. 1989. Preferential microbial reduction of hematite over goethite in a Brazilian oxisol. Soil Sci. Soc. Am. J. 53:1114-1118.

Matthews, E.D. 1960. Soil survey report of Frederick county, Maryland. U.S. Gov. Print. Office, Washington, DC.

Matthews, E.D., E.Z.W. Compy, and J.C. Johnson. 1961. Soil survey report of Montgomery county, Maryland. U.S. Gov. Print. Office, Washington, DC.

McCracken, R.J., S.B. Weed, and E.F. Goldston. 1964. Planosolic Piedmont soils of North Carolina. I. Morphology and composition. Soil Sci. 98:22-32.

Mehra, O.P., and M.L. Jackson. 1960. Iron oxide removal from soils and clays by a dithioinite-citrate system buffered with sodium bicarbonate. In Clays Clay Miner. Proc. 7 t h Conf., pp.317- 327. Natl. Acad. Sci.-Natl Res. Council Publ., Washington, DC.

Niroomand, G., and J.C.F. Tedrow. 1991. Importance of the parent material on gley formation. Manuscript in preparation.

Norrish, K., and R.M. Taylor. 1961. The isomorphous replacement of iron by aluminum in soil goethites. J. Soil Sci. 12:294-306.

Pickering, E.W., and P.L.M. Veneman. 1984. Moisture regimes and morphological characteristics in a hydrosequence in central Massachusetts. Soil Sci. Soc. Am. J. 48:113-118.

Rabenhorst, M.C. 1978. A study of the soils derived from serpentinite and associated rocks in Maryland. M.S. thesis. Univ. of Maryland, College Park.

Richardson, J.L., and F.D. Hole. 1979. Mottling and iron distribution in a Glossoboralf-Haplaquoll hydrosequence on a glacial moraine in northwestern Wisconsin. Soil Sci. Soc. Am. J. 43:552-558.

Schwertmann, U. 1964. Differenzierung der eisenoxide des bodens durch photochemische extraktion nit saurer ammoniumoxalate-losung. Z. Pflanzenernahr. Dueng. Bodenk. 105:194-202.

Schwertmann, U., and D.S. Fanning. 1976. Iron-manganese concretions in hydrosequences of soils in loess in Bavaria. Soil Sci. Soc. Am. J. 40:731-738.

Schwertmann, U., E. Murad, and D.G. Schultze. 1982. Is there Holocene reddening (hematite formation) in soils of axeric temperate climates. Geoderma 27:209-223.

Schwertmann, U., and R.M. Taylor. 1972. The influence of silicate on the transformation of lepidocrocite to goethite. Clays Clay Miner. 20:159-164.

Schwertmann, U., and R.M. Taylor. 1989. Iron oxides. p. 379-438. In J.B. Dixon and S.B. Weed (ed.) Minerals in soil environments. Second Edition. SSSA, Madison, Wisconsin.

Schwertmann, U., R.W. Fitzpatrick, R.M. Taylor, and D.G. Lewis. 1979. The influence of aluminum on iron oxides. II. Preparation and properties of Al-substituted hematites. Clays Clay Miner. 27:105-112.

Simonson, G.H., and L. Boersma. 1972. Soil morphology and water table relations: II. Correlation between annual water table fluctuation and profile features. Soil Sci. Soc. Am. Proc. 36:649-653.

Soil Conservation Service. 1984. Procedures for collecting soil samples and methods of analysis for soil survey. USDA-SCS Soil Surv. Invest. Rep. no. 1. U.S. Gov't. Print. Office, Washington, DC.

Soil Survey Staff. 1975. Soil taxonomy: A basic system of soil classification for making and interpreting soil surveys. USDA-SCS Agric. Handb. 436. U.S. Gov. Print. Office, Washington, DC.

Soil Survey Staff. 1990. Keys to soil taxonomy (fourth printing). SMSS technical monograph no. 19. Virginia Polytechnic Institute and State Univ., Blacksburg, Va.

Stumm, W., and J.J. Morgan. 1981. Aquatic chemistry: An introduction emphasizing chemical equilibria in natural waters. 2nd edition. John Wiley and Sons, New York, New York.

Tabatabai, M. A., and J.M. Bremner. 1970. Use of the Leco automatic 70-second carbon analyzer for total carbon analysis in soils. Soil Sci. Soc. Am. Proc. 34:608-610.

Taylor, R.M., and U. Schwertmann. 1978. The influence of aluminum on iron oxides. Part I. The influence of Al on Fe oxide formation from the Fe(II) system. Clays Clay Miner. 26:373-383.

Taylor, R.M., and U. Schwertmann. 1980. The influence of aluminum on iron oxides. VII. Substitution of Al for Fe in synthetic lepidocrocite. Clays Clay Miner. 28:267-271.

Torrent, J., U. Schwertmann, and D.G. Schultze. 1980. Iron oxide mineralogy of some soils of two river terrace sequences in Spain. Geoderma 23:191-208.

Torrent, J., U. Schwertmann, H. Fechter, and F. Alferez. 1983. Quantitative relationships between soil color and hematite content. Soil Sci. 136:354-358.

Veneman, P.L.M., M.J. Vepraskas, and J. Buoma. 1976. The physical significance of soil mottling in a Wisconsin toposequence. Geoderma 15:103-118.

Vepraskas, M.J., and L.P. Wilding. 1983. Aquic moisture regimes in soils with and without low chroma colors. Soil Sci. Soc. Am. J. 47:280-285.

Vokes, H.E., and J. Edwards. 1974. Geology and Geography of Maryland. Maryland Geological Survey Bulletin 19. 242p.

Wright, W.R. 1972. Pedogenic and geomorphic relationships of associated Paleudults in southern Maryland. Ph.D. diss. Univ. of Maryland, College Park.

Zobeck, T.M., and A. Ritchie, Jr. 1984. Analysis of long-term water table records from a hydrosequence of soils in central Ohio. Soil Sci. Soc. Am. J. 48:119-125.

APPENDIX A

SOIL DESCRIPTIONS

Pedon: MC1
Classification: fine-loamy, mixed, mesic Typic Ochraqualf
Series: outside range of Croton (less silty and no fragipan)
Site Location: Walter Reilly farm, Rte 28 near intersection with Rte 117, Montgomery County.
Geomorphic Position: Toeslope
Parent Materials: Red Triassic shales and sandstones
Described By: Mark Elless, Martin Rabenhorst, and Margaret Condron
Date: October 9, 1989
Notes: Depth to gleyic features is 22 cm; several rounded quartz gravels and cobbles throughout.

A --- 0-10 cm; dark brown to brown (10YR 4/3) loam; weak to moderate medium granular structure; very friable; approximately 5% rounded iron-manganese concretions; clear smooth boundary.

Ap --- 10-22 cm; dark yellowish brown (10YR 4/4) silt loam; few fine faint light brownish gray to light yellowish brown (2.5Y 6/3) and yellowish brown (10YR 5/6) mottles in lower 4 cm of the horizon; weak medium subangular blocky structure; friable; approximately 5-10% rounded iron-manganese concretions; abrupt smooth boundary.

Btg1 --- 22-41 cm; light brownish gray (2.5Y 6/2) silty clay loam; many (25%) fine distinct reddish yellow (7.5YR 6/6) and many (30%) medium to large distinct yellowish brown (10YR 5/4) mottles; medium moderate to large subangular blocky structure; friable to firm; very few iron-manganese concretions within upper few cm of horizon; continuous clay films on all ped surfaces; abrupt smooth boundary.

Btg2 --- 41-65 cm; grayish brown to light olive brown (2.5Y 5/3) clay loam; common (10%) large distinct grayish brown (2.5Y 5/2) thick, continuous clay films mainly on ped surfaces; many (25%) medium to large prominent yellowish red (5YR 5/6), and many (25%) medium distinct strong brown (7.5YR 5/8) mottles; medium moderate platy parting to medium coarse subangular blocky structure; firm to very firm; few soft iron-manganese concretions; clear wavy boundary.

Btg3 --- 65-71 cm; light brownish gray (2.5Y 6/2) clay loam; common medium faint brown (7.5YR 5/4) and common medium faint strong brown (7.5YR 5/8) mottles; weak moderate subangular blocky structure; friable; clay coatings on flags; abrupt smooth boundary.

2BC --- 71-114 cm; reddish brown (2.5YR 4/4) sandy loam; common (5%) medium distinct pinkish gray to light brown (7.5YR 6/3), common (15%) medium to large distinct pink (5YR 7/3), common (5%) fine to medium faint strong brown (7.5YR 4/6), and common (4%) fine distinct brownish yellow (10YR 6/8) mottles; weak moderate subangular blocky structure; friable; concentration of flags (red sandstone) at top of horizon.

Pedon: MC2
Classification: fine-loamy, mixed, mesic Typic Fragiaqualf
Series: outside range of Croton (less silty)
Site Location: Walter Reilly farm, Rte 28 near intersection with Rte 117, Montgomery County.
Geomorphic Position: Footslope
Parent Materials: Red Triassic shales and sandstones
Described By: Mark Elless, Martin Rabenhorst, and Margaret Condron
Date: October 9, 1989
Notes: Depth to gleyic features is 25 cm; several rounded quartz gravels and cobbles throughout.

A --- 0-9 cm; dark brown to brown (10YR 4/3) loam; weak to moderate medium granular structure; very friable; few iron-manganese concretions (1-3 mm); clear smooth boundary.

Ap --- 9-25 cm; dark yellowish brown (10YR 4/4) loam; few fine faint yellowish brown (10YR 5/6) mottles; weak medium subangular blocky structure; friable; 5-10% iron-manganese concretions (1-10 mm); abrupt smooth boundary.

Btg --- 25-44 cm; brown (10YR 5/3) clay loam; common (10%) faint pale brown (10YR 6/3), common (5%) faint grayish brown (10YR 5/2), common (10%) prominent yellowish red (5YR 5/6), and many (30%) distinct strong brown (7.5YR 5/8) mottles; moderate medium subangular blocky structure; firm; continuous clay coatings on ped surfaces; clear smooth boundary.

Bx1 --- 44-69 cm; red (2.5YR 4/6) silt loam; common (20%) medium faint yellowish red (5YR 5/8), common (10%) large distinct brown (7.5YR 5/2), and common medium to large faint dark brown to brown (7.5YR 5/4) mottles; weak coarse prismatic parting to moderate coarse platy structure; very firm; continuous clay coatings on all vertical ped faces; gradual smooth boundary.

Bx2 --- 69-83 cm; red (2.5YR 4/6) silt loam; common (20%) medium faint yellowish red (5YR 5/8), common (10%) large distinct brown (7.5YR 5/2), and common medium to large faint dark brown to brown (7.5YR 5/4) mottles on old root channels; moderate medium to coarse platy structure; firm; clear smooth boundary.

2BC --- 83-101 cm; yellowish red (5YR 4/6) sandy loam; very weak medium subangular blocky to platy structure; very friable to loose; clear smooth boundary.

3BCg --- 101-120 cm; light gray (10YR 7/1) in upper part and reddish brown (2.5YR 4/4) in lower part, silt loam; common prominent light gray to gray (10YR 6/1) and common distinct strong brown (7.5YR 5/6) mottles in lower part of the horizon; weak medium platy to subangular blocky structure; slightly firm.

Pedon: MC3
Classification: fine-loamy, mixed, mesic Aeric Fragiaqualf
Series: Abbottstown
Site Location: Walter Reilly farm, Rte 28 near intersection with Rte 117, Montgomery County.
Geomorphic Position: Lower Backslope
Parent Materials: Red Triassic shales and sandstones
Described By: Mark Elless and Margaret Condron
Date: October 27, 1989
Notes: Depth to gleyic features is 38 cm.

Ap --- 0-22 cm; dark brown to brown (10YR 4/3) loam; weak medium subangular blocky structure; very friable; iron-manganese concretions near lower boundary; abrupt smooth boundary.

Bt --- 22-38 cm; brown (10YR 5/3) loam; common medium distinct strong brown (7.5YR 5/6) and few fine distinct yellowish red (5YR 5/8) mottles; moderate coarse subangular blocky structure; friable; clear smooth boundary.

Bx1 --- 38-57 cm; dark reddish brown (5YR 3/4) loam; few fine distinct reddish yellow (7.5YR 6/8) mottles associated with clay; moderate medium subangular blocky structure; friable; light brownish gray (10YR 6/2) continuous clay coatings on ped faces.

Bx2 --- 57-82 cm; yellowish red (5YR 4/6) loam; few fine distinct yellowish brown (10YR 5/6) mottles; moderate medium prismatic structure; firm; light gray to gray (5Y 6/1) continuous clay coatings on ped faces; clear smooth boundary.

Bx3 --- 82-110 cm; dark reddish brown (5YR 3/4) silt loam; few fine distinct brownish yellow (10YR 6/8) mottles; moderate medium prismatic structure; friable; light gray to gray (5Y 6/1) continuous clay coatings on ped faces; abrupt smooth boundary.

2BCg --- 110-118 cm; light gray (2.5Y 7/2) loam/sandy loam; common fine distinct strong brown (7.5YR 5/8) and common medium distinct reddish brown (5YR 5/4) mottles; water intercepted in this horizon, could not determine structure or consistence.

3Cr --- 118+ cm; sandy loam

Pedon: MC4
Classification: fine-loamy, mixed, mesic Aquic Fragiudalf
Series: Readington
Site Location: Walter Reilly farm, Rte 28 near intersection with Rte 117, Montgomery County.
Geomorphic Position: Backslope
Parent Materials: Red Triassic shales and sandstones
Described By: Mark Elless, Martin Rabenhorst, and Margaret Condron
Date: November 3, 1989
Notes: Depth to gleyic features is 55 cm.

Ap --- 0-18 cm; reddish brown (5YR 4/4) silt loam; weak to moderate medium granular structure; friable; rare, fine iron manganese concretions; clear smooth boundary.

Bt1 --- 18-36 cm; dark red (2.5YR 3/6) silt loam; moderate medium subangular blocky; friable; thin discontinuous clay coatings on ped faces; gradual smooth boundary.

Bt2 --- 36-55 cm; dark red (2.5YR 3/6) silt loam; few medium distinct strong brown (7.5YR 5/6) and common medium distinct brown (7.5YR 5/4) mottles; moderate medium subangular blocky structure; friable; thin discontinuous reddish brown (5YR 5/4) clay coatings on both vertically and horizontally oriented ped surfaces; 5-10% coarse fragments (red shale and fine-grained sandstone); black Mn coatings on unweathered shale fragments; gradual smooth boundary.

Btx1 --- 55-90 cm; dark red (2.5YR 3/6) gravelly loam; common medium distinct pinkish gray (5YR 6/2) and few fine distinct strong brown (7.5YR 5/6) mottles; moderate medium to coarse subangular blocky structure; firm; continuous clay coatings on vertical faces and in pores; approximately 20% coarse fragments; gradual smooth boundary.

Btx2 --- 90-120 cm; dark red (2.5YR 3/6) gravelly loam; few fine distinct strong brown (7.5YR 5/6) and common medium to large prominent light gray (10YR 7/2) mottles; weak medium to coarse subangular blocky structure; very firm; continuous light brownish gray (2.5Y 6/2) clay coatings on ped surfaces; common black (N 2/0) Mn coatings on some ped surfaces; gravel is soft, weathered shale fragments; diffuse smooth boundary.

Cr --- 120-145 cm; dark red (2.5YR 3/6) gravelly loam; common large prominent light brownish gray (2.5Y 6/2) mottles.

Pedon: MC5
Classification: coarse-loamy, mixed, mesic Alfic Hapludult
Series: outside range of Penn (slightly lower base saturation).
Site Location: Walter Reilly farm, Rte 28 near intersection with Rte 117, Montgomery County.
Geomorphic Position: Summit
Parent Materials: Red Triassic shales and sandstones
Described By: Mark Elless and Margaret Condron
Date: November 15, 1989
Notes: No gleyic features observed.

Ap --- 0-23 cm; dark yellowish brown (10YR 4/4) loam; weak medium subangular blocky structure; friable; few medium sandy iron-manganese concretions in lower portion of the horizon; abrupt smooth boundary.

Bt1 --- 23-33 cm; strong brown (7.5YR 4/6) loam; moderate medium subangular blocky structure; friable; yellowish brown (10YR 5/4) clay coatings along root channels; few medium sandy iron-manganese concretions; clear wavy boundary.

Bt2 --- 33-41 cm; dark brown to brown (7.5YR 4/4) sandy loam; few fine distinct strong brown (7.5YR 5/8) mottles; weak medium subangular blocky structure; friable; few medium iron-manganese concretions throughout horizon; clear smooth boundary.

BC --- 41-79 cm; dark reddish brown (5YR 3/4) sandy loam; common fine distinct strong brown (7.5YR 5/6) mottles; weak medium subangular blocky structure; friable; light reddish brown (5YR 6/4) clay coatings; fine iron-manganese nodules; clear wavy boundary.

C1 --- 79-89 cm; reddish brown (5YR 4/3) sandy loam; many fine distinct yellowish red (5YR 5/8) mottles; weak medium prismatic structure; very friable; reddish brown (5YR 5/4) clay coatings; clear smooth boundary.

2C2 upper --- 89-121 cm; reddish brown (5YR 5/4) silt loam; few fine distinct strong brown (7.5YR 5/8) mottles; moderate medium prismatic parting to moderate coarse subangular blocky structure; firm; very pale brown (10YR 7/3) clay coatings; small weathered sandstone pebbles occur throughout the horizon; clear smooth boundary.

2C2 lower --- 121-150 cm; dark red (2.5YR 3/6) gravelly silt loam; moderate coarse prismatic parting to moderate coarse subangular blocky structure; firm to friable; reddish yellow (5YR 6/6) clay coatings; many (>20%) sandstone gravels.

3R --- 150+ cm; dark red (2.5YR 3/6) sandstone.

Pedon: FC1
Classification: clayey, mixed, mesic Ultic Ochraqualf
Series: outside range of Croton (more clayey, no fragipan).
Site Location: Mt. St. Mary's College, Emmittsburg east of Rte 15N behind athletic field.
Geomorphic Position: Toeslope
Parent Materials: Red Triassic shales and sandstones
Described By: Mark Elless and Martin Rabenhorst
Date: January 28, 1991
Notes: Depth to gleyic features is 33 cm. Quartz cobbles at lower boundary of 2BC.

Ap --- 0-33 cm; dark brown to brown (10YR 4/3) loam; moderate medium granular structure; friable; few iron-manganese concretions; abrupt smooth boundary.

Btg1 --- 33-54 cm; light brownish gray (10YR 6/2) silty clay; many (40%) fine distinct strong brown (7.5YR 5/6) mottles; weak medium prismatic parting to moderate medium subangular blocky structure; firm; gradual smooth boundary.

Btg2 --- 54-75 cm; grayish brown (10YR 5/2) clay; many (35%) fine distinct strong brown (7.5YR 5/6) mottles; weak medium prismatic parting to moderate medium subangular blocky structure; firm; clear wavy boundary.

2BC --- 75-125 cm; reddish brown (5YR 4/3) silty clay loam; common (15%) fine distinct light gray to gray (10YR 6/1) just behind ped faces, common (5%) fine distinct dark gray (10YR 4/1) on ped faces, and many (30%) fine distinct strong brown (7.5YR 5/8) mottles; weak coarse prismatic parting to moderate medium platy structure; firm; grayish brown clay films on old root channels; range in horizon thickness is 30-70 cm; clear wavy boundary.

3BC --- 125-160 cm; light olive brown (5Y 5/2) sandy loam; many (25%) large faint grayish brown (2.5Y 5/2) on prism faces and many (25%) fine to medium prominent red (2.5YR 4/6) mottles; moderate medium to coarse subangular blocky structure; friable; abrupt smooth boundary.

4BCg1 --- 160-195 cm; olive gray (5Y 5/2) loamy sand/sandy loam; prominent reddish brown (5YR 4/4) on ped faces which are horizontally oriented, prominent yellowish red (5YR 5/8) on ped faces which are horizontally oriented, and distinct light brownish gray (2.5Y 6/2) mottles; weak coarse platy to prismatic structure; friable.

4BCg2 --- 195-215 cm; olive gray (5Y 6/2) sandy loam; prominent reddish brown (5YR 4/4) on ped faces which are horizontally oriented, prominent yellowish red (5YR 5/8) on ped faces which are horizontally oriented, and distinct light brownish gray (2.5Y 6/2) mottles; sampled by auger.

4BCg3 --- 215-225 cm; olive gray (5Y 6/2) loam; prominent reddish brown (5YR 4/4) on ped faces which are horizontally oriented, prominent yellowish red (5YR 5/8) on ped faces which are horizontally oriented, and distinct light brownish gray (2.5Y 6/2) mottles; sampled by auger.

5Cr --- 225+ cm; gravelly sandy loam.

Pedon: FC1A
Classification: clayey, mixed, mesic Aeric Fragiaqualf
Series: outside range of Abbottstown (more clayey)
Site Location: Mt. St. Mary's College, Emmittsburg east of Rte 15N behind athletic field.
Geomorphic Position: Upper toeslope
Parent Materials: Red Triassic shales and sandstones
Described By: Mark Elless and Martin Rabenhorst
Date: January 28, 1991
Notes: Depth to gleyic features is 54 cm. Quartz cobbles at upper boundary of fragipan.

Ap --- 0-32 cm; dark brown to brown (10YR 4/3) silt loam; moderate medium granular structure; friable; abundant worm channels; 5% iron-manganese concretions (0.5-3 mm in diameter); abrupt smooth boundary.

Bt1 --- 32-54 cm; strong brown (7.5YR 5/8) silty clay; many few distinct pale brown (10YR 6/3) to many medium distinct light brown (7.5YR 6/4) mottles; moderate fine to medium subangular blocky structure; friable; thin pale brown (10YR 6/3) to light brown (7.5YR 6/4) clay films on ped surfaces and 30% of ped interiors; clear smooth boundary.

Bt2 --- 54-74 cm; dark reddish brown (2.5YR 3/4) silty clay loam; this color mainly in ped interiors,; few (< 1%) fine distinct red (2.5YR 5/8), many (35%) fine distinct brown (7.5YR 5/2) mainly as thin clay films on ped surfaces, and many (25%) fine distinct yellowish red (5YR 4/6) mottles within some peds; moderate medium prismatic parting to moderate fine to medium subangular blocky structure; friable; clear smooth boundary.

2Bx upper --- 74-110 cm; dark reddish brown (2.5YR 3/4) loam; common (15%) fine prominent grayish brown (2.5Y 5/2) along prism faces, common (5%) fine prominent dark gray (10YR 4/1) along prism faces adjacent to roots, and common (5%) fine prominent light brown (7.5YR 6/4) mottles on some ped surfaces; moderate medium and coarse prismatic parting to moderate medium subangular blocky structure; firm; separation between Bx upper and Bx lower is by the abundance of coatings on prism faces; few (< 1%) black (N 2/0) Mn coatings on old fracture surfaces; 5% coarse fragment content; gradual smooth boundary.

2Bx lower --- 110-158 cm; dark reddish brown (2.5YR 3/4) loam; common (10%) fine prominent grayish brown (2.5Y 5/2) and common (3%) fine prominent dark gray (10YR 4/1) mottles; similar, but thicker, materials coating prism faces in this horizon compared to Bx upper horizon; black (N 2/0) Mn coatings more abundant also (3%); 40% coarse fragment content; abrupt smooth boundary when underlying discontinuous white seam is present, gradual smooth boundary when this seam is absent.

white seam --- 158-160 cm; light gray (2.5Y 7/2) silty clay; 1-2 cm thick, discontinuous all around the pit but continuous for 1 meter on one face of the pit; abrupt smooth boundary.

2Cr --- 160-205 cm; dark reddish brown (2.5YR 3/4) sandy loam; extremely gravelly ; few pinkish gray (7.5YR 6/2) clay films; black (N 2/0) Mn coatings mainly on rock faces, coatings approximately 40% of all rock faces; very shaly.

3R --- 205+ cm; shale dipping towards the northeast.

Pedon: FC2
Classification: fine-loamy, mixed, mesic Aquic Fragiudalf
Series: Readington
Site Location: Mt. St. Mary's College, Emmittsburg east of Rte 15N behind athletic field.
Geomorphic Position: Footslope
Parent Materials: Red Triassic shales and sandstones
Described By: Mark Elless, Martin Rabenhorst, David Verdone, and Carl Robinnette.
Date: July 27, 1990
Notes: Depth to gleyic features is 60 cm.

Ap --- 0-25 cm; reddish brown (5YR 4/4) silt loam; moderate medium granular structure; friable; abrupt smooth boundary.

BE --- 25-40 cm; reddish brown (5YR 5/3) silty clay loam; common fine distinct yellowish red (5YR 5/6) mottles; moderate medium subangular blocky structure; friable; few iron-manganese nodules; horizon thickness ranges from 0-18 cm; clear smooth boundary.

Bt --- 40-60 cm; reddish brown (2.5YR 4/4) silty clay loam; common fine distinct yellowish red (5YR 5/8) mottles; moderate medium prismatic to subangular blocky structure; friable; prominent clay coatings having matrix color on ped faces; clear smooth boundary.

2Bx --- 60-90 cm; dark reddish brown (2.5YR 3/4) loam; few fine distinct light gray (5YR 7/1) mottles; very strong coarse prismatic structure; very firm; reddish brown (5YR 4/4) and strong brown (7.5YR 5/8) weathered shale fragments also evident; clear smooth boundary.

2BC --- 90-110 cm; dark reddish brown (2.5YR 3/4) gravelly loam; common fine distinct pinkish gray (5YR 7/2) and common fine prominent grayish brown (10YR 5/2) mottles; weak medium subangular blocky structure; very firm; clay coatings having matrix color on ped surfaces; gradual smooth boundary.

3Crt --- 110-150 cm; dark reddish brown (2.5YR 3/4) extremely gravelly sandy loam; massive structure; firm; pinkish white (5YR 8/2) clay coatings on both ped faces and along fractures in shale; abrupt smooth boundary.

White seam --- 150-151 cm; light gray (5YR 7/1) clay; exists as clay coatings on ped faces.

4R --- 151+ cm; dark reddish brown (2.5YR 3/4) shale; pinkish white (5YR 8/2) coatings along fractures within the shale.

Pedon: FC3
Classification: fine-loamy, mixed, mesic Aquic Hapludult
Series: outside range of Readington (no fragipan, lower base saturation).
Site Location: Mt. St. Mary's College, Emmittsburg east of Rte 15N behind athletic field.
Geomorphic Position: Lower Backslope
Parent Materials: Red Triassic shales and sandstones
Described By: Mark Elless, Martin Rabenhorst, David Verdone, and Carl Robinnette.
Date: July 27, 1990
Notes: Depth to gleyic features is 96 cm.

Ap --- 0-20 cm; weak red to reddish brown (2.5YR 4/3) silt loam; moderate fine subangular blocky parting to moderate fine granular structure; friable; many fine and medium roots; gradual smooth boundary.

BA --- 20-28 cm; dark reddish brown (2.5YR 3/4) silt loam; weak medium subangular blocky structure; friable; few fine roots; gradual smooth boundary.

Bt1 --- 28-44 cm; dark reddish brown (2.5YR 3/4) silt loam; moderate medium subangular blocky structure; friable; few fine roots; gradual smooth boundary.

Bt2 --- 44-64 cm; dark reddish brown (2.5YR 3/4) gravelly silt loam; moderate medium subangular blocky structure; friable; few fine roots; gradual smooth boundary.

Bt3 --- 64-96 cm; dark reddish brown (2.5YR 3/4) very gravelly loam; common fine distinct yellowish red (5YR 4/6) mottles; weak medium prismatic parting to moderate medium subangular blocky; friable; few fine roots; clear smooth boundary.

2Crt --- 96-150 cm; dark reddish brown (2.5YR 3/4) loam; common fine distinct gray (5YR 5/1) coatings in upper portion of horizon and common fine distinct light gray (5YR 7/1) mottles; structureless massive; common black (N 2/0) Mn coatings; no roots present; clear smooth boundary.

3R --- 150+ cm; dark reddish brown (2.5YR 3/4) shale or sandstone.

Pedon: FC4
Classification: fine-loamy, mixed, mesic Typic Eutrochrept
Series: outside range of Penn (no argillic horizon)
Site Location: Mt. St. Mary's College, Emmittsburg east of Rte 15N behind athletic field.
Geomorphic Position: Upper Backslope
Parent Materials: Red Triassic shales and sandstones
Described By: Mark Elless, Martin Rabenhorst, David Verdone, and Carl Robinnette.
Date: July 27, 1990
Notes: Depth to gleyic features is 62 cm.

Ap --- 0-19 cm; dark reddish brown (5YR 3/3) silt loam; weak medium subangular blocky structure; friable; many fine and medium roots; gradual smooth boundary.

Bw1 --- 19-35 cm; dark reddish brown (2.5YR 3/4) loam; weak medium subangular blocky structure; friable; many fine to medium roots; gradual smooth boundary.

Bw2 --- 35-62 cm; dark reddish brown (2.5YR 3/6) loam; few fine prominent yellowish brown (10YR 5/6) mottles; moderate medium subangular blocky; friable; many fine roots; clear wavy boundary.

BC --- 62-81 cm; reddish brown (5YR 4/3) gravelly sandy loam; moderate medium subangular blocky structure; friable to firm; many very dark gray (N 3/0) Mn stains and iron-manganese concretions; some reddish yellow (7.5YR 6/6) shale fragments; few very fine roots; clear smooth boundary.

Cr --- 81-105 cm; reddish brown (5YR 4/3) gravelly loam; firm; very dark gray (N 3/0) Mn coatings and iron-manganese concretions; no roots present; abrupt smooth boundary.

R --- 105+ cm; reddish brown (5YR 4/3) shale.

Pedon: FC5
Classification: fine-loamy, mixed, mesic Ultic Hapludalf
Series: Penn
Site Location: Mt. St. Mary's College, Emmittsburg east of Rte 15N behind athletic field.
Geomorphic Position: Summit
Parent Materials: Red Triassic shales and sandstones
Described By: Mark Elless, Martin Rabenhorst, David Verdone, and Carl Robinnette.
Date: July 27, 1990
Notes: No gleyic features observed.

Ap --- 0-22 cm; dark reddish brown (5YR 3/3) silt loam; weak medium subangular blocky structure; friable; common fine roots; gradual smooth boundary.

Bt1 --- 22-44 cm; dark reddish brown (5YR 3/3) loam; moderate medium subangular blocky structure; friable; few fine roots; clear smooth boundary.

Bt2 --- 44-66 cm; dark reddish brown (5YR 3/4) cobbly loam; moderate medium subangular blocky structure; friable; few fine roots; 30% cobbles; clear wavy boundary.

Bt3 --- 66-110 cm; dark reddish brown (5YR 3/4) cobbly silt loam; moderate medium subangular blocky structure; friable few fine roots; 30% cobbles; clear wavy boundary.

2BCt1 --- 110-132 cm; dark reddish brown (2.5YR 3/4) very gravelly silt loam; weak medium platy structure; friable; few fine roots in upper portion of the horizon; 50% gravels of shale; clear smooth boundary.

3BCt2 --- 132-158 cm; dark reddish brown (2.5YR 3/4) very gravelly loam; weak medium subangular blocky structure; friable; no roots present; 50% gravels of sandstone; clear smooth boundary.

4Crt --- 158-172 cm; dark reddish brown (2.5YR 3/4) very gravelly sandy loam; loose fine single-grained structure; friable, 50% gravels of shale; clear smooth boundary.

4R --- 172+ cm; dark reddish brown (2.5YR 3/4) shale.

APPENDIX B

pH AND CEC

Table B-1. CEC and pH data for both sites.

Sample	pH	Exchangeable Bases K	Na	Ca	Mg	Total	Exch Acdty	Avg CEC	Avg Base Sat'n.
		<-----meq/100g----->							%
MC1 A	5.2	0.09	0.22	2.92	0.59	3.83	5.54	9.15	42
		0.08	0.20	2.93	0.61	3.82	5.09		
Ap	6.1	0.06	0.28	2.67	0.70	3.71	3.80	8.23	47
		0.04	0.26	3.00	0.72	4.03	4.93		
Btg1	7.0	0.09	0.51	4.02	1.96	6.58	2.69	9.21	71
		0.10	0.56	3.87	1.92	6.45	2.69		
Btg2	7.5	0.09	0.72	4.22	2.47	7.50	0.71	8.40	90
		0.09	0.66	4.29	2.55	7.60	1.00		
Btg3	7.7	0.11	0.51	8.22	2.68	11.51	0.29	11.59	99
		0.11	0.51	8.05	2.71	11.38	0.00		
2BC	7.8	0.07	0.23	10.44	1.22	11.96	0.00	11.92	100
		0.23	0.22	10.26	1.17	11.88	0.00		
MC2 A	5.5	0.09	0.09	3.95	0.64	4.79	6.21	10.77	43
		0.08	0.10	3.71	0.61	4.51	6.05		
Ap	6.5	0.04	0.14	2.75	0.64	3.58	3.47	6.72	51
		0.04	0.14	2.52	0.59	3.29	3.11		
Btg	7.4	0.15	0.43	5.12	2.13	7.83	1.49	9.62	84
		0.16	0.41	5.48	2.34	8.39	1.53		
Bx1	7.6	0.08	0.37	3.83	1.96	6.25	0.00	6.86	93
		0.19	0.41	3.89	2.03	6.52	0.95		
Bx2	7.9	0.08	0.32	4.40	1.72	6.52	0.70	7.00	94
		0.08	0.31	4.44	1.77	6.61	0.17		
2BC	7.7	0.04	0.15	1.78	0.70	2.67	1.24	3.67	72
		0.04	0.15	1.71	0.69	2.59	0.84		
3BCg	8.0	0.07	0.28	7.40	1.49	9.23	1.70	10.45	89
		0.07	0.29	7.37	1.61	9.33	0.64		
MC3 Ap	5.8	0.07	0.08	2.56	0.36	3.07	5.13	7.49	39
		0.06	0.08	2.28	0.34	2.76	4.02		
Bt	5.1	0.07	0.16	1.52	0.62	2.37	9.53	11.65	21
		0.07	0.15	1.60	0.62	2.44	8.95		
Bx1	5.0	0.10	0.25	1.07	1.59	3.00	7.79	11.16	27
		0.11	0.24	1.17	1.59	3.11	8.41		
Bx2	5.5	0.11	0.33	1.85	2.96	5.24	5.84	10.45	50
		0.10	0.36	1.80	2.94	5.20	4.60		
Bx3	6.7	0.07	0.31	1.78	2.70	4.87	2.90	8.16	60
		0.10	0.30	1.79	2.70	4.89	3.65		
2BCg	6.9	0.04	0.23	1.96	2.04	4.29	1.90	6.19	68
		0.05	0.23	1.79	2.02	4.09	2.11		
3Cr	6.8	0.08	0.18	1.35	1.35	2.96	2.15	5.65	53
		0.09	0.18	1.40	1.31	2.97	3.22		

Table B-1 (cont). CEC and pH data for both sites.

Sample	pH	Exchangeable Bases K	Na	Ca	Mg	Total	Exch Acdty	Avg CEC	Avg Base Sat'n.
		<-----meq/100g----->							%
MC4 Ap	5.7	0.15	0.08	3.55	0.46	4.24	6.85	10.89	39
		0.12	0.07	3.52	0.47	4.18	6.52		
Bt1	4.6	0.13	0.11	2.19	0.66	3.10	11.66	14.04	21
		0.16	0.12	2.01	0.64	2.93	10.41		
Bt2	4.2	0.24	0.17	0.98	0.95	2.36	10.41	13.25	18
		0.13	0.15	1.08	0.97	2.33	11.41		
Btx1	4.3	0.14	0.18	0.94	1.49	2.73	8.52	11.06	25
		0.13	0.19	0.98	1.53	2.83	8.02		
Btx2	4.8	0.27	0.22	2.24	2.17	4.90	6.02	11.21	44
		0.25	0.26	2.35	2.20	5.06	6.44		
Cr	5.1	0.33	0.23	3.16	2.29	6.00	4.76	10.75	56
		0.37	0.23	3.30	2.21	6.10	4.64		
MC5 Ap	5.0	0.22	0.01	1.53	0.17	1.92	4.70	6.93	29
		0.21	0.05	1.63	0.19	2.07	5.16		
Bt1	5.5	0.38	0.00	2.20	0.21	2.79	4.04	7.29	40
		0.35	0.02	2.44	0.23	3.06	4.70		
Bt2	5.6	0.29	0.01	1.98	0.21	2.50	3.16	5.82	43
		0.34	0.02	1.92	0.20	2.48	3.50		
BC	4.8	0.36	0.01	1.39	0.19	1.96	3.75	5.89	33
		0.28	0.03	1.45	0.20	1.95	4.12		
C1	4.3	0.12	0.04	1.18	0.60	1.95	6.10	8.09	23
		0.18	0.03	1.04	0.56	1.81	6.30		
2C2 up	4.4	0.19	0.07	1.24	1.64	3.14	8.24	11.61	29
		0.22	0.05	1.63	1.70	3.60	8.24		
2C2 lo	4.5	0.22	0.06	1.35	2.43	4.06	8.49	12.41	32
		0.23	0.06	1.30	2.39	3.99	8.28		
3R	4.5	0.12	0.06	1.40	1.66	3.24	3.07	5.97	53
		0.14	0.07	1.20	1.69	3.10	2.53		
FC1 Ap	6.2	0.29	0.07	5.11	0.56	6.04	7.71	13.44	46
		0.30	0.07	5.32	0.59	6.29	6.85		
Btg1	5.2	0.20	0.11	3.61	0.83	4.75	10.74	15.30	31
		0.21	0.10	3.53	0.84	4.67	10.45		
Btg2	4.5	0.37	0.19	3.60	1.55	5.70	18.81	24.48	24
		0.31	0.14	3.95	1.61	6.01	18.43		
2BC	4.5	0.27	0.28	2.27	1.93	4.75	11.16	15.50	31
		0.23	0.32	2.32	1.91	4.77	10.32		
3BC	5.5	0.07	0.20	1.84	1.58	3.69	6.56	10.52	36
		0.10	0.23	1.89	1.59	3.80	6.98		
4BCg1	5.7	0.06	0.15	1.23	1.07	2.51	2.74	5.18	50
		0.06	0.12	1.40	1.08	2.67	2.45		
4BCg2	4.9	0.10	0.27	1.65	1.42	3.44	4.67	8.07	44
		0.12	0.30	1.76	1.51	3.68	4.35		

Table B-1 (cont). CEC and pH data for both sites.

Sample	pH	Exchangeable Bases K	Na	Ca	Mg	Total	Exch Acdty	Avg CEC	Avg Base Sat'n.
		<-----meq/100g----->							%
4BCg3	4.9	0.22	0.53	3.75	3.19	7.70	6.13	13.98	56
		0.26	0.61	3.91	3.24	8.01	6.13		
5Cr	4.6	0.46	0.72	5.20	3.98	10.35	7.39	17.81	58
		0.35	0.71	5.21	3.99	10.27	7.60		
FC1A Ap	5.6	0.20	0.07	4.66	0.51	5.43	5.14	10.75	50
		0.20	0.05	4.62	0.49	5.37	5.56		
Bt1	6.2	0.15	0.20	3.29	1.01	4.65	13.09	17.95	26
		0.16	0.21	3.31	1.02	4.70	13.46		
Bt2	5.7	0.19	0.31	1.90	1.69	4.09	17.46	21.17	19
		0.20	0.31	1.87	1.71	4.10	16.70		
2Bx up	5.3	0.16	0.33	2.09	2.31	4.88	11.32	16.19	30
		0.20	0.34	2.04	2.27	4.85	11.32		
2Bx lo	4.8	0.16	0.38	2.42	2.54	5.49	7.23	13.08	42
		0.15	0.37	2.44	2.55	5.51	7.94		
wh seam	4.7	0.29	0.57	3.75	3.88	8.49	7.92	16.05	52
		0.24	0.54	3.66	3.79	8.24	7.46		
2Cr	4.6	0.23	0.56	3.48	3.26	7.52	5.83	13.67	55
		0.23	0.55	3.41	3.20	7.39	6.59		
FC2 Ap	5.8	0.30	0.08	4.99	0.58	5.94	7.01	12.53	47
		0.29	0.06	4.86	0.58	5.79	6.32		
BE	4.3	0.15	0.16	2.93	0.93	4.17	9.68	13.51	31
		0.11	0.20	3.00	0.98	4.29	8.87		
Bt	3.8	0.17	0.25	2.55	1.71	4.68	14.57	19.10	24
		0.16	0.25	2.46	1.68	4.54	14.40		
2Bx	4.4	0.18	0.37	2.41	2.60	5.56	14.83	20.68	27
		0.14	0.36	2.36	2.62	5.47	15.50		
2BC	4.4	0.18	0.44	2.84	3.01	6.47	13.65	20.55	32
		0.18	0.43	2.90	3.01	6.51	14.48		
wh seam	4.3	0.22	0.62	4.54	3.91	9.29	12.46	21.97	42
		0.19	0.61	4.52	3.93	9.24	12.94		
3Crt	4.6	0.19	0.56	4.36	3.66	8.78	9.55	18.64	47
		0.19	0.56	4.34	3.64	8.72	10.24		
FC3 Ap	5.0	0.42	0.09	4.98	0.52	6.00	5.71	11.81	50
		0.45	0.07	4.85	0.50	5.87	6.04		
BA	6.1	0.18	0.09	3.21	0.37	3.85	5.56	9.28	44
		0.17	0.09	3.68	0.41	4.35	4.81		
Bt1	4.4	0.18	0.13	3.46	0.47	4.24	4.34	9.08	47
		0.16	0.09	3.61	0.49	4.35	5.22		
Bt2	4.3	0.17	0.09	4.21	0.90	5.36	7.56	13.02	41
		0.16	0.09	4.22	0.90	5.37	7.73		
Bt3	4.5	0.14	0.08	2.06	0.95	3.24	10.96	14.29	23
		0.13	0.08	2.12	0.96	3.30	11.09		

Table B-1 (cont). CEC and pH data for both sites.

Sample	pH	Exchangeable Bases K	Na	Ca	Mg	Total	Exch Acdty	Avg CEC	Avg Base Sat'n.
		<----------meq/100g---------->							%
2Crt	4.6	0.13	0.08	1.15	0.89	2.25	9.01	11.29	20
		0.13	0.08	1.25	0.89	2.34	8.97		
FC4 Ap	4.6	0.68	0.08	4.67	0.81	6.24	nd	5.58	111
		0.65	0.08	4.64	0.79	6.17			
Bw1	4.8	0.22	0.09	5.33	0.99	6.63	nd	7.60	87
		0.20	0.07	5.36	1.00	6.63			
Bw2	5.9	0.19	0.07	3.15	1.30	4.70	nd	6.11	76
		0.19	0.09	3.05	1.26	4.58			
BC	4.8	0.15	0.05	2.91	1.83	4.94	nd	6.54	71
		0.15	0.03	2.50	1.60	4.29			
Cr	4.1	0.18	0.06	1.84	1.79	3.87	nd	6.20	62
		0.25	0.10	1.71	1.79	3.84			
FC5 Ap	4.5	0.59	0.09	3.02	0.42	4.11	5.23	9.85	42
		0.50	0.05	3.22	0.47	4.24	6.13		
Bt1	4.6	0.07	0.08	3.21	0.43	3.80	4.50	9.36	44
		0.08	0.07	3.75	0.47	4.37	6.05		
Bt2	4.7	0.09	0.08	3.67	0.95	4.78	4.93	10.12	47
		0.11	0.09	3.61	0.94	4.75	5.78		
Bt3	4.9	0.13	0.11	3.28	1.22	4.74	4.51	9.23	47
		0.12	0.10	2.57	1.12	3.91	5.31		
2BCt1	5.0	0.18	0.10	2.67	2.06	5.01	8.04	12.93	38
		0.19	0.11	2.58	2.02	4.90	7.91		
3BCt2	5.9	0.10	0.08	1.40	1.32	2.90	5.37	8.27	36
		0.10	0.07	1.44	1.37	2.97	5.29		
4Crt	6.2	0.20	0.11	2.75	2.78	5.85	9.03	15.15	38
		0.20	0.11	2.60	2.77	5.69	9.73		

APPENDIX C

SEMIQUANITITATIVE MINERALOGICAL ANALYSIS OF THE SAND, SILT, AND CLAY FRACTIONS

Methodology

The semiquantitative mineralogical analysis employed in this research used the following approach based upon peak shapes (i.e height and width).

tr.= mineral abundance < 2%

X = mineral abundance between 2-10%

XX = mineral abundance between 10-30%

XXX = mineral abundance between 30-70%

XXXX = mineral abundance between 70-100%

Table C-1. Semiquantitative Mineralogical Analysis of the Sand Fraction.

Sample	Qz	Mica	K-sp	Na-pl	Kao	Chl	Hem
MC1 A	XXX		X	X			X
MC1 Ap	XXX		X	X			
MC1 Btg1	XXX	tr.	X	X			
MC1 Btg2	XXX	X	X	X			
MC1 Btg3	XXX	X	X	X			
MC1 2BC	XXX	X	X	X			X
MC2 A	XXX		X	X			
MC2 Ap	XXX		X	X			
MC2 Btg	XXX		X	X			
MC2 Bx1	XXX	X	X	X			
MC2 Bx2	XXX	X	X	X			
MC2 2BC	XXX	X	X	X			
MC2 3BCg	XXX	X	X	X			
MC3 Ap	XXX		X	X			
MC3 Bt	XXX	X	X	X			
MC3 Bx1	XXX	X	X	X			
MC3 Bx2	XXX	X	X	X			tr.
MC3 Bx3	XXX	X	X	X			
MC3 2BCg	XXX	X	X	X			
MC3 3Cr	XXX	X	X	X			
MC4 Ap	XXX	X	X	X			tr.
MC4 Bt1	XXX	X	tr.	X	X	X	tr.
MC4 Bt2	XXX	XX	X	X	X	X	X
MC4 Btx1	XXX	XX		X	X		X
MC4 Btx2	XX	XX	tr.	X	X	X	X
MC4 Cr	XX	XX	tr.	X	X	tr.	X
MC5 Ap	XXX		X	X			
MC5 Bt1	XXX	X	X	X			
MC5 Bt2	XXX	X	X	X			
MC5 BC	XXX	X	X	X			X
MC5 C1	XXX	X	X	X			tr.
MC5 2C2 up	XX	X	X	X	X	tr.	tr.
MC5 2C2 lo	XX	X	X	X	tr.	X	X
MC5 3R	XXX	X	X	X			

Table C-1 (cont). Semiquantitative Mineralogical Analysis of the Sand Fraction.

Sample	Qz	Mica	K-sp	Sand Na-pl	Kao	Chl	Hem
FC1 Ap	XXXX			tr.			
FC1 Btg1	XXXX			tr.			
FC1 Btg2	XXXX			X			
FC1 2BC	XXXX			X			tr.
FC1 3BC	XXX	tr.		X			
FC1 4BCg1	XXX	X		X			
FC1 4BCg2	XXX	X		X			
FC1 4BCg3	XXX	X		X			
FC1 5Cr	XX	X		X			
FC1A Ap	XXXX			X			
FC1A Bt1	XXXX			X			
FC1A Bt2	XXXX			X			
FC1A 2Bxup	XXX	X		X			X
FC1A 2Bxlo	XXX	X		X			X
FC1A w.seam	XXX	X		X			
FC1A 2Cr	XXX	X		X			X
FC2 Ap	XXX			X			
FC2 BE	XXX			X			
FC2 Bt	XXX	tr.		X			
FC2 2Bx	XX	X		X			X
FC2 2BC	XX	X		X			X
FC2 w.seam	XXX	X					tr.
FC2 3Crt	XX	X		X			X
FC3 Ap	XXX	tr.		X			
FC3 BA	XXX	tr.		X			tr.
FC3 Bt1	XXX	X		X			tr.
FC3 Bt2	XXX	X		X			X
FC3 Bt3	XXX	X		X			X
FC3 2Crt	XXX	X		X			X
FC4 Ap	XXX	X		X			X
FC4 Bw1	XXX	X		X			X
FC4 Bw2	XXX	X		X	tr.	tr.	X
FC4 BC	XXX	X		X	tr.	tr.	X
FC4 Cr	XXX	X		X			X

Table C-1 (cont). Semiquantitative Mineralogical Analysis of the Sand Fraction.

Sample	Qz	Mica	K-sp	Sand Na-pl	Kao	Chl	Hem
FC5 Ap	XXX	X		X	tr.	tr.	X
FC5 Bt1	XXX	X		X	tr.	tr.	X
FC5 Bt2	XXX	X		X	tr.		X
FC5 Bt3	XXX	X		X	tr.		X
FC5 2BCt1	XXX	X		X	tr.	tr.	X
FC5 3BCt2	XXX	X		X			X
FC5 4Crt	XXX	X		X			X

Table C-2. Semiquantitative Mineralogical Analysis of the Silt Fraction.

Sample	Qz	Mica	K-sp	Silt Na-pl	Kao	Chl	Hem
MC1 A	XXX	XX	X	X			
MC1 Ap	XXX	XX	X	X	X		
MC1 Btg1	XXX	XX	X	X	X		
MC1 Btg2	XXX	XX	X	X	X		
MC1 Btg3	XXX	XX	X	X	X	X	tr.
MC1 2BC	XXX	XX	X	X	X	X	X
MC2 A	XXX	XX	X	X			
MC2 Ap	XXX	XX	X	X	X		
MC2 Btg	XXX	XX	X	X	X		
MC2 Bx1	XXX	XX	X	X	X		X
MC2 Bx2	XXX	XX	X	X	X	X	tr.
MC2 2BC	XXX	XX	X	X	X		X
MC2 3BCg	XXX	XX	X	X	X	X	tr.
MC3 Ap	XXX	XX	X	X	X	tr.	
MC3 Bt	XXX	XX	X	X	X	X	
MC3 Bx1	XXX	XX	X	X	X	X	X
MC3 Bx2	XXX	XX	X	X	X	X	X
MC3 Bx3	XXX	XX	X	X	X		X
MC3 2BCg	XXX	XX	X	X	X	tr.	tr.
MC3 3Cr	XXX	XX	X	X	X	X	X
MC4 Ap	XXX	XX	tr.	X	X	X	X
MC4 Bt1	XXX	XX	X	X	X	X	X
MC4 Bt2	XXX	XX	X	X		X	X
MC4 Btx1	XXX	XX	tr.	X	X	X	X
MC4 Btx2	XXX	XX	tr.	X	X	X	X
MC4 Cr	XXX	XX		X	X	X	X
MC5 Ap	XXX	XX	X	X	X	X	X
MC5 Bt1	XXX	XX	X	X	X	X	X
MC5 Bt2	XXX	XX	X	X	X	X	X
MC5 BC	XXX	XX	X	X	X	X	X
MC5 C1	XXX	XX	X	X	X		X
MC5 2C2 up	XXX	XX	tr.	X	X	X	X
MC5 2C2 lo	XXX	XX	tr.	X	X	X	X
MC5 3R	XXX	XX	X	X	X	X	X

Table C-2 (cont). Semiquantitative Mineralogical Analysis of the Silt Fraction.

Sample	Qz	Mica	K-sp	Silt Na-pl	Kao	Chl	Hem
FC1 Ap	XXX	XX	X	tr.	tr.	tr.	tr.
FC1 Btg1	XXX	XX	X	X	X		
FC1 Btg2	XXX	XX	X	X	X		
FC1 2BC	XXX	XX	X	X	X		X
FC1 3BC	XXX	XX		tr.	tr.		
FC1 4BCg1	XXX	XX		X	X		tr.
FC1 4BCg2	XXX	XX		X	X		
FC1 4BCg3	XXX	XX		tr.	tr.		
FC1 5Cr	XXX	XX					X
FC1A Ap	XXX	XX	X				tr.
FC1A Bt1	XXX	XX	tr.	tr.	tr.		
FC1A Bt2	XXX	XX	tr.				X
FC1A 2Bxup	XXX	XX	tr.	tr.	tr.		X
FC1A 2Bxlo	XXX	XX	tr.				X
FC1A w.seam	XXX	XX					
FC1A 2Cr	XXX	XX					X
FC2 Ap	XXX	XX	X	X	tr.	X	tr.
FC2 BE	XXX	XX	X	X	X		X
FC2 Bt	XXX	XX	tr.	X	X	X	X
FC2 2Bx	XXX	XX	tr.	X			X
FC2 2BC	XXX	XX	X	X			X
FC2 w.seam	XXX	XX	tr.	X			X
FC2 3Crt	XXX	XX	X	X			X
FC3 Ap	XXX	XX	X	X	tr.	tr.	X
FC3 BA	XXX	XX	X	X	X	X	X
FC3 Bt1	XXX	XX	tr.	X	tr.	tr.	X
FC3 Bt2	XXX	XX	tr.	X	X	tr.	X
FC3 Bt3	XXX	XX		X	tr.	tr.	X
FC3 2Crt	XXX	XX		X			X
FC4 Ap	XXX	XX	X	X	X	X	X
FC4 Bw1	XXX	XX	X	X	X	X	X
FC4 Bw2	XXX	XX	tr.	X	tr.	tr.	X
FC4 BC	XXX	XX		X	X	tr.	X
FC4 Cr	XXX	XX				tr.	X

Table C-2 (cont). Semiquantitative Mineralogical Analysis of the Silt Fraction.

Sample	Qz	Mica	K-sp	Silt Na-pl	Kao	Chl	Hem
FC5 Ap	XXX	XX	X	X	X	X	X
FC5 Bt1	XXX	XX	tr.	X	X		X
FC5 Bt2	XXX	XX	tr.	tr.	tr.		X
FC5 Bt3	XXX	XX		tr.	tr.		X
FC5 2BCt1	XXX	XX		X	X	X	X
FC5 3BCt2	XXX	XX					X
FC5 4Crt	XXX	XX	tr.				

Table C-3. Semiquantitative Mineralogical Analysis of the Clay Fraction.

Sample	Clay							
	Chl	Vermic	Mica	Kao	Qz	Gth	Hem	Lep
MC1 A	X	X	XX	XX	X	X		
MC1 Ap	X	X	XX	XX		X		
MC1 Btg1	X	XX	XX	XX	X	X	X	
MC1 Btg2	X	XX	XX	XX	X	X	X	
MC1 Btg3	X	XX	XX	XX				
MC1 2BC	X	XX	XX	XX				
MC2 A	X	X	XX	XX		X		
MC2 Ap	X	X	XX	XX	tr.	X		
MC2 Btg	X	XX	XX	XX		X		
MC2 Bx1	X	XX	XX	XX	tr.	X		
MC2 Bx2	X	XX	XX	XX				
MC2 2BC	X	XX	XX	XX				
MC2 3BCg	X	XX	XX	XX				
MC3 Ap	X	X	XX	XX	X	X		
MC3 Bt	X	X	XX	XX	tr.	X	X	
MC3 Bx1	X	X	XX	XX		X	X	
MC3 Bx2	X	XX	XX	XX		X		
MC3 Bx3	X	XX	XX	XX				
MC3 2BCg	X	X	XX	XX		X		
MC3 3Cr	X	X	XX	XX		X		
MC4 Ap	X	X	XX	XX	tr.	X	tr.	
MC4 Bt1	X	X	XX	XX		X	tr.	
MC4 Bt2	X	X	XX	XX		X	X	
MC4 Btx1	X	X	XX	XX				
MC4 Btx2	X	X	XX	XX	tr.			
MC4 Cr	X	X	XX	XX				
MC5 Ap	X	X	XX	XX				
MC5 Bt1	X	X	XX	XX	tr.	tr.	tr.	
MC5 Bt2	X	X	XX	XX	X	tr.	tr.	
MC5 BC	X	X	XX	XX	X			
MC5 C1	X	X	XX	XX	X		X	
MC5 2C2 up	X	X	XX	XX				
MC5 2C2 lo	X	X	XX	XX			tr.	
MC5 3R	X	X	XX	XX				

Table C-3 (cont). Semiquantitative Mineralogical Analysis of the Clay Fraction.

Sample	Clay							
	Chl	Vermic	Mica	Kao	Qz	Gth	Hem	Lep
FC1 Ap	X							
FC1 Btg1	X	X	XX	XXX				
FC1 Btg2	X	X	XX	XXX	X	X		
FC1 2BC		X	XX	XXX		X		
FC1 3BC		X	XX	XXX	X	X		X
FC1 4BCg1		X	XX	XXX	tr.			
FC1 4BCg2		XX	XX	XXX				
FC1 4BCg3		XX	XX	XXX				
FC1 5Cr		XX	XX	XXX	tr.			
		XX	XXX	XX				
FC1A Ap	X							
FC1A Bt1	X	XX	XX	XXX	X	X		
FC1A Bt2	X	XX	XX	XXX	X	X		
FC1A 2Bxup	X	XX	XX	XXX		X		
FC1A 2Bxlo	X	XX	XX	XXX	tr.			
FC1A w.sm	X	X	XXX	X				
FC1A 2Cr		XX	XXX	XX				
		XX	XXX	XX				
FC2 Ap	X							
FC2 BE	X	X	XX	XX	X	X	X	
FC2 Bt	X	X	XX	XX	X	X	X	
FC2 2Bx	X	X	XX	XX	tr.	X	X	
FC2 2BC	tr.	X	XX	XX		X	X	
FC2 w.sm	tr.	XX	XX	XX	tr.		X	
FC2 3Crt	tr.	XX	XX	XX	X		X	
		XX	XX	XX	tr.		X	
FC3 Ap	X							
FC3 BA	X	tr.	XX	XX	X			
FC3 Bt1	X	tr.	XX	XX	X		X	
FC3 Bt2	X	X	XX	XX	X		X	
FC3 Bt3	X	X	XX	XX	X	tr.	X	
FC3 2Crt	tr.	X	XX	XX	X		X	
		XX	XX	XX	tr.		X	
FC4 Ap	X							
FC4 Bw1	X	X	XX	XX	X			
FC4 Bw2	X	X	XX	XX	X		X	
FC4 BC	X	X	XX	XX	X	X	X	
FC4 Cr	X	X	XX	XX	X	X	X	
		X	XX	XX			X	
							X	

Table C-3 (cont). Semiquantitative Mineralogical Analysis of the Clay Fraction.

Sample	Clay							
	Chl	Vermic	Mica	Kao	Qz	Gth	Hem	Lep
FC5 Ap	XX	tr.	XX	XX			tr.	
FC5 Bt1	X	X	XX	XXX			X	
FC5 Bt2	X	X	XX	XX	X	tr.	X	
FC5 Bt3	X	X	XX	XX			X	
FC5 2BCt1	X	X	XX	XX			X	
FC5 3BCt2	X	X	XX	XX			X	
FC5 4Crt	X	X	XX	XX			X	